SCINTILLATION COUNTER STUDIES OF PHOTODISINTEGRATION AND OF THE DECAY SCHEMES OF SOME RADIOACTIVE NUCLEI

by

J. D. Prentice

Department of Natural Philosophy
University of Glasgow

Presented at the University of Glasgow
in May, 1959
as a Thesis for the Degree of
Doctor of Philosophy

ProQuest LLC.
789 East Eisenhower Parkway
P.O. Box 1346
Ann Arbor, MI 48106 – 1346

PREFACE

In this thesis are discussed four experimental investigations in low energy nuclear physics which test the validity of certain applications of the nuclear shell model. The experiments described were carried out by the author between October, 1953 and June, 1957 in the Department of Natural Philosophy of the University of Glasgow.

The review of the shell model and of three types of experiment in the interpretation of which it is useful, is given in Chapter I, to show the relevance of the experimental work to an understanding of the nucleus. The material for this chapter has been drawn mainly from the current literature on the subject.

All the experiments were original in planning and execution. In two cases it was discovered when the work was almost completed that similar work, concurrently performed elsewhere, had yielded similar results. Accounts of three of the experiments have been published and the fourth was reported by Dr. K. G. McNeill at a meeting of the Canadian Association of Physicists in June, 1956. The author's degree of responsibility for the various parts of each investigation is outlined below.

Chapter II describes an investigation of the production of an isomeric state of Pb^{207} by a photoneutron reaction.

The identification of the radioactivity, described in section 2.2(i), was performed in collaboration with Mr. J. M. Reid and Dr. K. G. McNeill. The author was responsible for the experiments to measure the yield of the isomeric state from the photoneutron experiment and the experiments with Bi^{207} to attempt to clarify the energy level scheme of Pb^{207}, but is indebted to Dr. McNeill for help in analysing the results of the former. The conclusions, and the discussion of the relevance of the experiment to the theory of photodisintegration are due to the author.

In Chapter III is described a search for a reported isomeric state of Mn^{54}. The experiments reported in section 3.2 were performed by the author except for those, briefly mentioned at the end, which were carried out at the University of Saskatchewan and are clearly indicated in the text. The author is indebted to Dr. McNeill for helpful discussions concerning the conclusion in section 3.3.

An investigation of the radioactive decay scheme of the ground state and isomeric state of Mo^{91} is described in Chapter IV. The author was responsible for the experimental work, some of which was performed and analysed in collaboration with Dr. McNeill.

In Chapter V is described the investigation of the radioactive decay scheme of I^{128}. The planning and execution of the experiments were the responsibility of the author who is nevertheless indebted to Dr. McNeill for

assistance in the performance and analysis of some of them. The discussion of the results, and the conclusions drawn from them are the author's.

ACKNOWLEDGEMENTS

The author would like to thank Professor P. I. Dee for his interest and encouragement during the course of this work and for the opportunity to perform it in the Natural Philosophy Department of the University of Glasgow.

The author is very grateful to Dr. K. G. McNeill for his assistance and advice and to Dr. G. M. Lewis for several helpful discussions and for the loan of a coincidence circuit.

The assistance of Mr. J. C. Telfer in maintaining the 23 MeV synchrotron is gratefully acknowledged.

Finally, the author acknowledges with gratitude the receipt of the McGill-Glasgow Exchange Fellowship for the session 1953-1954 and a Glasgow University Research Studentship during the remainder of the period occupied by this work.

CONTENTS

CHAPTER I INTRODUCTION

Section 1.1 The Role of Models in Nuclear Physics

In 1911 Lord Rutherford proposed an atomic model consisting of a small, dense, positively charged nucleus at the centre of the atom, surrounded by negative electrical charge. Structure was detected within the nucleus itself and since then much of the research in physics has concerned attempts to understand the atomic nucleus.

Two contrasting approaches to the problem, each partially successful in the past, are still being pursued today. The nucleus was found to consist of protons and neutrons: one may perform experiments to measure their mutual interactions and try to develop a consistent theory of these forces in terms of which to predict the properties of nuclei containing large numbers of the basic particles. Alternatively, by examining the properties of a large number of nuclei, attempts may be made to deduce generalities which apply to all nuclei. The first approach has led to the study of the nuclear force law: the second has encouraged the proposal of a number of models of the nucleus.

Since the discovery that nuclei are composed of particles it has been apparent that there must be a specific inter-nucleon force to overcome the electrostatic repulsion between the protons and to confine the nucleons in the small volume which the nucleus was found to occupy.

Some features of the force law can be deduced from general properties of nuclei such as the variation of nuclear volume and binding energy with the number of constituent nucleons. To determine the forces between pairs of nucleons more specifically, nucleon-nucleon scattering has been studied over the wide range of energies now available in the laboratory, from thermal neutrons up to 10,000 Mev protons.

That the nuclear force field should be characterized by massive "quanta" was predicted by Yukawa in 1935 and the discovery of π-mesons in cosmic rays, by the study of tracks in photographic emulsions, confirmed the existence of these short-lived particles which interacted strongly with nuclei. It was found that π-mesons could be produced in the laboratory and the contemporary investigation of the nuclear force law includes experiments involving light and heavy mesons as well as the scattering experiments which are still being checked and extended. There remain, however, many unknown factors in the meson theory of nuclear forces and even when these are eliminated the second approach to the problem of the nucleus will be fruitful in describing heavy nuclei, because of the difficulty of finding even approximate solutions to the many-body problem.

The experiments described in this thesis contribute to the latter approach. Much information has been amassed

about the properties of nuclei, by many different types of experiments: significant general features have been observed and have inspired the proposal of models of the nucleus based on analogies to other branches of physics. Each of the models so far proposed has been successful in explaining some properties of nuclei or nuclear reactions but has been found unable to predict correctly other nuclear phenomena: several have been modified, in the light of newer experimental evidence, to widen their application. The liquid drop model, the optical model and the shell model are examples.

The first was suggested by the constancy of nuclear density throughout the periodic table and the smallness of the variation of binding energy with nuclear size, both features being suggestive of the properties of molecules in a liquid drop. The model proved particularly useful in the treatment of fission but failed in its predictions of the energy spectrum of the excited states of nuclei. It was also applied to the theory of nuclear reactions by Bohr and led to the idea of the compound nucleus, and the concepts of nuclear temperature and evaporation of particles.

The concept of the compound nucleus is, however, only applicable to reactions in which a bombarding particle is captured by the target nucleus and to describe the initial stage of the reaction it is necessary to consider the

abrupt change in potential which the incoming particle experiences at the nuclear surface. Representing the nucleus by a complex potential well predicts both scattering and absorption of the incident wave packet. The optical model of the nucleus, which is based on this idea, has been successful in explaining many of the resonance features of nuclear reactions.

The fact that several nuclear properties, such as the binding of the last added nucleon, varied smoothly over wide regions of the periodic table but showed sharp discontinuities as the number of neutrons or protons passed certain values, suggested that nuclei were constructed by filling successive shells with nucleons. Thus as each extra proton or neutron was added it would occupy a state of particular angular momentum and energy, the number of nucleons allowed in each level being determined by the Pauli principle, and the magic numbers being explained by postulating large gaps between certain energy levels and the succeeding ones.

All these models are at present used to interpret various experimental results; experiments are conducted to determine the regions of applicability of the models; and attempts are made to modify their theoretical basis in order to extend the range of nuclear phenomena to which they can be applied.

Even models which are insufficiently detailed to

predict quantitatively the values of particular nuclear parameters may still infer the variations of certain general features throughout the periodic table. When such trends are revealed by reviews of experimental data such as those described in "The Properties of Medium-weight Nuclei" (Way, 1956), then further experiments which either corroborate the observed generalities or show exceptions to them contribute empirical evidence which, together with other results, forms a useful proving ground for the models.

To further our understanding of the nucleus by the phenomenological approach experiments must, therefore, be performed which help to define the limits of applicability of the models or which confirm or deny the observed empirical trends. In this thesis are presented the results of experiments on four nuclei, Mn^{54}, Mo^{91}, I^{128} and Pb^{207}. The interpretation of these results in terms of the shell model throws light on the validity of applying it to various nuclear phenomena.

In the remainder of the introduction the shell model and some of its improvements are described (section 1.2): the interaction of electromagnetic radiation with nuclei is discussed (section 1.3): and finally the application of these theories to three types of experimental work which appear in the following chapters, is briefly outlined (section 1.4).

Section 1.2 The Nuclear Shell Model

The suggestion that the motion of nucleons in the nucleus is determined by an average potential rather than by strong interactions with their nearest neighbours seems unreasonable in view of the strength and short range of the two body force found in nucleon-nucleon scattering experiments. Nevertheless the model has been widely used since 1949, when the introduction of the strong spin-orbit coupling (Mayer, 1949 and Haxel, 1949) gave correct predictions of the observed magic numbers. Its success in predicting most of the static and some of the dynamic properties of nuclei overshadowed the apparent weakness of its theoretical basis. Recently major advances in the treatment of the many-body problem have revealed the possibility of building the nuclear shell model on a firm theoretical foundation.

Historically, the shell model was proposed in analogy with the successful model of the atom in which the basic motion of the electrons was determined by the field of the nucleus and their mutual interactions treated as a perturbation. Certain discontinuities in nuclear properties such as α- and β-decay energies and neutron capture cross sections, which occurred at points in the periodic table corresponding to particular nucleon numbers suggested a similarity to the closing of electron shells at the inert gases. The assumption of some nuclear potential, such as

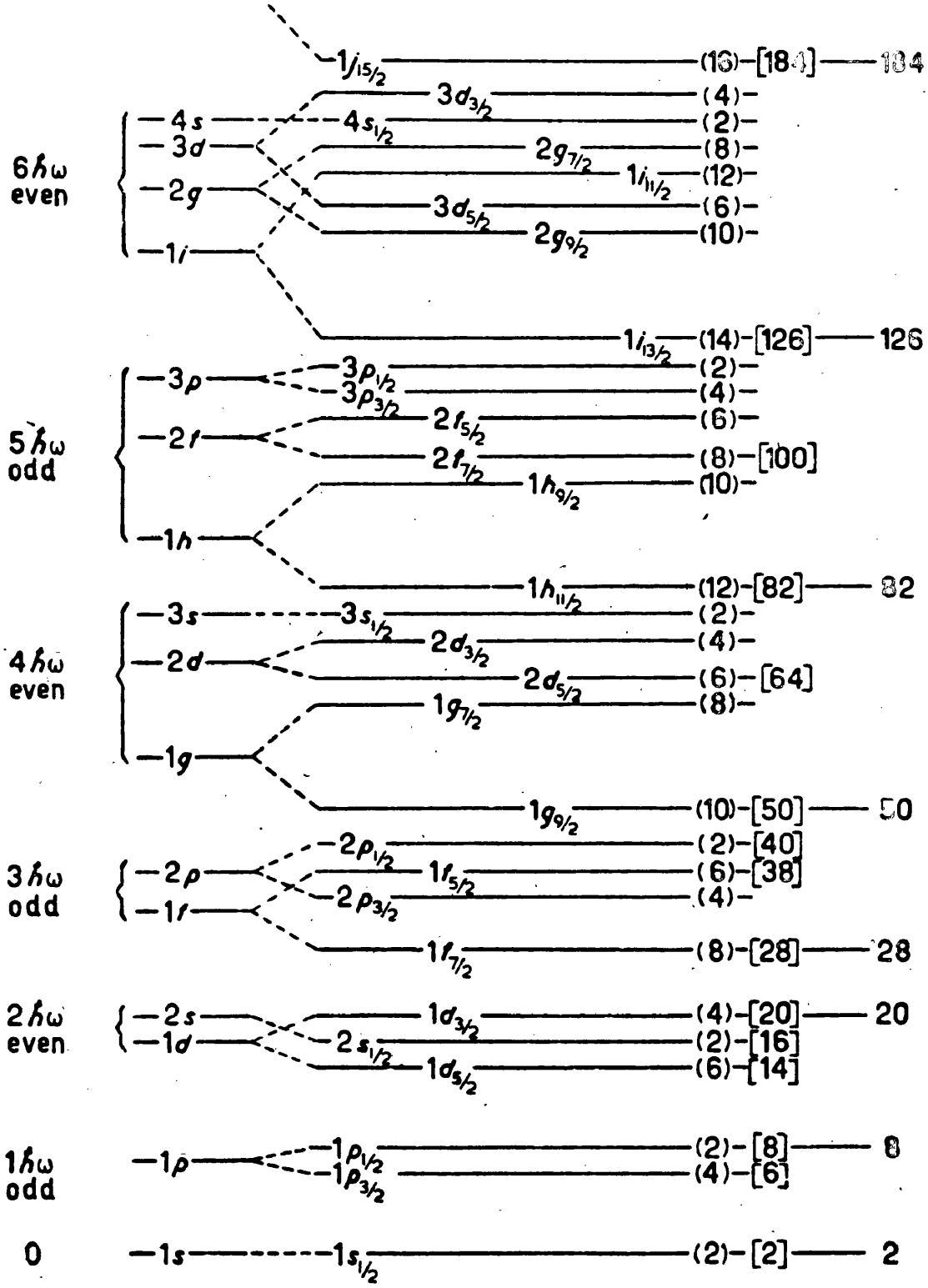

Fig. 1.1

Energy level scheme for protons as predicted by the single particle shell model for a spherically symmetric potential intermediate between the harmonic oscillator and the square well of infinite depth. The harmonic oscillator grouping and the parity are shown on the left. Numbers on the right are level degeneracies (curved brackets) and total occupation numbers [square brackets].

a three-dimensional square well or harmonic oscillator, yielded bound states of increasing energy which could be filled consecutively with protons and neutrons as the mass number, A, increased. No potential was found, however, which successfully predicted shell closures at the observed magic numbers 50, 82 and 126 until, with the aid of j-j coupling and a strong spin-orbit interaction, the doublets of high orbital angular momentum were shown to be sufficiently widely split for the high spin member to join the next lower shell. In fig. 1.1 is shown the level order predicted for protons by Jensen (1955). In the harmonic oscillator potential the bracketed sets of levels are degenerate. The order shown, ignoring the spin-orbit splitting, is the same as that found for the infinite square well potential, up to the 3s level. The order for neutrons is predicted to be the same up to N = 50 but thereafter low neutron angular momenta are more favoured than the corresponding proton states and some levels will cross. At best the diagram is approximate but with its aid and some very simple assumptions many of the nuclear ground state spins and parities can be predicted.

In nuclei containing an even number of protons and an even number of neutrons (hereinafter called even nuclei) each successive pair of neutrons couples together to give zero angular momentum and the protons behave similarly.

The ground states of even nuclei have thus unambiguously zero spin and even parity. No exceptions have been found to this rule.

For odd proton or odd neutron nuclei the simplest assumption is that all the nucleons, except the odd one, pair in the above way and that the ground state properties are determined by the spin and parity of the one unpaired nucleon. This single particle shell model provides many correct predictions but needs certain modifications. In an unfilled shell we must take some account of the nucleon-nucleon interaction; firstly, the effect of pairing energy must be included. If, to an even nucleus with Z protons, two more protons are added the pairing energy is defined as the binding energy of the two protons minus twice the binding energy of the $(Z + 1)^{st}$ proton. The sign is always positive, and the magnitude is almost the same for nearby odd-N nuclei particularly if the last added neutrons are in a different shell from the last added protons. Neutron pairing energy can be defined in a similar way. The most significant feature is that the pairing energy increases for levels of higher orbital angular momenta. The pairing energies (of the order of 1 to 3 Mev) of two successive levels may differ by as much as 1 Mev which is sometimes more than the spacing between the levels. This effect eliminates many of the expected high spin ground states. In the

region N = 82 to N = 126 the $i_{13/2}$ shell is expected to be the last to fill (see fig. 1.1). Pb^{207}, with 125 neutrons, should therefore have one neutron missing from the $i_{13/2}$ shell. Instead of a ground state spin and parity of $\frac{13}{2}+$, however, experiments show values of $\frac{1}{2}-$ (Strominger, 1958). The explanation of this result is that the pairing energy gained in completing the $i_{13/2}$ shell is greater than the energy needed to raise a neutron from the $3p_{1/2}$ shell to the $1i_{13/2}$ shell. In fact the pairing energy is so great that the same holds true for both the $2f_{5/2}$ and $3p_{3/2}$ states as is indicated by the $\frac{5}{2}-$ and $\frac{3}{2}-$ natures of the first two excited states of Pb^{207}. No $i_{13/2}$ ground state has been observed in any of the nuclei with $112 < N < 126$.

A similar argument explains the absence of spin $\frac{11}{2}$ ground states in either the neutron or proton $h_{11/2}$ shells although there is still some doubt about the order of the $\frac{11}{2}-$ and $\frac{3}{2}+$ states in Sn^{125} and Sn^{123}.

In the $g_{9/2}$ shell which closes at Z = 50 the pairing energy is almost equal to the gap between the $g_{9/2}$ and $p_{1/2}$ states. Thus in 26 odd-Z isotopes in the region Z = 41 to Z = 49 whose ground state spins have been directly measured, or estimated from experimental evidence on β-decay, the value $\frac{9}{2}$ occurs in 17 cases and the value $\frac{1}{2}$ in 7 cases. (The occurrence of two ground states of spin and parity $\frac{7}{2}+$ is explained below.) Similarly in the $g_{9/2}$ neutron shell there are 9 known $\frac{9}{2}+$ ground states, 7 nuclei with $\frac{1}{2}-$

ground states and 5 with spin and parity $\frac{7}{2}+$ or $\frac{5}{2}+$.

For nuclei containing an odd number of nucleons in a shell which is neither nearly empty nor nearly full the single particle shell model is not a good approximation and the coupling of several nucleons to give spin and parity values different from any of the available single particle levels is possible. The Independent Particle model considers the states which can be constructed by coupling together all the nucleons outside closed shells and can thus explain the occurrence of ground states such as that of Mn^{55} with spin and parity $\frac{5}{2}-$, in the middle of the $f_{7/2}$ shell and the above mentioned exceptions.

In nuclei of even A but odd Z and N (odd nuclei) the properties of the ground state depend on the coupling of an odd proton with an odd neutron. If the state of each of the odd particles can be guessed from knowledge of the nearest corresponding odd-Z or odd-N nucleus, Nordheim's rules (Nordheim, 1951) give an estimate of the resultant spin. His weak rule, however, gives several possible values for the spin and exceptions to both rules are known so predictions about the ground states of odd nuclei require more detailed calculations.

Such calculations have been successfully performed for nuclei with one or two neutrons and protons outside closed shells (de Shalit, 1953, Kurath, 1953) but the calculations become rapidly more difficult as the numbers

of equivalent particles to be considered increases.

The success of the single particle shell model (SPSM) and the more sophisticated independent particle model (IPM) in explaining the observed ground state spins and parities is strong evidence for their validity and provides an incentive to investigate their application to other nuclear phenomena such as the well defined low lying excited states of nuclei.

Again, the SPSM is useful in certain regions of the periodic table near the magic numbers. In particular for one nucleon outside a closed shell or for one "hole", that is one nucleon missing from a closed shell, the excited states might be expected to correspond to excitations of single particles to the available shell model levels. Pb^{208} has closed shells of both protons ($Z = 82$) and neutrons ($N = 126$) and Pb^{207}, therefore, with $N = 125$ should be particularly amenable to this type of analysis. The $\frac{1}{2}-$ ground state has been explained above in terms of the pairing energy in the $i_{13/2}$ state. Excited states can be formed by exciting one neutron from the $i_{13/2}$, $p_{3/2}$, $f_{5/2}$ and $f_{7/2}$ states to complete the $p_{1/2}$ shell and these spins and corresponding parities can plausibly be assigned to the known low-lying excited states. In odd neutron or odd proton nuclei with N or $Z = 41$ to 49 inclusive, a $\frac{9}{2}+$ ground state is predicted except in those nuclei for which the pairing energy makes

the $\frac{1}{2}-$ state lower. It is expected that the other level will be sufficiently close to form the first excited state. Thus in these regions many nuclei are found whose first excited state differs by 4 units of angular momentum from the ground state. This is particularly likely near the beginning and end of the $g_{9/2}$ shell; in nuclei where the shell is about half full odd numbers of equivalent $g_{9/2}$ nucleons sometimes couple to give $\frac{7}{2}+$ states as alternatives to the $\frac{9}{2}+$ states. Similarly for odd nuclei the spin and parity depend on the coupling of two or more nucleons and predictions are less reliable. There is, however, the possibility of high spins resulting from the coupling of the odd nucleons in the same regions of the periodic table. Adjacent nuclear levels of widely different spin lead to the phenomenon of isomerism and the possibility of studying the transitions between these levels in some detail as described below in section 1.4(ii).

The energies of particular excited states are scarcely predictable from the shell model even near magic numbers where fairly well defined single particle states are found. Ignorance of the shape and the depth of the central potential and the form of the interaction which should be used to calculate the pairing energy leads to uncertainties in the energy of single particle levels which are large compared to their separations and not even the order of the states can be accurately predicted. In configurations involving

two or more equivalent nucleons there are so many parameters available that virtually any experimental results can be fitted by theoretical calculations. Certain strikingly regular nuclear spectra have, however, demanded an explanation; it was not immediately supplied by the shell model.

In the rare earth region of the periodic table series of excited states of even nuclei have been found with spin and parity assignments 2+, 4+, 6+- - - and whose energies were fitted by the simple relationship $E = E_0 l(l + 1)$. Such regularity suggests a simple model and Bohr and Mottelson have interpreted these levels in terms of rotation of the whole nucleus (Bohr, 1953). Despite the success of the shell model, the strong inter-nucleon forces make it likely that collective motions of the nucleons will be possible. It has been shown theoretically that with many particles outside closed shells, the nucleon-nucleon forces lead to deformations of the nucleus and that the lowest energy state may be one of spheroidal, rather than spherical, shape. This in turn changes the shape of the potential and produces different single particle states, but a non-spherical equilibrium shape permits the explanation not only of the level schemes mentioned above as excitations of the nucleus by unified rotation but also of the very high electric quadrupole moments which occur in the same region of the periodic

table. The rotational spectrum is perturbed by coupling between the independent particle motions and the collective rotations and the model which takes this into account is successful in classifying the states of some nuclei in the region $A \simeq 25$ as members of rotational bands (Litherland, 1956). This Unified Model admits the possibilities of either a spherical configuration or a spheroidal equilibrium shape produced by the interactions of many particles outside closed shells, of collective oscillations of the shape, of rotations and finally of coupling between the single particle motions and the collective motions. Many of the nuclear spectra and transition probabilities which it predicts can also be predicted by the independent particle model, taking account of the coupling between all the particles outside closed shells and also of the perturbations caused by the mixing of configurations. Very near to closed shells the pure shell model is applicable. In the rare earth region large equilibrium deformations yield rotational excitations of very low energy compared to single particle transitions and thus very pure rotational spectra. In the remaining regions the various models are applicable to different phenomena.

In particular Way et al (1956) have shown that the excited states of even nuclei in the region $22 < N < 90$ display marked regularities. The energies of the second and first excited states are in the ratio $E_{2nd}/E_{1st} \simeq 2.2$

and the product of the mass number and E_{1st}, the energy of the first excited state, $E_{1st}A \simeq 60$ MeV. The ground states are all 0+ and almost all the first excited states 2+ and the second excited states are mostly 0+, 2+ or 4+. The energy distribution ratio can be explained in terms of the IPM with a short range attractive force between particles (Schwartz, 1954). The success, however, of the collective model in explaining the energy and spin patterns of the rare earth nuclear spectra suggests a similar attempt in this region. Scharff-Goldhaber (1955) and Wilets (1956) have explained the regularities in terms of vibrational excitations of the nuclear core.

The success of both the IPM and the Unified Model in explaining the same phenomena suggests a fundamental similarity between the two models and it is now believed that the same results can be obtained by treating the nucleons as individual particles moving in an average field, with their specific interactions as a correction or considering the collective motions of a nucleus, deformed by particle interactions, with the coupling between collective motions and independent particle motions as a correction.

In spite of the success of the IPM in explaining observed nuclear data doubts have often been expressed about its theoretical basis because it is difficult to see how a strong, short range, two-body force can supply

a smooth average potential leading to undisturbed independent motion of each nucleon within the nucleus. An early suggestion by Weisskopf that the Pauli exclusion principle might preclude the nucleon-nucleon interactions which would be expected to disturb such motion gave a qualitative explanation of this effect but only recently has the work of Brueckner and others shown how these ideas can be quantitatively introduced. These major advances in the treatment of the many-body problem (reviewed by Weisskopf, 1958) have greatly strengthened the theoretical basis of the independent particle model.

The variety of models still required to explain the current knowledge of the nucleus affirms the need for further experimental results to clarify the proper region of application of each model. The experiments described in this thesis provide information concerning the ground and excited states of nuclei and the interpretation of these results in terms of the IPM further confirms its validity in explaining certain nuclear properties.

Much of the experimental work concerns the emission or absorption of electromagnetic radiation by nuclei and it is therefore necessary briefly to review the theory of this process in the next section.

Section 1.3 Interaction of Electromagnetic Radiation with Nuclei

Transitions between different energy levels of the

same nucleus may take place by emission or absorption of γ-rays and thus some of the dynamic properties of nuclei are disclosed by a study of the interaction of electromagnetic radiation with nuclei.

The nucleus is a quantum-mechanical system and a full treatment of this problem would involve quantum field theory. However, a semi classical treatment, developed by Weisskopf (1952) and others, successfully explains many of the experimental results.

For radiation, the wavelength of which is long compared to the nuclear radius, the electromagnetic field may be expanded in terms of vector spherical harmonics and then the periodically varying field corresponding to an outgoing wave from the nucleus at the origin can be expressed as a sum of electric and magnetic multipole fields each of which carries a particular angular momentum and parity.

The source of the field is the nucleus and Weisskopf shows that each of the multipole fields is related to a "multipole moment" of the nucleus. Classically the multipole moments are proportional to integrals over the nuclear volume of certain functions of the charge and current density. The rate of emission of energy in each of the multipole fields may then be calculated from the nuclear properties. Up to this point the treatment is purely classical; the system must now be quantized.

Firstly the radiation field is quantized by replacing the rate of emission of energy by the rate of creation of

quanta times the energy, $\hbar\omega$, of each quantum. Then by dividing by the latter, the transition probability, i.e. the rate of emission of quanta, is obtained. Secondly the nucleus must be considered as a number of particles and the integrals of functions of continuously varying charge and current distributions are replaced by the matrix elements of the corresponding operators between initial and final nuclear states. Additional terms must be included to take account of the intrinsic magnetic moments of the neutron and proton.

Conservation of angular momentum and parity impose selection rules, and nuclear states a and b of spin and parity J_a, π_a and J_b, π_b can only be connected by γ-rays of multipolarity ℓ which satisfies $|J_a - J_b| \leq \ell \leq J_a + J_b$. The electric or magnetic nature is decided by the parities. If $\pi_a\pi_b = (-1)^\ell$ we have an electric transition: $\pi_a\pi_b = (-1)^{\ell+1}$ gives a magnetic multipole.

For systems with spherical symmetry the dependence of the transition probabilities on the z components of angular momenta only introduces statistical factors. These are explained by Weisskopf (1952).

The total electric and magnetic multipole transition probabilities are found to decrease rapidly with increasing ℓ so that only the lowest or perhaps lowest two values of ℓ permitted by the selection rule will contribute significantly in any experimental situation. For simple assumptions

about the nucleus the magnetic multipole transition, Mℓ, is calculated to be about 10 times weaker than the corresponding electric multipole, Eℓ. Thus appreciably more mixing is likely when the selection rules permit Mℓ and E(ℓ + 1) transitions than in the converse situation.

In view of the success of the single particle shell model in describing some properties of low lying nuclear states it appeared worthwhile to calculate the transition probabilities for a single particle transition. Making the simplest possible assumption about the nuclear wave function, i.e. that the radial wave function is a constant inside the nucleus and drops to zero at the nuclear limit, Weisskopf (1952) estimated the electric transition probability. The magnetic one is determined from general arguments showing that the magnetic multipole matrix element should be a factor of $\frac{\hbar}{McR}$ smaller than the corresponding electric multipole moment but that the intrinsic magnetic moment contributes 2 or 3 times as much. Thus the magnetic transition probability, proportional to the square of the matrix element is approximately $10\left(\frac{\hbar}{McR}\right)^2$ smaller than the equivalent electric transition probability. These assumptions permit the expression of the transition probabilities in terms of the nuclear radius, the energy of the transition and the multipolarity.

Better approximations to the single particle wave functions are expected to reduce these values, owing to the

smaller overlap of the initial and final state radial wave functions so a lower limit can be placed on the lifetime of the excited states in the single particle approximation.

Other nuclear models will, however, give quite different results. The collective model for instance predicts very fast E2 transitions connecting rotational states (Bohr, 1953). The experimental results in the region $90 \leq N \leq 112$ show transition probabilities about 100 times greater than the single particle estimate. The large static electric quadrupole moments which occur in the same region of the periodic table confirm the existence of strongly deformed nuclei which are expected to show these rotational spectra with the enhanced transition probabilities associated with collective nuclear motions.

The probability associated with a γ-ray transition thus depends on the spins and parities of initial and final nuclear states and also on the details of the nuclear wave function. Thus if the lifetime of an excited state and the multipolarity of the transition are known the validity of alternative descriptions of the nucleus may be tested, or in regions where a particular model is known to be applicable the multipolarity may be deduced from the measured transition probability and information may be inferred about the ground and excited states of the nuclei.

These theoretical ideas about emission and absorption transition probabilities will be seen to play an important

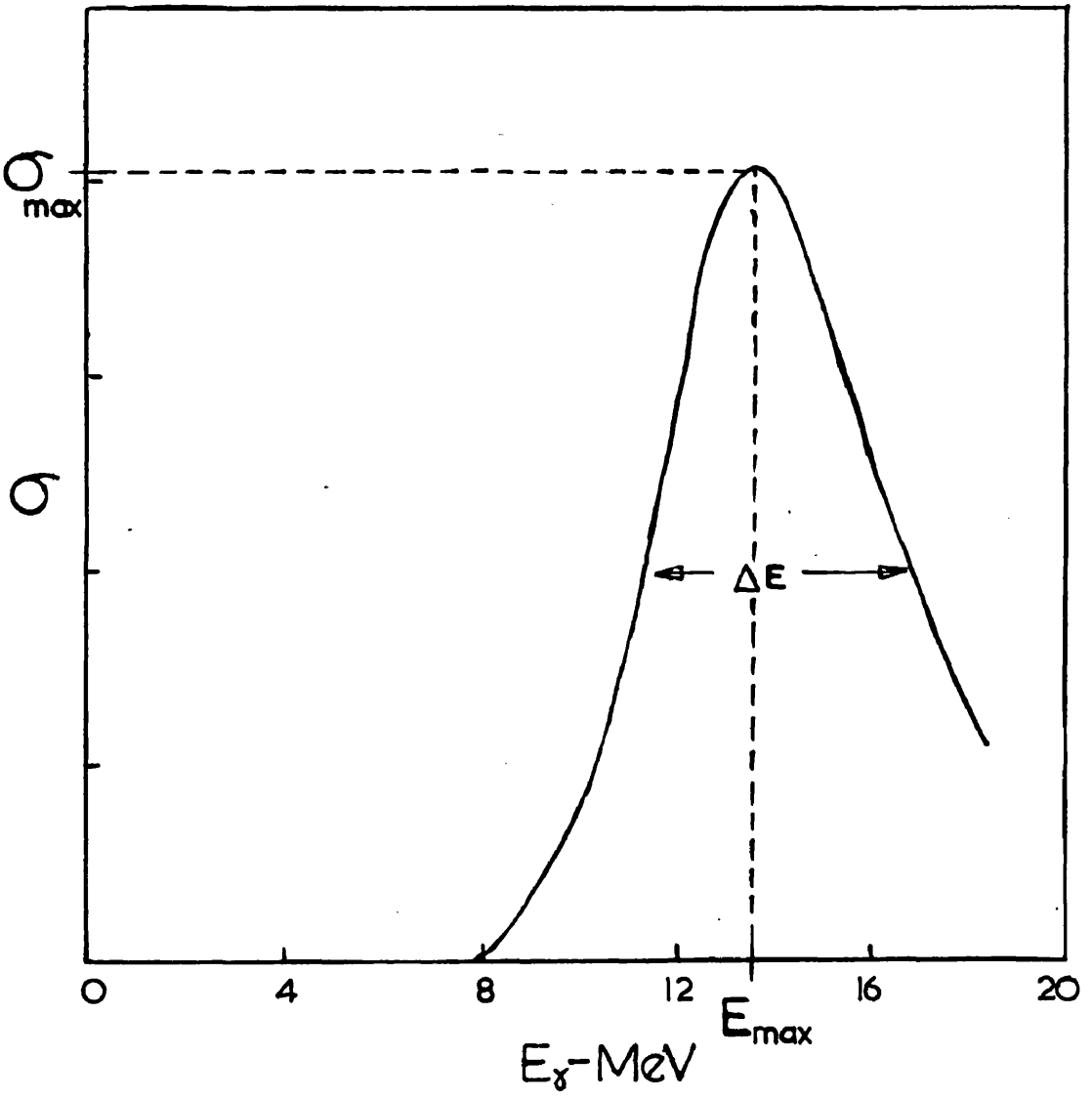

Fig. 1.2

The cross section for the (γ,n) reaction in Pb
(Montalbetti, 1953)

role in the analysis of the formation and decay of the isomeric states in Pb^{207} and Mo^{91} and in the analysis of the complex decay scheme of I^{128}.

1.4 Experimental Investigations

Many fields of experimental work have contributed the results on which the above theories are based and to which they can be applied. Three particular types of investigation which are relevant to the experiments described in this thesis are briefly reviewed below.

(i) Photodisintegration

Studies of the interaction of electromagnetic radiation with nuclei include not only the emission, but also the absorption of γ-rays. If sufficient energy is imparted to the nucleus by an incoming photon a nucleon or light nucleus (deuteron, α-particle) may be emitted. Extensive experiments on this phenomenon of photodisintegration have revealed certain features common to elements throughout the periodic table.

If the cross section for a particular reaction such as the absorption of a γ-ray by a Pb^{208} nucleus followed by the emission of a neutron $\left(Pb^{208}(\gamma,n)Pb^{207}\right)$ is studied as a function of the γ-ray energy it is found to vary as shown in fig. 1.2. Similar curves have been observed for a large number of photonuclear reactions and the general characteristics of a broad peak occurring at an energy a

few MeV above the threshold for the reaction (the binding energy of the emitted particle) appear to be common to all such reactions.

The variation throughout the periodic table of the following parameters connected with these peaks has been observed and theoretical attempts have been made to explain them:

(i) $E_{max.}$ the γ-ray energy for which the maximum cross section occurs.

(ii) $\sigma_{int.}$ the integrated cross section (the upper limit of integration for many of the experimental results is often imposed by the energy of the available bremsstrahlung at 23 or 30 MeV. For comparison with theory the limit is seldom taken above about 100 MeV because of effects connected with meson production which become important above this energy).

(iii) ΔE the full width at half maximum of the resonance.

The peak in a particular reaction cross section, such as $\sigma(\gamma,n)$, might arise from the combination of two independent effects. The rise might be due to the energy dependence of the γ-ray absorption probability and the fall be caused by the increasing competition from other possible modes of decay of the intermediate nucleus such as the emission of two neutrons. Alternatively the peak might show the presence of a resonance effect in the γ-ray absorption process. The former explanation was proven wrong, at least

for the photodisintegration of Cu^{63}, by experiments which showed the (γ,2n) yield to be small compared to the (γ,n) yield from this isotope even for peak bremsstrahlung energies well above the (γ,2n) threshold (Perlman, 1948). The latter explanation emphasized the importance of the variation of the γ-ray absorption cross section as a function of γ-ray energy. A sufficiently excited nucleus may, however, emit one or more of a number of different particles and the theoretically important absorption cross section is a sum of all possible A(γ,x) cross sections where A stands for the initial nucleus and x represents the emitted particle or γ-ray since we must also consider the possibility of re-emission of a γ-ray. Most of the experimental results were obtained for (γ,n) reactions: in only a few isolated cases were several cross sections measured for the same initial isotope and estimates thus made of total γ-ray absorption cross sections. As Z increases, however, this limitation becomes less serious because the emission of one or two neutrons rapidly becomes predominant over other modes of de-excitation owing to the increasing potential barrier which charged particles have to penetrate when leaving the nucleus. Thus for heavy elements a measure of the neutron emission or the residual radioactivities produced by (γ,n) and (γ,2n) reactions can give a close approximation to the total γ-ray absorption cross section. Attempts were therefore made to formulate

theories which would predict both the resonance energy, $E_{max.}$, and the total absorption strength, $\sigma_{int.}$, of the broad peaks, known as "giant resonances".

An early theory of these resonances (Goldhaber, 1948), proposed oscillations of all the protons of the nucleus relative to all the neutrons. The incoming photon could thus excite electric dipole vibrations in the nucleus. Three different modes of oscillation were suggested: the first involved harmonic vibrations of each proton about its equilibrium position and predicted a constant resonance energy, independent of A. The second, in which the nuclear surface remained fixed and neutron and proton density variations were excited within the nuclear volume, predicted $E_{max.} \propto A^{-1/3}$. Finally, a model, in which the neutrons and protons were considered as two intermingled and incompressible fluids which could be displaced with respect to one another, was used to perform more detailed calculations. The resulting variation of the resonant energy with mass number, $E_{max.} \propto A^{-1/6}$, agreed with the current experimental results. The formula for $E_{max.}$ contained two parameters one depending on the slope of the nuclear potential at the nuclear boundary and the other on the energy of interaction of a neutron and proton. With reasonable values for these parameters the formula gave values for $E_{max.}$ for carbon and copper in good agreement with the observed maxima of the (γ,n) cross sections.

Calculations based on the second model, which considered neutron-proton oscillations within a fixed nuclear surface, were extended by other authors (Steinwedel, 1950 and Danos, 1952). They again found the resonant energy to be inversely proportional to the nuclear radius, R, but also obtained the constant of proportionality $E_{max.} = 60A^{-1/3}$ MeV using $r_o = 1.42$ and $R = r_o A^{-1/3}\ 10^{-13}$ cm. This value is rather low when compared with experimental results but $r_o = 1.2$ is probably a better value and this would improve the value for E_{max}.

Neither model makes quantitative predictions about the width of the giant resonance although Goldhaber and Teller suggest that coupling between the proton-neutron oscillation and other possible motions of the nucleons broadens the resonance.

Any satisfactory theory must also predict a value of $\sigma_{int.}$ in agreement with experiment. The above theories and the experimental results which they set out to explain showed the importance of dipole absorption in the nuclear photoeffect. The Thomas-Reiche-Kuhn sum rule for the absorption of dipole radiation by the electrons in an atom was extended to apply it to the nucleus (Levinger, 1950). It was shown that considering the motions of nucleons with respect to the nuclear center of mass the protons had an effective charge $e\frac{N}{A}$ and the neutrons also contributed with an effective charge $-e\frac{Z}{A}$. Summing contributions from all possible dipole transitions of all the nucleons gave the

result $\sigma_{int.} = 0.015A$ MeV barns in the approximation $N = Z = \frac{A}{2}$. This result requires further correction, however, to take account of the exchange nature of the nuclear force and should be modified to $\sigma_{int.} = 0.015A(1 + 0.8x)$ MeV-barns where x is the fraction of the nuclear force which has exchange character, a result which is consistent with the experimental data.

As both the above mentioned collective models of photo-disintegration involve all the nucleons they can be expected to give the full absorption strengths predicted by this sum rule.

In the second part of a photonuclear reaction the excited nucleus emits one or more nucleons. Both the above models predicted a sharing of the γ-ray energy by all the nucleons and, therefore, the subsequent emission of particles should be described by the statistical theory of the compound nucleus which had been successfully applied to other types of nuclear reactions. For heavier nuclei proton emission would be expected to be strongly inhibited relative to neutron emission. Measurements for elements near A = 100 with 17.6 MeV γ-rays (Hirzel, 1947) showed (γ,p) cross sections of a few per cent of the corresponding (γ,n) cross sections. The statistical theory predicted values of $\frac{\sigma(\gamma,p)}{\sigma(\gamma,n)}$ between 10^{-3} and 10^{-5} in this region so the experimental values were 20 to 1000 times higher than the theoretical ones. To account for these results it was suggested that most of the proton emission was due to the

absorption of the γ-ray energy by a single proton which was then directly emitted before sharing its energy with other nucleons (Courant, 1951). A combination of this direct nuclear photoeffect and the collective models could then account for both the (γ,n) and (γ,p) experimental results.

A theory has, however, been proposed which consistently explains the current knowledge of photodisintegration in terms of a single model of the photonuclear reaction. Furthermore it acknowledges the success of the independent particle model (IPM) in describing the initial state of the nucleus and assigns the γ-ray absorption to single particle transitions between shell model states (Wilkinson, 1954 and 1956a). A difficulty in this theory immediately arises because the agreement between the sum rules and the experimental cross sections implies that all the nucleons contribute to the absorption. But nucleons in the lower shells cannot make dipole transitions of energy appropriate to the giant resonance because the final states are already occupied. It therefore appears that the nucleons in the few closed sub shells nearest to the top of the potential with available final states cannot account for the total absorption strength. Wilkinson has shown, however, that single particle transitions which complete a sub shell are expected to be strongly favoured (Wilkinson, 1956b) and absorptions that disrupt closed shells should be similarly enhanced. The lower lying nucleons also contribute by

preventing downward transitions, induced emissions, which if allowed would detract from the absorption strength of a particular level. Thus the available single particle dipole transitions are shown to account for the observed giant resonance absorption (Wilkinson, 1956a).

The near equality of the energy of the various transitions, which gives the resonance nature, is also shown to be consistent with the IPM. The width of the resonance is attributed to three effects (i) a slight variation in the energies of the contributing transitions, (ii) a broadening of the shell model state by the interaction of the excited nucleon with the remainder of the nucleons and (iii) coupling between the nucleons outside closed shells and the core.

In a highly excited state the IPM gives a less valid approximation to the actual nuclear properties than in the ground state because the interactions with other nucleons, which in the ground state are prevented by the lack of unoccupied final states, are in the excited state allowed. If a nucleon is excited by γ-ray absorption there is a considerable probability of it scattering other nucleons and thus sharing its energy. The result is a compound nucleus. If the γ-ray energy is above the binding energy a particle may be emitted: either the excited nuclean may escape before interaction or the compound nucleus may emit another particle. The latter process is described by the

statistical theory of the decay of the compound nucleus worked out for nuclear reactions (Weisskopf, 1952). The former, named by Wilkinson the "resonance direct" effect, accounts for the observed (γ,p) cross sections for heavy nuclei being higher than those predicted by the statistical theory, and for the excess of high energy protons and neutrons. The relative contributions of the two effects can be described in terms of the energy of excitation, the size of the nucleus, the barrier (coulomb or centrifugal) which the proton or neutron must penetrate, and the strength of the interaction between the excited nucleon and the remainder of the nucleons. The last term is related to the imaginary part of the potential which gives the absorption in the optical model, and information about its strength can be obtained from other nuclear reactions.

All of these theories of photodisintegration are of a very approximate nature. Insufficient information is available about the nuclear wave functions to allow exact predictions: most of the experimental evidence deals with broad features of the giant resonance. Each theory contains sufficient adjustable parameters, such as the shape and depth of the potential well used to calculate the independent particle energy levels, to allow it to fit the experimental results.

The shell model interpretation appears preferable, however, because it is an extension of the theory which is

known to be very useful in describing low energy nuclear properties and also because it postulates only one absorption mechanism whereas the earlier theories require two quite separate mechanisms, one for the direct photo-effect and the other for the collective oscillations which lead to the giant resonance and compound nucleus formation.

The results of the experiments on $Pb^{208}(\gamma,n)Pb^{207}$, described in chapter II, appear to add evidence in favour of the Wilkinson theory.

(ii) Isomeric states

Photodisintegration experiments are concerned mainly with the absorption of electromagnetic radiation. Information concerning the emission of γ-rays can also contribute to our understanding of the nucleus.

The selection rule stated in section 1.3 implies that radiation connecting two nuclear states must be of multipole order at least equal to the difference between the initial and final angular momenta. As the transition probabilities decrease rapidly with increasing multipolarity, γ-ray emission lifetimes will depend strongly on the spin change involved.

In 1917 F. Soddy suggested that nuclei with the same Z and the same A might be able to decay in different manners, and proposed the name "isomers" for such nuclei. Not until 1938 (Feather, 1938) was it definitely proved that such a phenomenon could exist. Many examples have since been found and the term isomeric state is now often applied to any

nuclear excited state whose lifetime is experimentally measurable.

The long lived excited states were soon seen to form well defined groups in the periodic table just below some of the larger closed shells. The interpretation of this phenomenon in terms of the IPM is straightforward for these are just the regions where states of high angular momentum are being filled and where the model predicts adjacent states of widely different angular momenta. The known isomeric states have been classified according to their multipolarity (Goldhaber, 1951 and 1952). When the measured lifetimes were plotted against energy the different multipolarities were well separated. The M4 transitions in particular lay very close to a plot of the theoretical lifetimes predicted by Weisskopf. Values of K conversion coefficients and K to L conversion ratios assisted in the assignment of the multipolarities and all the known decay schemes listed by Goldhaber and Hill were in concord with the states expected from the strong spin-orbit coupling shell model.

There remained, however, problems in the interpretation of the transition probabilities. The formulae of Weisskopf were based on the simplest possible assumption of the radiation being entirely due to one proton moving in the field of the other nucleons. Thus specific properties of the nuclear wave functions were expected to produce wide divergences

between the predicted and measured lifetimes. Such were observed for the E3, E4 and M3 transitions. But the M4 transitions formed a remarkably homogeneous group including both odd-proton and odd-neutron transitions. According to Weisskopf's theory the latter should be much longer lived than the former.

Further experimental work was, therefore, of value to see if this agreement would be confirmed or denied by newly discovered isomers. This interest in M4 transitions provided part of the incentive to clarify the decay scheme of Mo^{91} which exhibits such a transition.

(iii) Studies of decay schemes

The collection of experimental information on isomeric states is a specialized branch of the general field of study of radioactive decay schemes.

Data on the energies, spins and parities of low lying nuclear levels can often be obtained from investigations of the β-transitions and the associated γ-rays in the decay of radioactive nuclei. The theory of β-decay shows that there are strong selection rules governing the transition probability and thus a knowledge of the half-life and energy of a β-transition may give evidence concerning the relative spins and parities of the states which it connects.

A full treatment of the theory of weak interactions involves field theory and is beyond the scope of this introduction. Only the simplest results which apply to

nuclear β-decay and can be justified approximately by simplifying assumptions will here be stated. The dependence of the interaction probability on energy and atomic number can be included in the so-called Fermi function $f(Z,E_0)$. These functions have been extensively tabulated for β^-, β^+ and K capture transitions (e.g. Siegbahn 1955). They express the dependence on the phase space available to the electron and neutrino and on the external coulomb field of the nucleus. The function f times the half-life t is called the comparative half-life and includes all the extranuclear effects but ignores all the effects of the nuclear initial and final states except their relative energy. Thus ignoring nuclear effects the product ft should be the same for transitions of different energy and different Z.

Two sets of selection rules are possible depending on the form of the interaction between the nucleon and the electron-neutrino field, and both are now believed to contribute. Both show that the strongest transitions will be those in which the β-particle and neutrino carry zero orbital angular momentum and the parity of the initial and final nuclear states is the same. All other transitions are predicted to be of much lower intensity. Fermi selection rules apply to cases in which the intrinsic spins of the neutrino and electron are anti-parallel and thus the net change in angular momentum is 0 for the allowed transitions

i.e. $\Delta I = 0$, $\pi_i = \pi_f$, where π_i and π_f are the parities of the initial and final nuclear states. The alternative Gamow-Teller selection rules apply to the interaction in which the spins are parallel. Then for an allowed transition, $\Delta I = 0, \pm 1$ (except that $I_i = I_f = 0$ is forbidden), and again $\pi_i = \pi_f$. The ft values give an indication of the allowed or forbidden nature of a transition and together with other considerations are a help in assigning the spins and parities of the nuclear states involved. For complex β-spectra where decay takes place to two or more states of the daughter nucleus the partial half-lives for each transition must be measured in order to calculate the ft value for each transition separately.

The decays to excited states are often followed by γ-rays and thus the detection of coincidences between the two types of radiation can help in measuring the branching ratio. The γ-ray energies themselves and the γ-ray branching ratios in cascades can also contribute information about the excited states.

Such information about nuclear level schemes is useful both in testing specific predictions of nuclear models and in contributing to the knowledge of empirical trends which suggest new models or the application of old ones in new regions of the periodic table. Thus even experiments which do not provide crucial tests of current theories can add to our understanding of the nucleus.

CHAPTER II THE PHOTOPRODUCTION OF Pb^{207*}

Section 2.1 The Nucleus $_{82}Pb^{207}$

The discussion of photodisintegration in section 1.4(i) demonstrated the possibility of explaining this phenomenon in terms of the nuclear shell model which was briefly reviewed in section 1.2. The nucleus Pb^{208} contains closed shells of both protons (Z = 82) and neutrons (N = 126) and therefore neighbouring nuclei in the periodic table are particularly well interpreted by the shell model. In this chapter an experiment on the (γ,n) reaction in lead is described in which the relative yields leading to two known states of Pb^{207} were measured. A similar experiment, using bromine, has been adequately explained by the statistical model of the complex nucleus (Katz, 1952). In contrast, the present results appear to require the resonance direct mechanism of the Wilkinson theory for their explanation. In this section the experiments which led to the discovery of the isomeric state in Pb^{207} and of its photoproduction are reviewed; in the following two sections the experimental methods and results are described; and in section 2.4 the agreement of the results with the current theories is discussed.

In the course of a search for short lived radioactive isotopes and isomers produced by the bremsstrahlung beam from the 23 MeV synchrotron Reid and McNeill (1953) bombarded

lead and discovered an activity of half-life 0.8 ± 0.1 seconds. They associated this with the isomeric state of Pb^{207} which had been studied by several other authors whose results are summarized below. Campbell and Gooderich (1950) irradiated lead with reactor neutrons and found two γ-rays of energies 0.5 and 1.0 MeV and a half-life of 0.9 seconds. G. Vendryés (1952) using neutrons from the $Be^{9}(d,n)B^{10}$ reaction to bombard lead, was able to confirm the energies of the γ-rays and improve the measurement of the half-life for which he obtained the value 0.82 ± 0.02 seconds. Vendryés attempted to identify the radioactivity and tentatively assigned it to an isomeric state in Pb^{207} for the following reasons. Neutrons slowed down in graphite produced much less activity, thus suggesting that neutron capture was not the reaction mainly responsible for its formation. The high coulomb barrier for lead makes reactions involving the emission of protons or α-particles unlikely and a fifteen minute irradiation showed no evidence for the production of the known Tl^{207}, Tl^{208}, or Hg^{205} activities. A (n,2n) reaction was impossible as the maximum neutron energy was less than 5 MeV and the smallest neutron binding energy involved was 6.9 MeV for Pb^{206}.

The conclusion was, therefore, that the activity was probably produced by a (n,n') reaction in one of the naturally occurring lead isotopes.

Pb^{208} was considered unlikely because, being a doubly

closed shell nucleus, it was not expected to have any low lying excited states and the 2.62 MeV state, known from Tl^{208} β-decay, was thought to be the lowest. Thus isomeric transitions involving γ-rays of 0.5 and 1.0 MeV could not be assigned to it. Similarly in Pb^{206} a level at 0.8 MeV found in α- and β-decay experiments was thought to be the lowest and the ratio of the K conversion coefficient to the L conversion coefficient for transitions from it to the ground state indicated E3 radiation and therefore a lifetime much shorter than 0.8 seconds. Also, other levels in Pb^{206} found by Harvey (1953) by the reaction $Pb^{207}(d,t)Pb^{206}$ did not explain the measured γ-ray energies. Finally Pb^{204} was ruled out as the two isomeric states which had already been found in this isotope did not agree in energy or lifetime with the activity under investigation. The activity was thus thought to be due to an isomeric state of Pb^{207} produced by (n,n') reactions and Vendryés discussed this assignment in the light of the work of Neumann and Perlman, Goldhaber and Sunyar, and Grace and Prescott presented below.

Neumann and Perlman (1951) measured the energy of conversion electrons emitted in the decay of Bi^{207} and also found three low energy groups of α-particles in the decay of Po^{211}. On the basis of these results they suggested a level scheme for Pb^{207} which was open to considerable doubt as, with no intensity or coincidence measurements it was impossible to know which transitions were in cascade. The

discovery of conversion electron groups corresponding to γ-rays of 0.565 and 1.063 MeV, however, increased the certainty of the above assignment of the isomeric state.

Goldhaber and Sunyar (1951) analysed a large number of known isomeric transitions and on the basis of Campbell and Goodrich's measurements of half-life and γ-ray energies they designated the isomeric transition M4. Using the shell model predictions they suggested the scheme $i_{13/2} \xrightarrow{1.06\ \text{MeV}\ \gamma\text{-ray}} f_{5/2} \xrightarrow{0.56\ \text{MeV}\ \gamma\text{-ray}} p_{1/2}$.

Grace and Prescott (1951) performed further experiments with Bi^{207} and showed by coincidence measurements that the 1.1 MeV and 0.56 MeV γ-rays were in cascade. Using their own results together with those of Neumann and Perlman they found a value of $K_{1.1}/K_{0.56}$ consistent with the M4, E2 assignment of Goldhaber and Sunyar for the isomeric state cascade.

Finally, Pryce (1952) investigated the predictions of the shell model for the ground and excited states of nuclei near the doubly closed shell nucleus $_{82}Pb^{208}$. On the basis of his calculations and the experimental evidence then available he deduced that the isomeric state was an $i_{13/2}$ level at 1.63 MeV which decayed to an $f_{5/2}$ level at 0.52 MeV which in turn decayed to the $p_{1/2}$ ground state. Thus the energies and multipolarities of the γ-rays associated with the isomeric state decay were known when the state was first produced by photon bombardment of lead (Reid, 1953).

Experiments to measure the relative photonuclear yields to ground and isomeric states had already been performed with other nuclei. In particular, Katz et al. (1952) investigated $Br^{81}(\gamma,n)Br^{80*}$, Goldemberg and Katz (1953) studied (γ,n) (γ,γ') and $(\gamma,2n)$ reactions in In^{115} leading to In^{114}, In^{114*}, In^{115*} and In^{113*} and Katz et al. (1953) measured (γ,n) yields to ground and isomeric states of Mo^{91} and Zr^{89}. In each of these cases the yields were determined by measuring the quantity of radioactivity produced, the isomeric and ground states having sufficiently different half-lives or decay schemes for them to be measured separately. The results were interpreted in terms of a compound nucleus model and the known or assumed spins and parities of the various states.

It was decided to investigate further the activity produced by Reid and McNeill to ascertain whether it was in fact the known isomeric state of Pb^{207} and to measure the relative numbers of (γ,n) events leading to the isomeric and ground states of the final nucleus.

This reaction was of particular interest because of the large spin change between the spin 0 ground state of Pb^{208} and the spin $\frac{13}{2}$ isomeric state of Pb^{207}. All the above mentioned similar experiments had concerned isomeric states in the group occurring just below the closing of the $g_{9/2}$ shells at nucleon number 50 and the spin changes involved in the photodisintegrations were much smaller.

The difficulty of the lead experiment was increased because the ground state of Pb^{207} is not radioactive and therefore the relative yields had to be measured by an indirect method:

(i) the relative yields of neutrons from the (γ,n) reactions in natural lead and lead enriched in Pb^{208} were measured,

(ii) the ratio of the yields for photoproduction of Pb^{207*} and Cu^{62} were measured,

(iii) the yields of Cu^{62} from $Cu^{63}(\gamma,n)$ and of neutrons from $Pb(\gamma,n)$ were taken from the papers of Katz and Cameron (1951) and Montalbetti et al. (1953) respectively.
The product of the three ratios gave the desired ratio of the yields of Pb^{207*} to the yield of Pb^{207} from (γ,n) reactions in Pb^{208}.

In the following sections the various parts of the work on lead are described. In section 2.2(i) experimental proof is presented that the radioactive decay produced by X-ray bombardment of lead is indeed due to the isomeric state of Pb^{207} produced by the reaction $Pb^{208}(\gamma,n)Pb^{207*}$. Section 2.2(ii) contains an account of the measurement of the relative photonuclear yields of the competing processes $Pb^{208}(\gamma,n)Pb^{207}$ and $Pb^{208}(\gamma,n)Pb^{207*}$, while section 2.3 is concerned with work on the possibility that the transition to the isomeric state is through an intermediate level of Pb^{207}. Finally in section 2.4 the results of all these

experiments are discussed in terms of the Wilkinson theory of photodisintegration.

Section 2.2 The Photoproduction Experiments

(i) Identification of the photoproduced radioactivity

As outlined in the previous section the first experiments by Reid and McNeill (1953) measured the half-life of the γ-ray activity produced in lead by bombardment with the bremsstrahlung beam from the 23 MeV synchrotron, as 0.8 ± 0.1 seconds which suggested that the isomeric state, Pb^{207*}, was being produced. The particular interest of this reaction prompted further investigation.

The same authors showed (Reid, 1954a), by comparison of the yields from natural lead and a Pb^{208} enriched sample, lent by Professor F. Soddy (Soddy, 1916), that the activity was almost certainly produced by $Pb^{208}(\gamma,n)Pb^{207*}$ and not $Pb^{207}(\gamma,\gamma')Pb^{207*}$ or $Pb^{206}(n,\gamma)Pb^{207*}$.

To confirm that the observed γ-rays were in fact from the decay of the known isomeric state in Pb^{207} it was necessary to measure their energies. A lead target was irradiated for short periods in the bremsstrahlung beam and immediately after the synchrotron was switched off the γ-rays from the decay of the induced activity were detected in a NaI(Tl) scintillation spectrometer placed below the target. Several extraneous longer lived radioactivities were produced in the crystal, crystal mounting and shielding

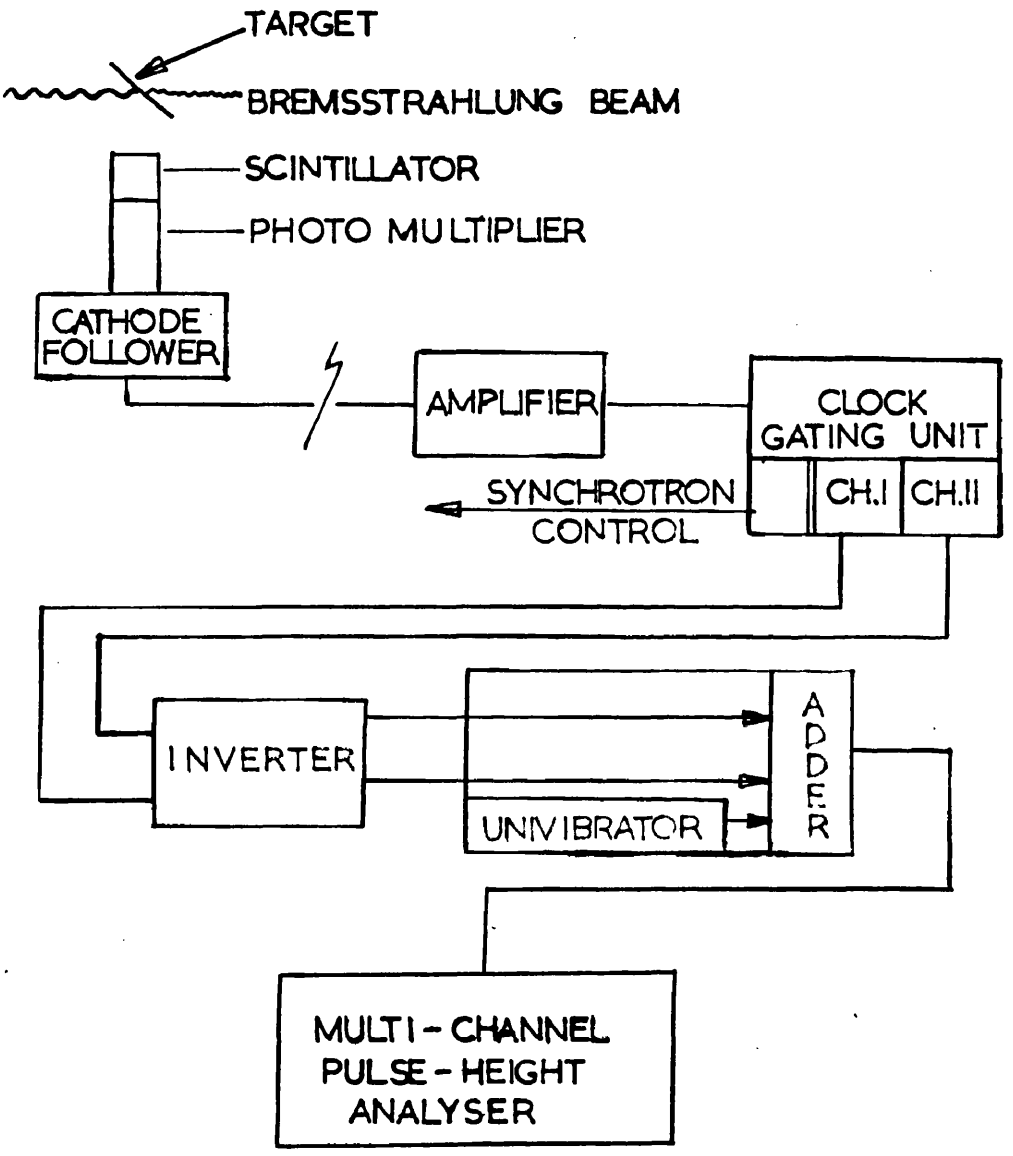

Fig. 2.1

Block diagram of the equipment for examining the spectrum of γ-rays from Pb^{207*} produced by bombarding lead with 22 MeV bremsstrahlung.

material, by the photoneutrons from material in the bremsstrahlung beam. In order to be able to obtain a reasonable number of counts from the Pb activity it was necessary to repeat many periods of alternate irradiation and counting and therefore the long lived background had to be eliminated. To accomplish this the following cycle was used: (i) the lead target was irradiated in the bremsstrahlung beam for 2.4 seconds, (ii) the synchrotron was switched off and the amplified pulses from the scintillation spectrometer were pulse-height analysed and recorded, (iii) the spectrum for a second counting period of 2.4 seconds was analysed and separately recorded. The cycle was repeated many times and two pulse height spectra were obtained. The second spectrum was subtracted from the first thus eliminating the effects of any activities of half-life long compared to 2.4 seconds, the contributions of which would be virtually the same to each spectrum.

As only one 100-channel differential pulse-height analyser was available it was necessary to use it for the analysis and recording of both spectra. The channels 0 to 45 were used to record the pulses occurring in the first 2.4 seconds after each irradiation and channels 50 to 99 for the pulses from the second counting period.

A block diagram of the equipment built to achieve this is given in fig. 2.1. The amplified pulses from the scintillation counter were fed to the inputs of two

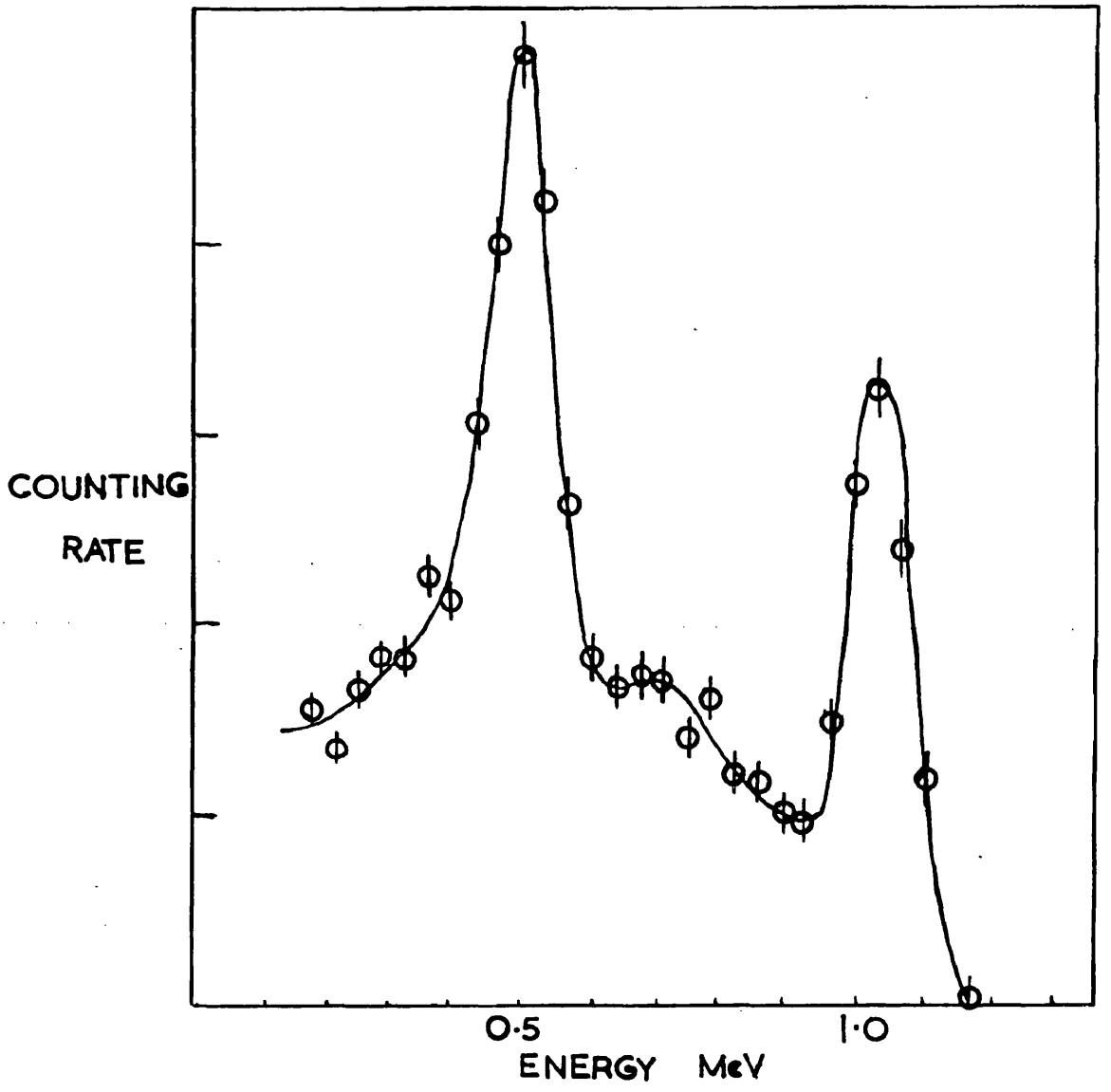

Fig. 2.2

The γ-ray spectrum of the 0.8 sec. radioactive decay produced in lead by 22 MeV bremsstrahlung.

proportional gate circuits which were opened in sequence by pulses from the decatron clock (Reid, 1954b). The negative outputs from these two circuits were fed through an inverter to the inputs of the univibrator mixer circuit. Pulses from one input were passed unchanged through the adding circuit and thence to the input of the pulse-height analyser. Pulses arriving at the other input triggered the univibrator, the pulse from which was added to the input pulse in the adding circuit. Thus the pulses from channel 1 were recorded in the first 45 channels and the spectrum in channel 2 was displayed on the pulse-height analyser with the zero of its energy scale in channel 46. The amplitude of the univibrator pulse and of both inputs was adjustable so that the gain in each channel and the position of the upper spectrum could be adjusted to allow a direct subtraction of the numbers in corresponding channels in the two spectra.

Test runs with radioactive sources and the gate in operation gave identical spectra thus demonstrating both the equality of the lengths of the two gate pulses and the proper operation of the univibrator mixer unit.

A lead target was irradiated in the bremsstrahlung beam and spectra obtained as described. Fig. 2.2 is a plot of the difference of the two spectra. Calibration spectra with radioactive sources replacing the target gave both the energy scale and the spectrum shape for γ-ray energies of 1.33, 1.17, 0.66 and 0.51 MeV. In fig. 2.2 there are seen

to be prominent peaks at 0.50 and 1.01 MeV indicating γ-ray energies in good agreement with the previous measurements of γ-rays from the decay of the known isomeric state of Pb^{207}.

The shapes of the experimental spectra provided the information necessary to separate the observed Pb^{207*} spectrum into contributions from the two γ-rays. The dependence of the total detection probability for γ-rays passing through the crystal on the γ-ray energy was calculated from tabulated values of absorption coefficients (Siegbahn, 1955). The intensity ratio for the two γ-rays at the crystal was then calculated and corrected for the absorption and scattering of γ-rays in the target to obtain the ratio of the intensities emitted by the Pb^{207*}. The final result was intensity 1.01 MeV/intensity 0.56 MeV = 1.2 ± 0.35 which is consistent with the assumption that the two γ-rays are in cascade, for in that case their intensities would be equal.

The half-life measurement and the γ-ray energy and intensity measurements were together considered adequate confirmation that the observed activity was identical with the isomeric state of Pb^{207} found in the other experiments discussed in section 2.1.

(ii) The measurement of the yield ratio

The reasons for wishing to measure the yield Pb^{207*}/yield Pb^{207} ratio from the $Pb^{208}(\gamma,n)$ reaction have been outlined

in section 2.1 and the indirect method by which it was achieved was described. The first step was to measure the relative yields of neutrons from the X-ray bombardment of Pb^{208} and natural lead.

The sample of lead, enriched in Pb^{208}, which was used in the earlier experiments (Reid, 1954a) discussed in section 2.2(i), was again borrowed from Professor Soddy. A target of natural lead was made of the same dimensions as the enriched sample. These two targets were irradiated alternately in the bremsstrahlung beam from the synchrotron, operated at 22 MeV peak energy and the neutron yields were measured by a method developed by McNeill (1955).

A $1\frac{3}{4}$" diameter by 2" long thallium activated sodium iodide crystal was used as neutron detector. The crystal was placed below the target and fast neutrons from the (γ,n) reaction in the lead produced radioactive I^{128} in the crystal. After the synchrotron was switched off the strength of the I^{128} source could be measured using the crystal itself as detector and thus a relative measurement of the total neutron flux during the synchrotron irradiation could be obtained. The 25 minute half-life of I^{128} made long irradiations impracticable and the small size of the enriched sample (30 gms.) and the rather small available bremsstrahlung beam of about 0.3 r/min. at 1 metre made it necessary to eliminate as completely as possible the effect of backgrounds.

It was thus necessary to shield the crystal from other sources of fast neutrons such as the internal synchrotron target and the wall of the room where the beam struck it, to shield it from external radiation during the counting period and to choose a discrimination level which gave the best ratio of detection efficiency for the I^{128} decay to the background counting rate. The crystal and photomultiplier were surrounded by 3 inches of iron, a layer of cadmium to absorb thermal neutrons and 1½ feet of paraffin wax. A horizontal tapered slot of rectangular cross section pierced this composite box to allow a path for the bremsstrahlung beam; the crystal was just below the lower side of the slot. The lead target was suspended in the slot, above the NaI crystal and in the centre of the X-ray beam. Even with this shielding the extraneous neutrons, produced by an irradiation with no target in position, created an I^{128} activity about one half as strong as that obtained with the lead target in position. The length of each irradiation was limited to 30 min. because of the relatively short half-life (25 min.) of the I^{128} activity. As the absolute counting rates obtained were small it was necessary to add the results of several irradiations to obtain satisfactory counting statistics.

The integrated flux of the bremsstrahlung beam was measured by counting in a standard geometry the Cu^{62} activity produced in a thin sheet of copper through which

the beam passed before reaching the target. As Cu^{62} has a half-life of 10 min. two sheets were used in each 30 min. run, one for the first 15 min. and the other for the second half. The bremsstrahlung intensity was continuously monitored by an ionization chamber and d.c. amplifier the output of which was displayed on a meter and the intensity was kept constant to within $\pm 10\%$.

Five sets of irradiations were made each set consisting of a run with no target, one with the natural lead target and one with the enriched lead target. The results were combined and the ratio of the yields from the two targets was

$$\frac{\text{yield}_{\text{natural}}}{\text{yield}_{\text{enriched}}} = 0.92 \pm 0.17$$

The atomic weight of natural lead is 207.21 and its composition is 52.3% Pb^{208} and 47.7% Pb^{207}, Pb^{206} and Pb^{204}. The enriched sample has extra Pb^{208} and a knowledge of its atomic weight, 207.7, and the isotopic abundances in natural lead allow one to calculate that it is 82% Pb^{208} and 18% other isotopes.

With this information and the measured yield ratio above it is possible to calculate that the ratio of the (γ,n) yields from natural lead and Pb^{208} is 0.87 ± 0.18 for bremsstrahlung of 22 MeV peak energy.

The second step was to measure the ratio of the yield of Pb^{207*} to the yield of Cu^{62} for irradiation by the same

integrated bremsstrahlung flux. The yields were measured by the activation method. Natural copper contains both Cu^{63} and Cu^{65} and thus Cu^{64} is produced as well as Cu^{62}. The latter can, however, be measured in the presence of the former by counting for several periods during the first few half-lives of the Cu^{62} decay and eliminating the effect of the long lived Cu^{64}.

The same experimental arrangement was used as in the previously described experiments with lead. The copper target placed above the scintillation spectrometer was irradiated for 15 minutes, the synchrotron was switched off and the 0.5 MeV annihilation radiation from the positrons emitted by the copper target was counted for 5 minute periods. A thin aluminium absorber prevented positrons from entering the crystal. The target was removed for one five minute period so that the I^{128} activity produced in the crystal by neutrons during the synchrotron irradiation could be measured. The counting rates were corrected for the long lived Cu^{64} activity, for the I^{128} activity and for natural background, and thus the yield of Cu^{62} was obtained. The integrated bremsstrahlung flux was again measured by the activity produced in a thin standard sheet of copper through which the beam passed before reaching the target.

For the measurement of the Pb^{207*} a lead target replaced the copper one. Its thickness was such that the correction for the different absorptions of the decay γ-rays

in the lead and copper targets was as small as possible, though the targets could not be made very thin because of the small yield obtained in the lead experiments. The clock gating unit (Reid, 1954b) was used to provide cycles of 1.2 second irradiations followed by three, 1.2 second, counting periods during each of which the counts were fed to separate scalers. Runs were limited to 15 min. to preserve accuracy of the bremsstrahlung flux measurement using the copper activation monitors. Successive fifteen minute runs had to be separated by an hour to allow the background of I^{128} activity to decay. From the differences between the total counts during the first and second counting periods of each cycle and the second and third counting periods, the Pb^{207*} activity was calculated independently of any longer lived activities which might be present. As a check on the apparatus the half-life of the Pb^{207*} decay was calculated for each run and only those runs were accepted for which the value was within the errors expected from statistical fluctuations in the counts.

In counting both the lead and copper activities the discrimination level of the counter was set at 0.4 MeV. The counting geometry in the two experiments was identical. The relative total counting efficiencies for 0.5 and 1.0 MeV γ-rays for the crystal were calculated and checked experimentally for 1.28 and 0.5 MeV γ-rays using a Na^{22} source. The spectrum shapes were determined experimentally using

radioactive sources. Then the relative yields were corrected for counting efficiency, absorption in the target and all backgrounds; as only a yield ratio was required it was not necessary to know the absolute integrated bremsstrahlung flux and the copper activation monitors provided a relative value.

The corrected ratio for irradiation with bremsstrahlung of peak energy 22 MeV was found to be

$$\frac{\text{yield}_{Pb^{207}*}/\text{per atom } Pb^{208}}{\text{yield}_{Cu62}/\text{per atom } Cu^{63}} = 0.27 \pm 0.03.$$

The ratio $\frac{Y_{Cu62}}{Y_{Pb(\gamma,n)}}$ obtained from the published values (Katz, 1951 and Montalbetti, 1953) is $\frac{2.6}{28}$ for a peak bremsstrahlung energy of 22 MeV. This last, together with the two measured ratios gives a value for

$$\frac{Y_{Pb207*}}{Y_{Pb207}} = \frac{Y_{Pb207*}}{Y_{Cu62}} \times \frac{Y_{Cu62}}{Y_{Pb(\gamma,n)}} \times \frac{Y_{Pb(\gamma,n)}}{Y_{Pb^{208}(\gamma,n)}}$$

$$= 0.27 \times \frac{2.6}{28} \times 0.87 = 0.022$$

$Y_{Pb(\gamma,n)}$ is the yield of neutrons from 22 MeV bremsstrahlung irradiation of natural Pb. Y_{Pb208} is the yield of neutrons from similar irradiation of Pb^{208}: $Y_{Pb^{208}(\gamma,n)}$ is very nearly equal to Y_{Pb207} as 98% of (γ,n) transitions lead to Pb^{207} and only 2% to Pb^{207*}. The inclusion, however, of neutrons from $(\gamma,2n)$ in $Y_{Pb^{208}(\gamma,n)}$ will make the observed value too large and the true ratio

is likely to be slightly larger than the value given above.

Section 2.3 The Delayed Coincidence Measurements Using Bi^{207}

A measurement of the threshold of the reaction $Pb^{208}(\gamma,n)Pb^{207*}$, based on the assumption that the activation curve would be similar in shape to those of $Ag^{109}(\gamma,n)Ag^{108}$ and $Ag^{107}(\gamma,n)\ Ag^{106}$, gave a value of 9.1 ± 0.1 MeV (Reid, 1954a). In the same paper it was shown that this value, together with the known values of the energy differences between the Pb^{208} and Pb^{207} ground states and between the Pb^{207} ground and isomeric states, proved it unlikely that the reaction took place by direct emission of a neutron from an excited state of Pb^{208} to the isomeric state of Pb^{207}. For if the γ-ray absorption near threshold were E2 or M1 as might be expected, then the emission of an $\ell = 4$ or $\ell = 6$ neutron would be required and the emission of such neutrons at the energy available should be strongly inhibited by the centrifugal barrier. Reid and McNeill therefore proposed the existence of a state of spin $\frac{11}{2}$ and odd parity just above the isomeric state. Such a state could be fed by E2 γ-ray absorption in Pb^{208} followed by emission of an $\ell = 3$ neutron and this they concluded was the most likely production mode in view of their threshold measurements.

Such a state of odd parity and spin $\frac{11}{2}$ in Pb^{207} should be detectable in the decay of Bi^{207}. Electron capture transitions to it from the $h_{9/2}$ Bi^{207} ground state would be

"allowed" and therefore expected to compete strongly with the other transitions. It would be expected to decay primarily by E1 γ-rays to the isomeric $i_{13/2}$ state.

The existence of a low energy γ-ray transition of energy 0.137 or 0.064 MeV in the decay of Bi^{207} was suggested (Neumann, 1951) to explain an observed electron group but this was later shown to be more probably an Auger electron group (Wapstra, 1953). No other low energy γ-rays had been reported but the results of Prescott (1954) indicated that there might be a second state very close to the $i_{13/2}$ state. Using a coincidence circuit of 1.5 microseconds resolving time Prescott found 1.07 MeV γ-rays in prompt coincidence with the K X-rays following electron capture in Bi^{207}. If an $\frac{11}{2}-$ state were close enough to the $i_{13/2}$ state the M3 transition of energy 1.07 MeV to the $f_{5/2}$ state, with an expected half-life about 1 to 5 microseconds, might compete appreciably with the E1 transition to the isomeric state and the latter might have escaped detection owing to its low energy. This situation could explain both the results of Reid (1954a) and the prompt coincidences found by Prescott (1954).

The lifetime of such a γ-ray, of energy about 1 MeV and M3 nature should be measurable by modern delayed coincidence methods and it was therefore decided to investigate the K X-ray - 1 MeV γ-ray coincidences using a shorter resolving time than that employed by Prescott.

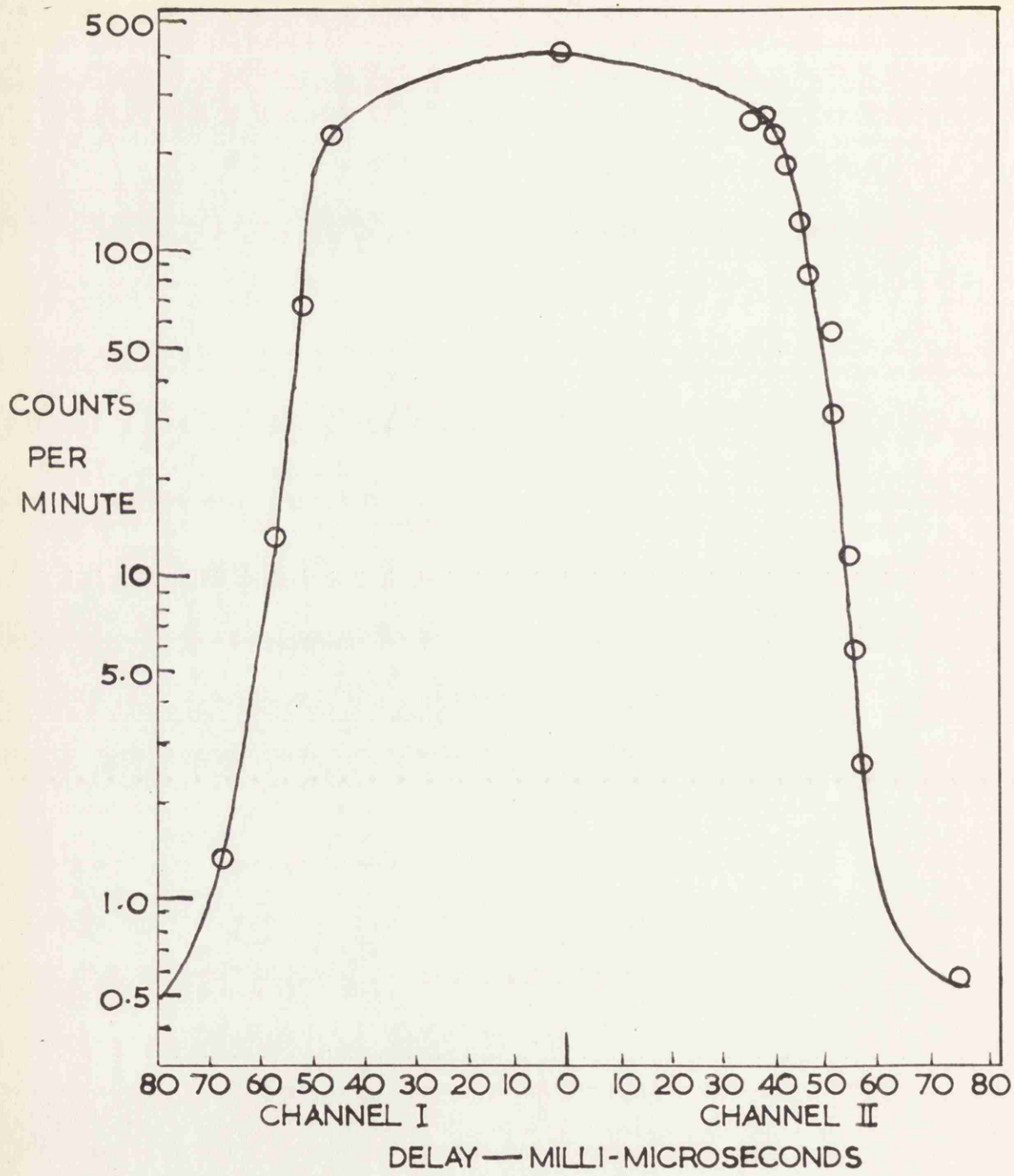

Fig. 2.3

Delayed coincidence counting rate between 1.06 MeV γ-rays and K X-rays, from a Bi^{207} source.

Channel I γ-rays - large crystal
Channel II X-rays - thin crystal

A Bell-Petch fast-slow coincidence circuit, kindly lent by Dr. G. M. Lewis, was used to examine coincidences between lead K X-rays and 1.06 MeV γ-rays emitted by a Bi^{207} source. Two NaI(Tl) scintillation counters were used as detectors. One crystal one inch square was only 1 mm. thick and had, therefore, a low detection efficiency for either 1.06 or 0.5 MeV γ-rays but an absorption probability of 70% for lead K X-rays of 75 keV. The other crystal, a 2" long by $1\frac{3}{4}$" diameter cylinder had a detection efficiency of 65% for 1.06 MeV γ-rays passing through it. The discriminator on the slow channel fed by the large crystal was set just above the total absorption peak in the spectrum of Cs^{137} γ-rays (0.66 MeV) so as to ensure rejection of all pulses from 0.5 MeV γ-rays but accept those from 1.06 MeV γ-rays. The other discriminator was set at the photopeak from RaD 45 keV γ-rays to give high efficiency for the lead K X-rays.

With the Bi^{207} source placed between the two counters the coincidence counting rate was measured for various additional delays between the counters. In fig. 2.3 the logarithm of the counting rate is plotted against delay in milli-microseconds. It can be seen that either the delay of the 1.06 MeV γ-ray after the K X-ray is $< 5 \times 10^{-8}$ sec. or that if there is any long-lived component it is of very low intensity.

The coincidence counting rate at large delays is $\backsimeq$ 0.5 counts/min. The random coincidence rate calculated from the

measured single channel counting rates and the measured resolving time is $\simeq$ 0.3 counts/min. Thus the counting rate from any long-lived component is $<<$ 0.1% of the prompt coincidence counting rate. It is therefore concluded that there are no M3 γ-rays of energy about 1 MeV of measurable intensity, following the decay of Bi^{207} unless the half-life of the transition is very much less than that predicted by Weisskopf's single particle formula and the existence of the state proposed by Reid and McNeill to explain their threshold measurements is unlikely.

(Shortly after this work was completed, the discrepancy noted by Reid and McNeill was resolved by the work of Bendel et al. (1955) who directly measured the effective threshold for the $Pb^{208}(\gamma,n)Pb^{207*}$ reaction and found it to be 10.2 MeV. Thus although the energy difference between the Pb^{208} ground state and (Pb^{207*} + n) is only 9.0 MeV the centrifugal barrier effectively prevents neutrons being emitted with less than 1 MeV energy. Once the energy is sufficient to overcome this barrier the cross section rises much more steeply with further increase of γ-ray energy than the cross sections for the (γ,n) reactions in the silver isotopes and this fact, unknown to Reid and McNeill, explains the error in their result. Later work by Lazar and Klema (1955) showed that all the K X-ray - 1.07 MeV prompt coincidences found by Prescott (1954) could be accounted for by coincidences between 1.07 MeV transitions and K X-rays from

internally converted 0.5 MeV transitions from the $f_{5/2}$ state to the Pb^{207} ground state.)

Section 2.4 Conclusions

The measured ratio of the relative yields of the isomeric and ground states of Pb^{207} may be compared with analagous results obtained for the isotopes Br^{80} (Katz, 1952), In^{114} (Goldemberg, 1953) and Zr^{89} (Katz, 1953). (The results in the last paper for Mo^{91} are in error owing to a mistake in the interpretation of the decay scheme of Mo^{91} and its isomeric state--see below, Chapter IV.)

In each of these three cases the ratio of the cross sections for production of the ground and isomeric states remains almost constant as the incident γ-ray energy increases through the giant resonance. As the variation with energy of the γ-ray absorption for higher multipolarities is expected to be quite different from that for the dipole resonance it appears that the measured ratio is that associated with production of both the states by dipole absorption.

Katz has shown that the assumption of dipole absorption of γ-rays and statistical emission of neutrons from the compound nucleus yields a plausible explanation of the measured ratio for Br^{80}.

A similar analysis of the lead experiment follows and will be seen to predict a ratio much smaller than the

observed one but if the reaction is described in terms of the Wilkinson theory of photodisintegration reasonable agreement with the observations is obtained. First let us consider dipole absorption of a γ-ray followed by statistical emission of neutrons from the excited Pb^{208} nuclei.

The spin and parity of the Pb^{208} ground state are 0+; therefore an intermediate state formed by dipole absorption will have spin and parity 1-. If this excited state emits a neutron Pb^{207} will be formed and subsequent γ-ray emission may leave it in either the $i_{13/2}$ isomeric state or the $p_{1/2}$ ground state. As there are known excited states of Pb^{207}, below 2.4 MeV, with spins $\frac{3}{2}$, $\frac{5}{2}$ and $\frac{7}{2}$ it is unlikely that any higher state will reach the $i_{13/2}$ state by γ-ray cascade unless its spin is at least $\frac{11}{2}$. To form such a state requires the emission of a neutron from a spin 1 state with orbital angular momentum $l \geq 4$. Such emission is highly inhibited, if the neutrons are emitted according to a statistical process, by the centrifugal barrier.

If the (γ,n) cross section curve for Pb^{208} is assumed to have the same form as that for natural Pb (Montalbetti, 1953) the relative numbers of reaction proceeding through a Pb^{208} excited state of energy between E_γ and $E_\gamma + dE_\gamma$ can be found by multiplying the ordinate of the cross section curve by the number of bremsstrahlung quanta in the energy range, as found from the tables published by Katz and Cameron (1951). The cross section as a function of E_γ and the

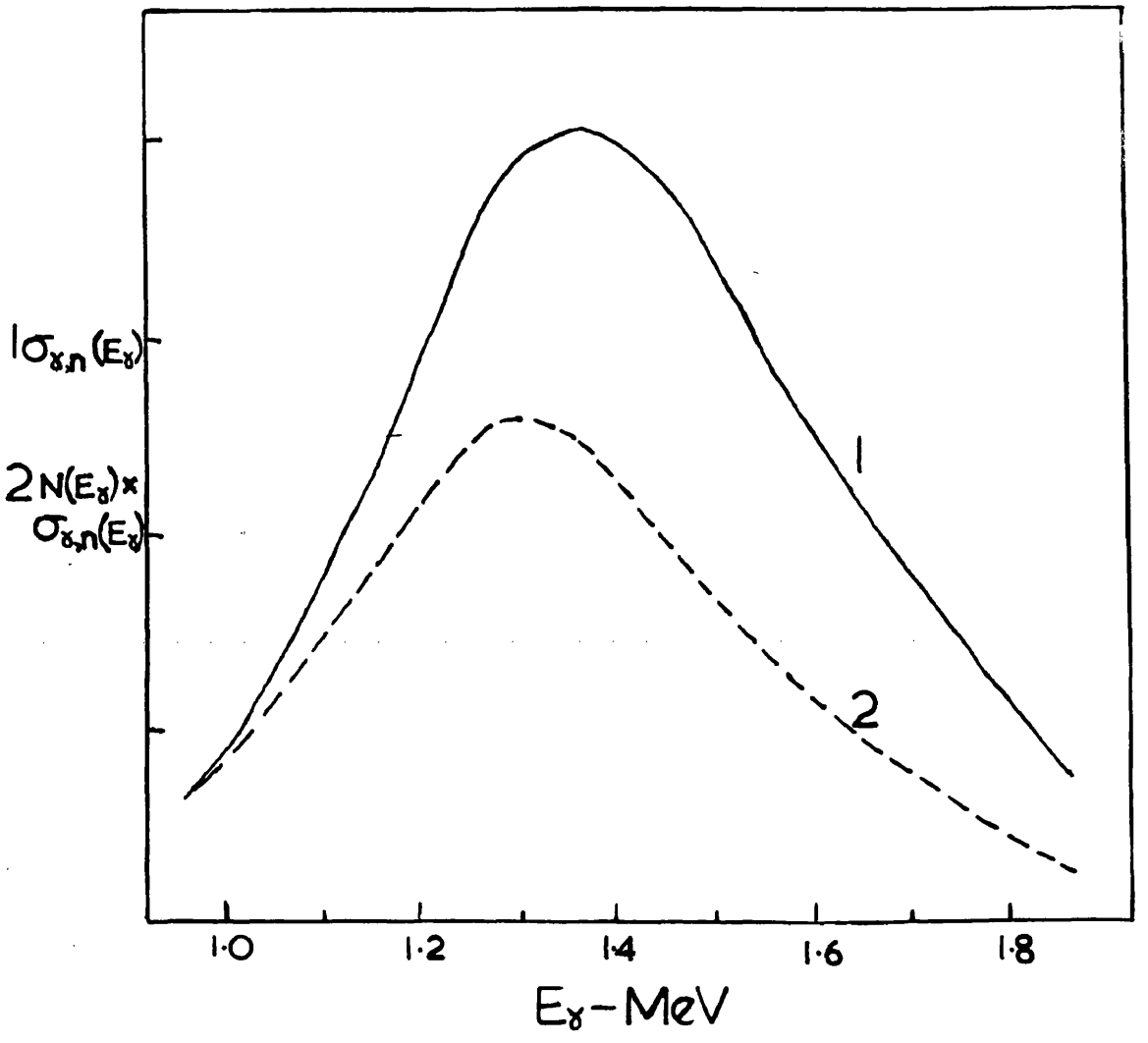

Fig. 2.4

Curve 1 - The (γ,n) cross section for Pb.

Curve 2 - The product of the (γ,n) cross section for lead and the bremsstrahlung spectrum.

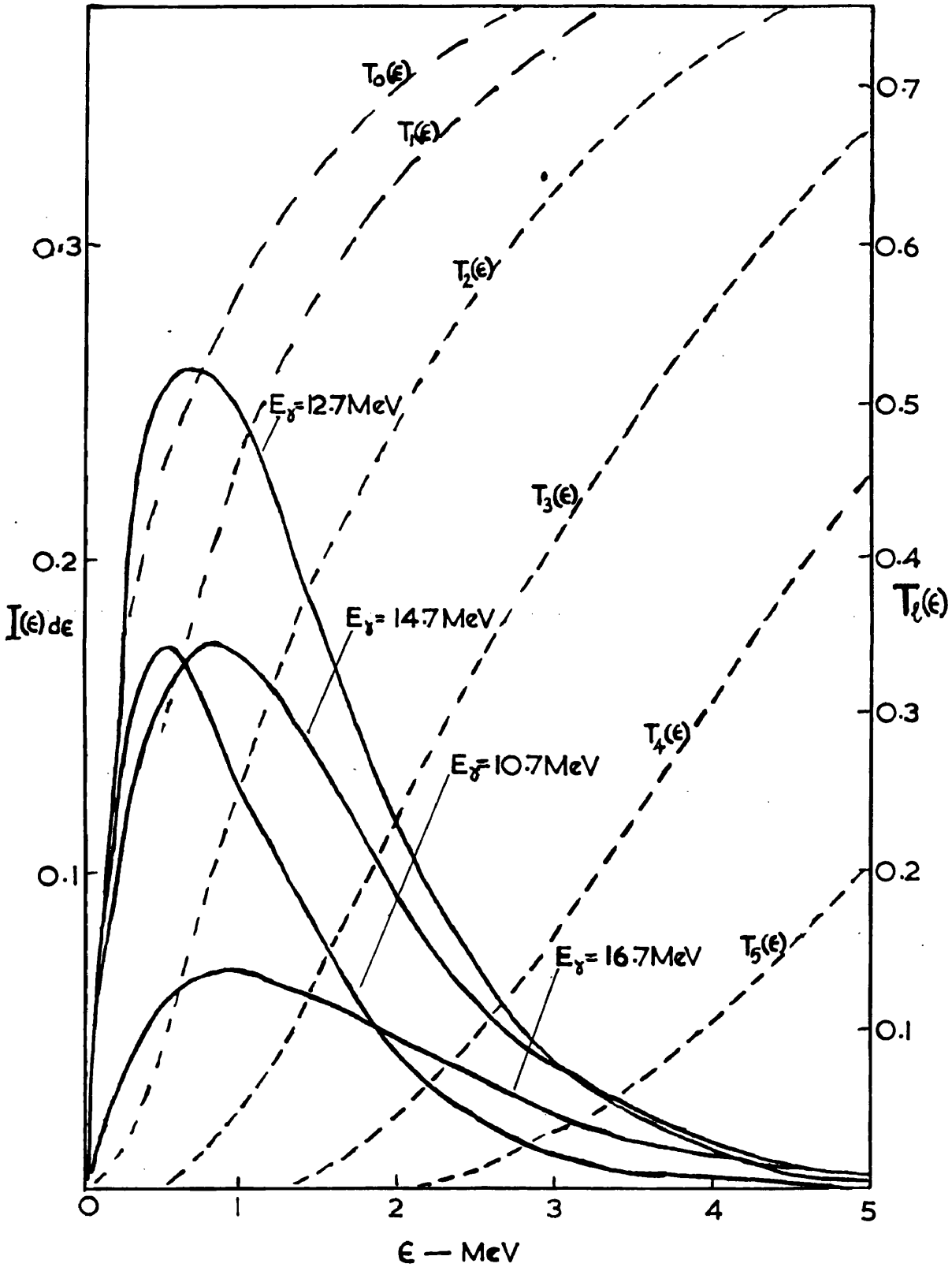

Fig. 2.5

Neutron energy distributions, predicted by the statistical theory, for the (γ,n) reaction in Pb^{208}, for various γ-ray energies (solid lines).

Transmission coefficients at the nuclear surface for neutrons (dotted lines).

product of the bremsstrahlung spectrum times the cross section are shown in fig. 2.4. For several excitations E_γ, the energy distribution of emitted neutrons was calculated using the statistical theory developed by Weisskopf (1952). The nuclear temperatures were calculated from the excitation energy, ϵ, available in the residual Pb^{207}. The curves plotted in fig. 2.5 (solid lines) are the predicted neutron energy distributions for excitations corresponding to absorption by Pb^{208} of γ-rays of energy 10.7, 12.7, 14.7 and 16.7 MeV respectively. The area under each curve is proportional to the corresponding ordinate in curve 2, fig. 2.4.

The emission of low energy neutrons with high angular momenta is inhibited by the centrifugal barrier. The probability of a neutron being emitted with given angular momentum, l, and energy, E, is given by the transmission coefficient $T_l(E)$. These functions have been plotted by Feld et al. (1951) and are shown in fig. 2.5 (dotted line). It can be seen that over 80% of the neutrons are expected to be emitted with energies below 2.5 MeV in a region where T_5 is negligible and T_4 is below 10%. From these curves it is estimated that very much less than 1% of the neutrons will be emitted with $l \geq 4$.

This theory is very approximate but it does seem to predict a considerably smaller ratio of the yields than that obtained experimentally.

Table II.1

Relative strengths of the single particle dipole transitions by which a γ-ray may be absorbed by Pb^{208}. The percentages shown were calculated using values of the enhancement factors and radial overlap integrals given by Wilkinson (1956a) and effective charges of $e\frac{N}{A}$ for protons and $-e\frac{Z}{A}$ for neutrons.

Neutron Transitions	
Transition	Percentage of total absorption
$1i_{13/2} - 1j_{15/2}$	16.0
$1i_{13/2} - 1j_{13/2}$	0.15
$1i_{13/2} - 2h_{11/2}$	0.80
$3p_{1/2} - 3d_{3/2}$	1.22
$3p_{1/2} - 4s_{1/2}$	0.37
$3p_{3/2} - 3d_{5/2}$	2.20
$3p_{3/2} - 3d_{3/2}$	0.25
$3p_{3/2} - 4s_{1/2}$	0.74
$2f_{5/2} - 2g_{7/2}$	4.66
$2f_{5/2} - 3d_{5/2}$	0.04
$2f_{5/2} - 3d_{3/2}$	0.62
$2f_{7/2} - 2g_{9/2}$	6.02
$2f_{7/2} - 2g_{7/2}$	0.17
$2f_{7/2} - 3d_{5/2}$	0.87
$1h_{9/2} - 1i_{11/2}$	11.2
$1h_{9/2} - 2g_{9/2}$	0.02
$1h_{9/2} - 2g_{7/2}$	0.59
$1h_{11/2} - 2g_{9/2}$	1.36
$1h_{11/2} - 1i_{11/2}$	0.33
Total =	47.61%

Proton Transitions	
Transition	Percentage of total absorption
$1h_{11/2} - 1i_{13/2}$	20.3
$1h_{11/2} - 1i_{11/2}$	0.26
$1h_{11/2} - 2g_{9/2}$	1.10
$3s_{1/2} - 3p_{3/2}$	1.68
$3s_{1/2} - 3p_{1/2}$	0.84
$2d_{3/2} - 2f_{5/2}$	4.46
$2d_{3/2} - 3p_{3/2}$	0.14
$2d_{3/2} - 3p_{1/2}$	0.68
$2d_{5/2} - 2f_{7/2}$	6.45
$2d_{5/2} - 2f_{5/2}$	0.32
$2d_{5/2} - 3p_{3/2}$	1.23
$1g_{7/2} - 1h_{9/2}$	13.2
$1g_{7/2} - 2f_{7/2}$	0.03
$1g_{7/2} - 2f_{5/2}$	0.74
$1g_{9/2} - 2f_{7/2}$	0.97
$1g_{9/2} - 1h_{9/2}$	0.31
Total =	52.71%

The theory of photodisintegration proposed by Wilkinson and discussed in the introduction provides an interpretation in terms of the resonance direct effect which comes closer to predicting the observed ratio. If the absorption of γ-rays by the Pb^{208} nucleus takes place by single particle transitions, and if some of the nucleons thus excited are emitted directly, certain of these events will leave the Pb^{207} nucleus in the isomeric state. An approximate calculation of the numbers of these events can be made.

Using the enhancement factors and radial overlap integrals given by Wilkinson (1956a) and the effective charges $e\frac{N}{A}$ for protons and $e\frac{Z}{A}$ for neutrons, contributions of the important neutron and proton transitions were calculated. Each of these transitions should contribute the percentage shown in table II.1 to the total dipole absorption assuming they are all of equal energy. If the energies of the individual transitions were known the percentages should be corrected for the increase in the transition probability proportional to $(E_\gamma)^3$ and for the reduction of the number of quanta in the bremsstrahlung spectrum with increasing energy, E_γ. From table II.1 it may be seen that there are three possible transitions for neutrons in the $i_{13/2}$ shell. Direct emission of one of these neutrons will leave the unperturbed core with one unpaired neutron in the $i_{13/2}$ state, the configuration corresponding to the isomeric state of Pb^{207}. The

probability for such emission is given by Wilkinson as

$$C = \frac{2kPh^2/MR}{2W}$$

k = wave number of excited nucleon

M = mass of nucleon

R = radius = $1.35 \times 10^{-13} A^{1/3}$ cm = 8×10^{-13} cm for Pb^{208}

W represents the complex part of the optical model potential of the nucleus and measures the interaction strength between the excited nucleon and the core. Wilkinson suggests a value, for lead, of 2W = 3 MeV.

P is the penetrability through the barrier which, for neutrons, is purely centrifugal and is therefore equal to $T_l(E)$ for a neutron of orbital angular momentum l and energy E (see fig. 2.5).

The energy of neutrons emitted from the $1j_{15/2}$ or $2h_{11/2}$ states leaving the Pb^{207} in the isomeric state will be given by

$$E = E_\gamma - 7.3 \text{ MeV} - 1.6 \text{ MeV}$$

where 7.3 MeV is the separation energy of a neutron from Pb^{208}, 1.6 MeV is the excitation of the isomeric state in Pb^{207} and E_γ the energy of the incident γ-ray.

For the $1j_{15/2}$ state, $P = T_7(E)$. If the $1i_{13/2} \rightarrow 1j_{15/2}$ transition, which gives the second strongest absorption, occurs at the centre of the giant resonance then E_γ = 13.7 MeV, E = 4.8 and the value of T_7 is sufficiently small to make the contribution of the resonance direct effect

negligible ($\lesssim 0.5\%$). The energy of the transition, however, may be somewhat higher. Wilkinson estimates that it occurs at 1.05 times the energy of the $h_{11/2} \rightarrow i_{13/2}$ proton transition, the strongest single transition. If we accept this ratio and set the latter at $E_\gamma = 13.7$, then E for the $j_{15/2}$ neutron becomes E = 5.5 MeV and the contribution of the resonance direct emission $\simeq 0.7\%$ of the total number of transitions. T_7E increases very rapidly with E in this region and thus for the transition to contribute the full measured value of 2.2% it would only be necessary to assign it to a γ-ray absorption energy of 15 MeV. Thus the contribution of the resonance direct emission, associated with this transition, to the formation of the isomeric state depends critically on the energy difference between the $i_{13/2}$ and $j_{15/2}$ states. Available nuclear data does not permit a decisively accurate calculation of this energy difference but a value which would allow the transition to contribute the whole observed yield of the isomeric state is not unreasonable.

The transition of an $i_{13/2}$ neutron to the $2h_{11/2}$ state might also make a significant contribution. Its strength as shown in table II.1 is only 0.81%. However, as it involves a change in principal quantum number, it is expected to occur at considerably higher energy than the transition to the $j_{15/2}$ state—in the analagous case for protons in lead Wilkinson places the $1h \rightarrow 2g$ transition at approximately

twice the energy of the $1h \rightarrow 1i$ transition. If the $i_{13/2} \rightarrow 2h_{11/2}$ energy difference is near the top of the observed giant resonance at say, 17.9 MeV then its strength would be expected to be enhanced by a factor $\left(\frac{17.9}{13.7}\right)^3$ over the strength for transitions at the giant resonance peak but reduced by a factor 0.62 for the reduced number of bremsstrahlung quanta giving a net enhancement of 1.4. As the penetrability of the centrifugal barrier is in this case $T_5(E)$, the total contribution to the isomeric state would be about 0.8%.

Thus with reasonable assumptions about the transitions the resonance direct emission of neutrons excited by dipole absorption from the $i_{13/2}$ level of Pb^{208} can account for the observed ratio of the production of the isomeric state of Pb^{207} to the production of the ground state whereas simple calculations with the statistical model predict a much smaller ratio. This experimental evidence thus strengthens the arguments in favour of Wilkinson's interpretation of the photodisintegration process.

CHAPTER III THE SEARCH FOR AN ISOMERIC STATE OF Mn^{54}

Section 3.1 The Nucleus Mn^{54} (Z = 25, N = 29)

The experiments discussed in the previous chapter were shown to throw light on the theoretical understanding of photonuclear reactions. In Chapter I it was also shown that the interpretation of long lived excited states of nuclei was one of the important applications of the shell model. A search was therefore made for other nuclei with isomeric states which had not been fully investigated and which might be produced by photonuclear reactions.

A report on a β-decay of half-life about 2 minutes was published by Caldwell and Stoddart (1951) and this activity was assigned by them to an isomeric state in Mn^{54} (Caldwell, 1951 and 1955). The activity was produced by bombarding iron with 10 MeV deuterons and 14 MeV neutrons. The assignment was based on the relative strengths of the sources produced in natural iron targets and Fe^{54} enriched targets and the assumption that the reactions taking place were (d,2p) and (n,p) respectively. Caldwell (1955) also reported that similar β-activities had been produced by 18 MeV protons in spectrographically pure targets of manganese and iron, presumably by the reactions $Mn^{55}(p,pn)$ and $Fe^{57}(p,\alpha)$ but that preliminary attempts to produce it by the reaction $Mn^{55}(\gamma,n)$, and by the reaction $Cr^{54}(p,n)$ using 10 MeV protons, were unsuccessful.

Considerable information about the ground state of Mn^{54}

and about the neighbouring isotopes Cr^{53} (29 neutrons) and Mn^{55} (25 protons) was available and predictions could be made on the basis of the shell model about other states of Mn^{54}.

The spin of Cr^{53} was measured by several methods (see Nuclear level schemes, 1955, for references) and found to be $\frac{3}{2}$ which suggests that the lowest state for the single neutron outside the closed shell at N = 28 is the $2p_{3/2}$ state and not the nearby $f_{5/2}$ state.

Mn^{55} is, however, one of the exceptions to the single particle shell model predictions of ground state spins and parities. Its 5 protons in the $f_{7/2}$ shell couple together to form a state of spin $\frac{5}{2}$ (Nuclear level schemes, 1955).

The ground state spin of Mn^{54} will thus probably depend on the particular configuration of five $f_{7/2}$ protons and one $p_{3/2}$ neutron which gives lowest energy and would be expected to have a spin between 2 and 5.

The electron capture decay of the Mn^{54} ground state to Cr^{54} was well known and the energy difference between the ground states of the three isobars Cr^{54}, Mn^{54}, and Fe^{54} had been established. The ground state spin and parity of Mn^{54} seemed almost certainly 3+ (Nuclear level schemes, 1955).

The existence of states of very high spin in this region of the periodic table was both predicted by Flowers (1952) and confirmed by experiment--e.g. the Sc^{44} isomeric state of spin 6 or 7, the V^{50} ground state of spin 6--and therefore

the existence of an isomeric state in Mn^{54} seemed quite reasonable. Such a state would be capable, at least from energetic considerations, of decaying by emission of negatrons, positrons or γ-rays. As the detection of γ-rays would permit the efficient use of a thicker source than could be used for detecting β^--particles and as γ-rays would be present in either of the last two types of decay, and possibly in the first one, it was decided to search for a γ-ray activity connected with this radioactivity.

If the reported activity was in fact the decay of an isomeric state of Mn^{54} it seemed reasonable that it could also be produced by $Mn^{55}(\gamma,n)$.

Section 3.2 The Experimental Search for the Reported Isomeric State

Solid samples of spectrographically pure manganese were irradiated in the 23 MeV peak energy bremsstrahlung beam from the synchrotron and quickly removed to a scintillation spectrometer consisting of a $1\frac{3}{4}$" diameter by 2" long NaI(Tl) crystal, a DuMont 6292 photomultiplier, and conventional electronics. It was found that a considerable Mn^{56} activity was produced in the sample by neutrons in the beam and this unwanted background was reduced by placing around the manganese target 4" of paraffin and a 0.01" thickness sheet of cadmium.

The pulse height spectrum from the scintillation

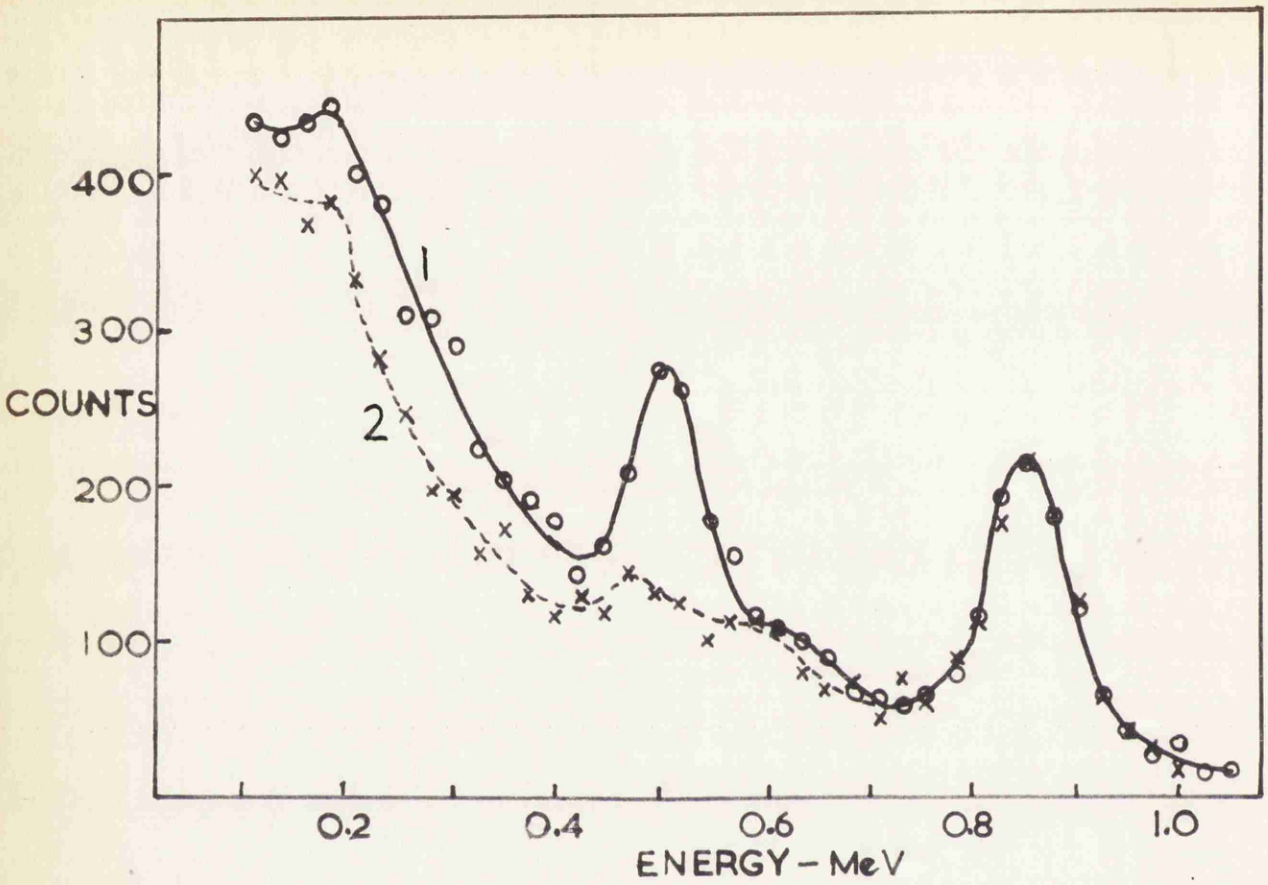

Fig. 3.1(a)

γ-ray spectra from manganese irradiated with 23 MeV bremsstrahlung.

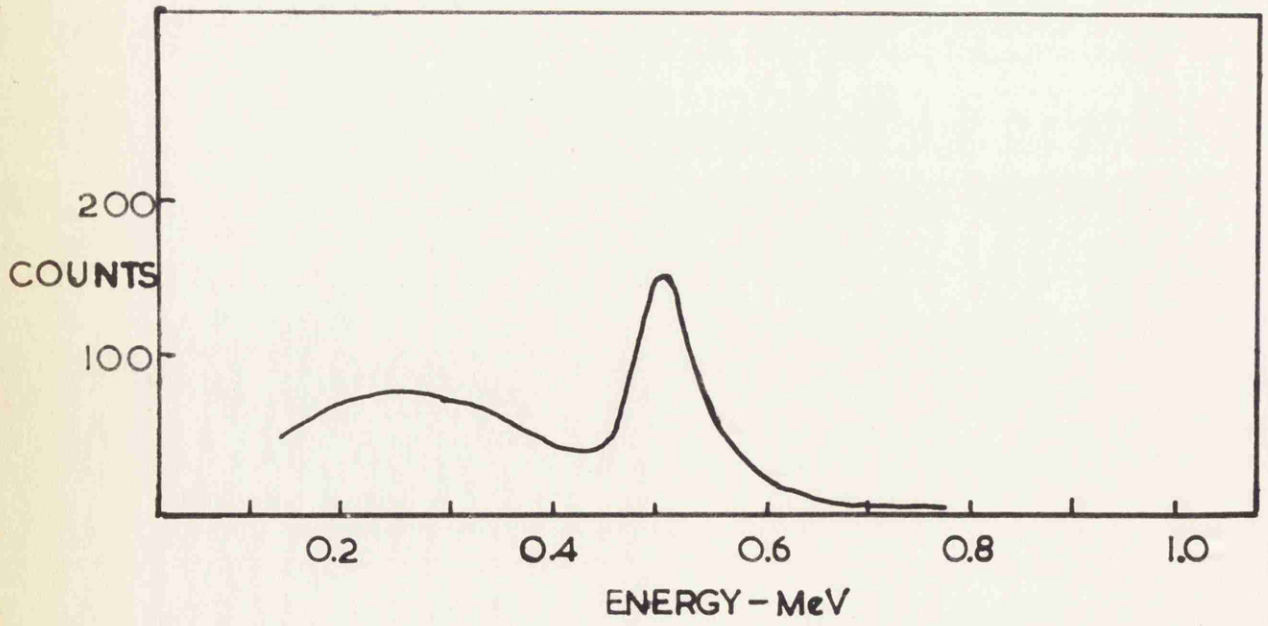

Fig. 3.1(b)

Difference of spectra 1 and 2 above, showing the short lived γ-rays.

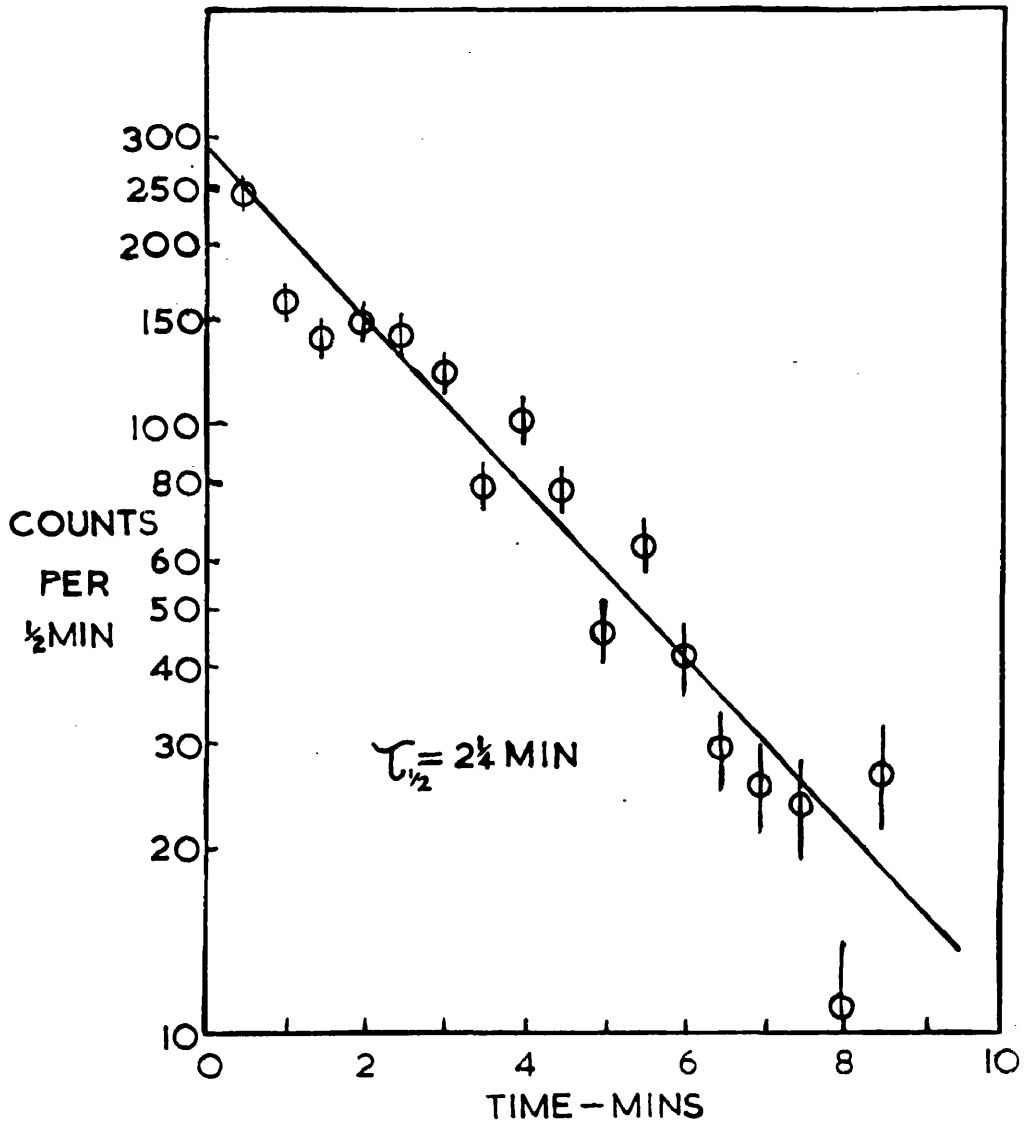

Fig. 3.2

Decay curve for 0.51 MeV γ-rays from bremsstrahlung irradiated manganese.

spectrometer was displayed on a 100 channel pulse-height analyser. Spectra were obtained for several short counting periods after each irradiation in order to be able to separate any short lived activities from longer lived backgrounds such as the Mn^{56} of half-life 2.6 hours.

The spectra shown in fig. 3.1(a) represent the counts obtained during the periods from one to seven minutes after the end of the irradiation and from $16\frac{1}{2}$ to $22\frac{1}{2}$ minutes after irradiation. In spectrum 1 there are peaks at 0.51 MeV and 0.85 MeV and in spectrum 2 a peak only at 0.85 MeV. In fig. 3.1(b) is shown the difference, 1 - 2, showing that the only short lived γ-ray is the one at 0.51 MeV. Several other runs with different amplifier gain settings, to look for higher or lower energy γ-rays showed the same peaks and no other short lived γ-rays.

Using a single channel pulse height analyser set to accept pulses in the 0.51 MeV total energy peak, the decay rate was measured. The counts from six such runs were added to reduce the statistical error and the results are plotted in fig. 3.2. The half-life thus obtained is 2.2 ± 0.2 minutes.

The energy of the γ-ray suggested that it was positron annihilation radiation: this was confirmed by a coincidence experiment. The irradiated manganese was placed between two 2" x $1\frac{3}{4}$" diameter NaI(Tl) crystal spectrometers arranged coaxially face to face. The pulses from one photomultiplier

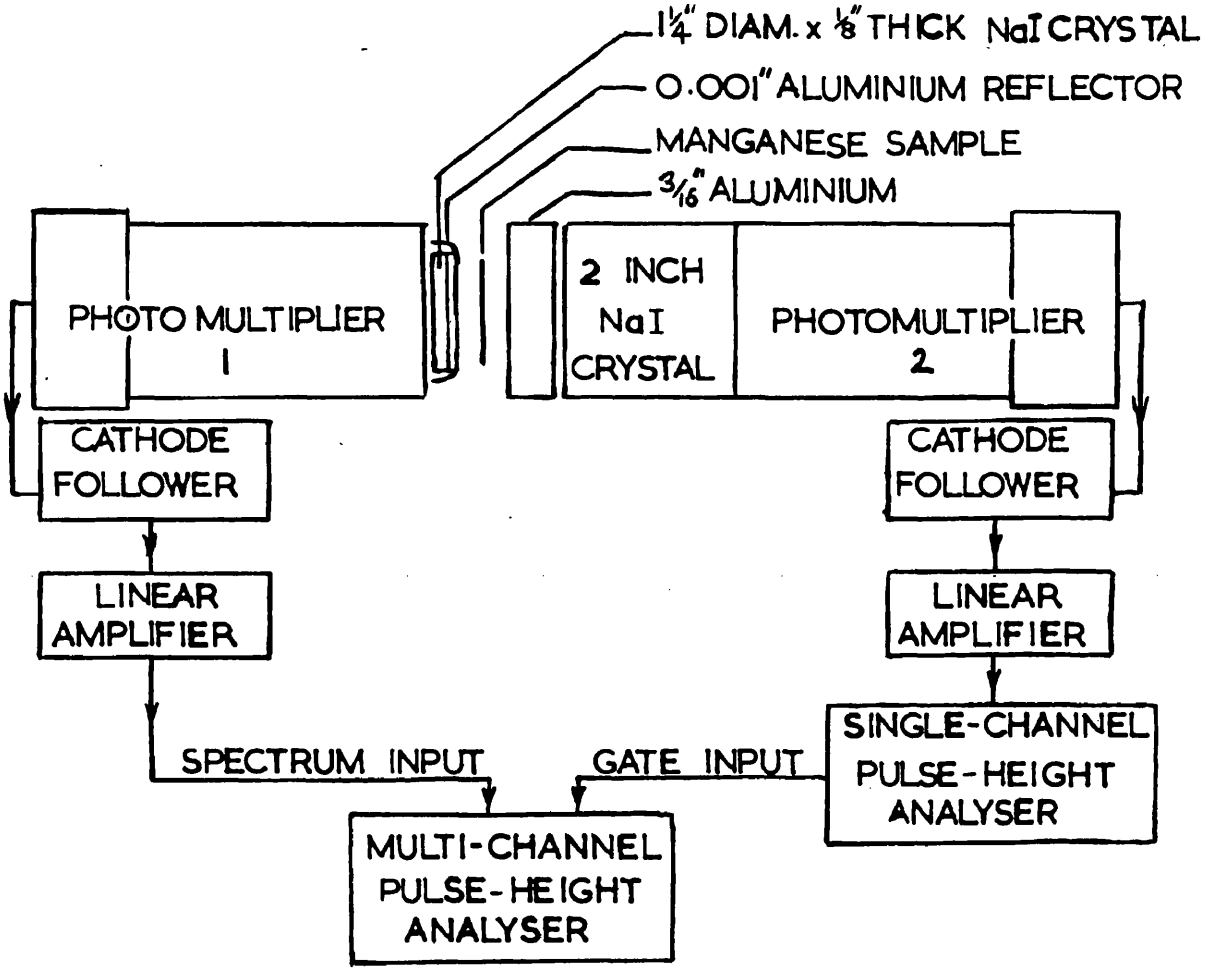

Fig. 3.3

Block diagram of the apparatus for measurement of the end point energy of the positrons emitted by manganese irradiated with 23 MeV bremsstrahlung.

went to the single channel analyser set to accept those from the 0.51 MeV total energy peak and its output was used to gate the 100 channel analyser. The pulses from the other photomultiplier were fed to the input of the 100 channel analyser. The coincidence spectrum thus obtained showed a peak at 0.51 MeV. A second run was made with the crystal axes perpendicular and the centre of the source located at their intersection. The counting rate was negligibly small showing that the 0.51 MeV coincident γ-rays had a strong 180° angular correlation and thus confirming that they were positron annihilation radiation. The coincidence counting rate was small but a decay curve was plotted and the half-life found to be 2.0 ± 0.5 min. in agreement with the earlier measurement.

It was thus shown that irradiation of manganese with bremsstrahlung of peak energy 23 MeV produced a very weak positron activity of half-life 2.2 ± 0.2 min. and no other detectable γ-rays.

An attempt was made to measure the positron end point energy. A thin NaI(Tl) crystal, approximately circular and about $1\frac{1}{4}$" diameter by $\frac{1}{8}$" thick, was used to detect the positrons. A piece of manganese 0.010" thick was irradiated for 4 minutes and placed against the thin NaI(Tl) crystal. Pulses from counter 2 (see fig. 3.3) were passed to the single channel analyser and its output used to gate the 100 channel analyser which recorded the coincident pulses

from the thin crystal. Thus the spectrum of pulses in the thin crystal in coincidence with 0.51 MeV annihilation radiation was obtained and the β^- backgrounds eliminated. The counting rate and spectra were obtained for the period from 1 to 4 minutes after each of 6 irradiations and added together. From their sum was subtracted the sum of the spectra obtained during the periods from 11 to 14 minutes after each irradiation. Thus the effects of long lived activities were eliminated. The resulting spectrum was consistent with a β^+ end point energy of approximately 2.0 MeV.

The weakness of the activity, its positron decay, half-life and end point energy all suggested that it might be due to O^{15} produced by (γ,n) reactions in a very small amount of oxygen impurity, possibly due to surface oxidation of the manganese samples. This possibility is further discussed below.

Another possible method of production of Mn^{54*} was $Mn^{55}(n,2n)$ and samples of the pure manganese were therefore irradiated with 14 MeV neutrons from the $H^3(d,n)He^4$ reaction for 4 minutes and then removed to the γ-ray spectrometer. In the ungated γ-ray spectrum a strong peak was observed due to a short lived γ-ray of 1.40 MeV. This was assigned both by its half-life and energy to the decay of V^{52} which could have been produced by the $Mn^{55}(n,\alpha)V^{52}$ reaction. γ-rays from Mn^{56} decay were also observed but no 0.5 MeV

γ-rays of sufficient intensity to be detected in the presence of the other activities. To confirm this result another sample was irradiated and the γ-ray spectrum in coincidence with 0.5 MeV pulses was measured with the source between the crystals. An aluminium absorber between each of the crystals and the source prevented β-particles from being detected. Although a small number of real coincidences was observed there was no sign of a peak at 0.51 MeV and the counts could be explained as coincidences between bremsstrahlung from the V^{52} β^+-particles and the associated Cr^{52} γ-rays.

If the weak β^+-activity produced in manganese by irradiation with 23 MeV bremsstrahlung was indeed to be assigned to the decay of the same state as produced by Caldwell then it should be detectable in samples of iron irradiated with fast neutrons. As separated isotopes were not available natural iron targets were irradiated with 14 MeV neutrons. Positrons were detected in the resulting decay but the measured half-life of about 9 minutes suggested that they were due to Fe^{53} produced by the reaction $Fe^{54}(n,2n)Fe^{53}$. The Q-value for this reaction is -13.2 MeV (Nuclear level schemes, 1955) and it was therefore possible to utilize the variation of energy with angle of the neutrons from $H^3(d,n)He^4$ to reduce it. The energy of the deuteron beam was 160 keV and the effective thickness of the tritium target (tritium absorbed in zirconium) 70 keV. Thus the

neutrons in the forward direction had energies from 14.8 MeV to 15.0 MeV and the energy available in the centre of mass frame, when interacting with an Fe^{54} nucleus, was from 14.55 to 14.75 MeV. With the iron target so placed that the neutrons reaching it came from the tritium target at an angle of $> 130^{o}$ to the incident deuteron direction the maximum energy available in the centre of mass frame was 13.3 MeV. Samples of iron irradiated in this latter position showed no detectable positron activity.

In all the γ-ray measurements aluminium absorbers were placed between the sources and NaI crystals to eliminate the direct detection of β^{+}- or β^{-}-particles. When the iron samples irradiated in the 135^{o} position were placed beneath a geiger counter a short lived activity was detected which, since it had no 0.51 MeV γ-rays associated with it, had to be a β^{-}-decay. Its half-life was measured and found to be 1.8 ± 0.2 min.

An attempt was made to measure the end point energy using a thin (0.006" thick) iron target and a plastic scintillator. As the counting rates were low the spectra from counts following six irradiations were combined. The result for the end point energy was 2.4 ± 0.3 MeV, the low counting rates making a more accurate measurement unfeasible. Two independent sets of runs gave similar results. The half-life and energy measurements permit the assignment of this activity to the decay of Mn^{57} produced by $Fe^{57}(n,p)Mn^{57}$

Thus from neutron irradiations of natural iron, no β^+-activity which could be associated with Mn^{54*} was observed and any 2 minute half-life β^--activity would be masked by the Mn^{57} decay.

At that time Dr. K. G. McNeill, who had collaborated in some of the preliminary measurements for the above work, was spending the summer at the University of Saskatchewan and had available a 23 MeV Betatron giving a bremsstrahlung intensity 20 times greater than that obtainable with the Glasgow synchrotron and the peak energy of which could be very accurately controlled. A sample of the pure manganese was therefore sent to him and he measured the threshold for the production of the 2 minute half-life positron activity. Both the threshold energy and the shape of the activation curve just above it were identical with those for $O^{16}(\gamma,n)O^{15}$. Further, a comparison of the strength of the activity with that produced in a copper target showed that (i) if it was due to Mn^{54*} the peak cross section in the giant resonance region for the reaction $Mn^{55}(\gamma,n)Mn^{54*}$ was $< 3 \times 10^{-29}$ cm^2 and (ii) all the observed activity could be accounted for by an oxygen impurity of 0.1%. Although this impurity was considerably greater than the maximum quoted by the suppliers of the manganese, in view of the possibility of surface oxidation and the experimental evidence it seemed most likely that the observed positron activity was O^{15}.

3.3 Conclusions

It was therefore concluded that there was no evidence for the production of a positron or γ-ray activity by bremsstrahlung irradiation of manganese or by neutron irradiation of iron. Although a 2 minute half-life negatron activity might be produced by $Fe^{54}(n,p)$ it could not be detected without a separated isotope target because of the large amount of Mn^{57} produced when natural iron was irradiated with 14 MeV neutrons. Finally, experiments performed by L. Katz and W. Link (McNeill, 1957) confirmed that the peak cross section for the production of a short lived negatron activity by the irradiation of manganese with bremsstrahlung was $< 10^{-28}$ cm^2 whereas the $Mn^{55}(\gamma,n)Mn^{54}$ (ground state) peak cross section is 10^{-25} cm^2.

The question therefore arises whether it is likely that Mn^{54*} might be produced by the $Fe^{54}(n,p)Mn^{54*}$ reaction (Caldwell, 1955) and yet not be formed by a photoneutron reaction. To consider this, let it first be assumed, for the sake of argument, that the original Caldwell and Stoddart result is correct--i.e. that there is an isomeric state of 2 minute half-life which decays by the emission of a negatron of peak energy 2 MeV. As the Mn^{54} ground state lies 0.54 MeV above that of Fe^{54} (Nuclear level schemes, 1955), the isomeric state must then be 1.46 MeV above the Mn^{54} ground state. The absence of γ-rays in the decay implies that the spin change involved must be at least $\Delta I = 4$ and as the spin of

the ground state is probably 3 (Nuclear level schemes, 1955) the spin of the isomeric state would have to be at least 7. As shown in section 3.1, shell model considerations suggest that this or larger values are quite probable.

Calculations of the probable orbital angular momentum values for 14 MeV neutrons interacting with nuclei (Katz, 1952) yield an average value of $l_{av.} = 3.5$ but considerable probability for l values up to 6. Thus the spin of the Fe^{55} compound nucleus in the reaction $Fe^{54}(n,p)Mn^{54*}$ could easily be the sum of the Fe^{54} ground state spin, 0, plus 6 for the l value of the neutron, plus $\frac{1}{2}$ for the spin of the neutron, that is $\frac{13}{2}$ and therefore excited states of Mn^{54}, produced by subsequent emission of a proton, might be expected to have spins of 7 or even higher.

The possibility of producing such a state by a photo-neutron reaction must next be considered. On the basis of the Wilkinson model the strongest neutron transition associated with the $Mn^{55}(\gamma,n)$ reaction is expected to be from the closed $f_{7/2}$ shell to the $g_{9/2}$ state and if a neutron were so excited, and then emitted by the resonance direct process there would remain an odd $f_{7/2}$ neutron and an odd $f_{7/2}$ proton which could couple to give a spin 7 intermediate state of Mn^{54}. Thus high spin excited states of Mn^{54} could easily be formed by either the (n,p) or the (γ,n) reaction.

Further difficulties arise, however, when the decay of

the state is considered. A 2-minute half-life for a β-decay of 2 MeV energy implies an allowed transition so the decay cannot take place from a high spin state to the spin 0 ground state of Fe^{54}. So the decay must take place to a higher spin excited state of Fe^{54} and the isomeric state must be a corresponding amount more than 1.46 MeV above the ground state of Mn^{54}. The lowest known excited state of Fe^{54} is of spin 2 and at 1.41 MeV and suggesting that Mn^{54*} lies more than (1.46 + 1.41) MeV above the Mn^{54} ground state requires an even higher spin to inhibit its decay by γ-ray emission with corresponding difficulties of formation of the state by either the (γ,n) or the (n,p) reaction. Alternatively the assumption that the β-decay energy is less than 2 MeV eliminates the spin change difficulties by permitting the assignment of spin 0 and an energy of excitation less than 0.1 MeV to the isomeric state. With this small energy and a spin change of 3, γ-ray emission to the ground state might be sufficiently inhibited to give the observed 2 minute half-life. Such a level should, however, be equally attainable by the $Fe^{54}(n,p)$ and $Mn^{55}(\gamma,n)$ reactions, and furthermore it would be expected to decay in part by positron emission to the 0+ ground state of Cr^{54}.

Assuming a β-decay energy larger than 2 MeV only accentuates the difficulties detailed above.

To summarize, if the β-decay energy is high it is difficult to interpret the decay of the state and in any

event its production by the (γ,n) reaction should be possible if it can be produced by Fe^{54}(n,p). If the β-decay energy were very much lower than reported the decay would be much more easily explicable but a positron branch would be expected. The experiments show that photoproduction of such an activity is at most very weak and that there is no evidence for the production of either a negatron or positron activity, associated with Mn^{54}, by fast neutron bombardment of natural iron.

Since the original report of the isomeric state two other isotopes in this region of the periodic table, V^{53} (Schardt, 1956) and Mn^{57} (Cohen, 1954) have been found to have negatron decays of 2.5 and 2.6 MeV energy and 2.0 and 1.7 minutes half-lives respectively.

In view of the these facts the existence of the isomeric state of Mn^{54} should not be accepted without reservations.

CHAPTER IV THE DECAY SCHEME OF Mo^{91} AND Mo^{91*}

Section 4.1 The Nucleus Mo^{91} (Z = 42, N = 49)

A further search for isomeric states which could be photoproduced and had not been fully investigated led to an examination of known isomers with odd neutron or proton numbers between 40 and 50.

In this region of the periodic table the $g_{9/2}$ shell is being filled and the independent particle model predicts that there will be a number of isotopes in which a $g_{9/2}$ state and $p_{1/2}$ state will be adjacent the upper of these states is then expected to be metastable and to decay by lepton or γ-ray emission or a combination of both. In these isotopes it is possible for either the $g_{9/2}$ or the $p_{1/2}$ level to form the ground state. The former situation arises when the odd nucleon fills a vacancy in the $g_{9/2}$ shell; but $p_{1/2}$ ground states occur in nuclei in which the pairing energy predominates and the addition of the last nucleon leads to an extra pair in the $g_{9/2}$ level leaving an unpaired nucleon in the $p_{1/2}$ state. Several isotopes of each type had been found to have isomeric states, among them Mo^{91}.

A number of experiments had established the existence of two decay modes with half-lives about 67 seconds and 15.3 minutes respectively, which could be attributed to Mo^{91} (Nuclear level schemes, 1955, contains references to early

papers on Mo^{91}). Disagreement had arisen, however, as to which of the half-lives should be attributed to the ground state and which to the isomeric state.

In the experiments of Katz et al. (1953) the two isomers were produced by the reaction $Mo^{92}(\gamma,n)$ and assignments of the 67 second decay to the ground state and the 15 minute half-life to the isomeric state were made on the basis of measurements which showed the threshold for the production of the latter activity to be higher than the threshold for the former. With this assignment and assuming that no isomeric transition from the upper state to the ground state occurred in the decay the relative (γ,n) yields to the two states were calculated from the measured β-particle strengths of the two activities. Finding the 15.5 minute state more abundant than the 67 second one they concluded the former was the $p_{1/2}$ level and the latter the $g_{9/2}$ level on the basis of the probable spin changes in the photonuclear reaction.

Subsequent experiments disclosed, however, a strong 0.65 MeV γ-ray in the 67 second decay, of intensity 2.3 times as great as the positron emission of the same half-life (Axel, 1955). As the electron capture competing with the positron emission was estimated to be very small the 0.65 MeV transition had thus to be assigned to a transition in Mo^{91} between the isomeric and ground states. It was further shown that existing discrepancies between the (n,2n)

and (γ,n) thresholds for the production of Mo^{91} could be resolved, and the measured activation ratio for the two levels, near the (γ,n) threshold, could be explained by a 67 second, 0.65 MeV, $p_{1/2}$ isomeric state and a 15 minute, $g_{9/2}$ ground state of Mo^{91} (Axel, 1955).

Further uncertainty existed in the measurement of the positron end point energies which had been variously reported as 2.6 MeV (Duffield, 1949) and 3.0 MeV (Katz, 1953) for the 67 second activity and 3.7 MeV (Duffield, 1949), 2.7 MeV (Sagane, 1940) and 3.32 MeV (Katz, 1953) for the 15.5 minute half-life. Finally, Katz et al. (1953) had re-analysed the experimental results of Duffield and Knight (1949) and obtained the value 3.2 MeV instead of 3.7 MeV.

Moreover, γ-rays of 1.2 and 1.5 MeV and several other possible transitions between 1.8 and 2.9 MeV from the 67 second activity, had been reported by Axel (1955) but had not been assigned places in the decay scheme.

It, therefore, seemed very worthwhile to clarify the decay schemes of these isomers and the following experiments were performed for that purpose.

Section 4.2 Experimental Methods and Results

Mo^{91} was produced by the reaction $Mo^{92}(\gamma,n)Mo^{91}$ by the irradiation of natural molybdenum in the X-ray beam of a 23 MeV synchrotron.

For examining the β^+- and γ-spectra of the Mo^{91}, plastic

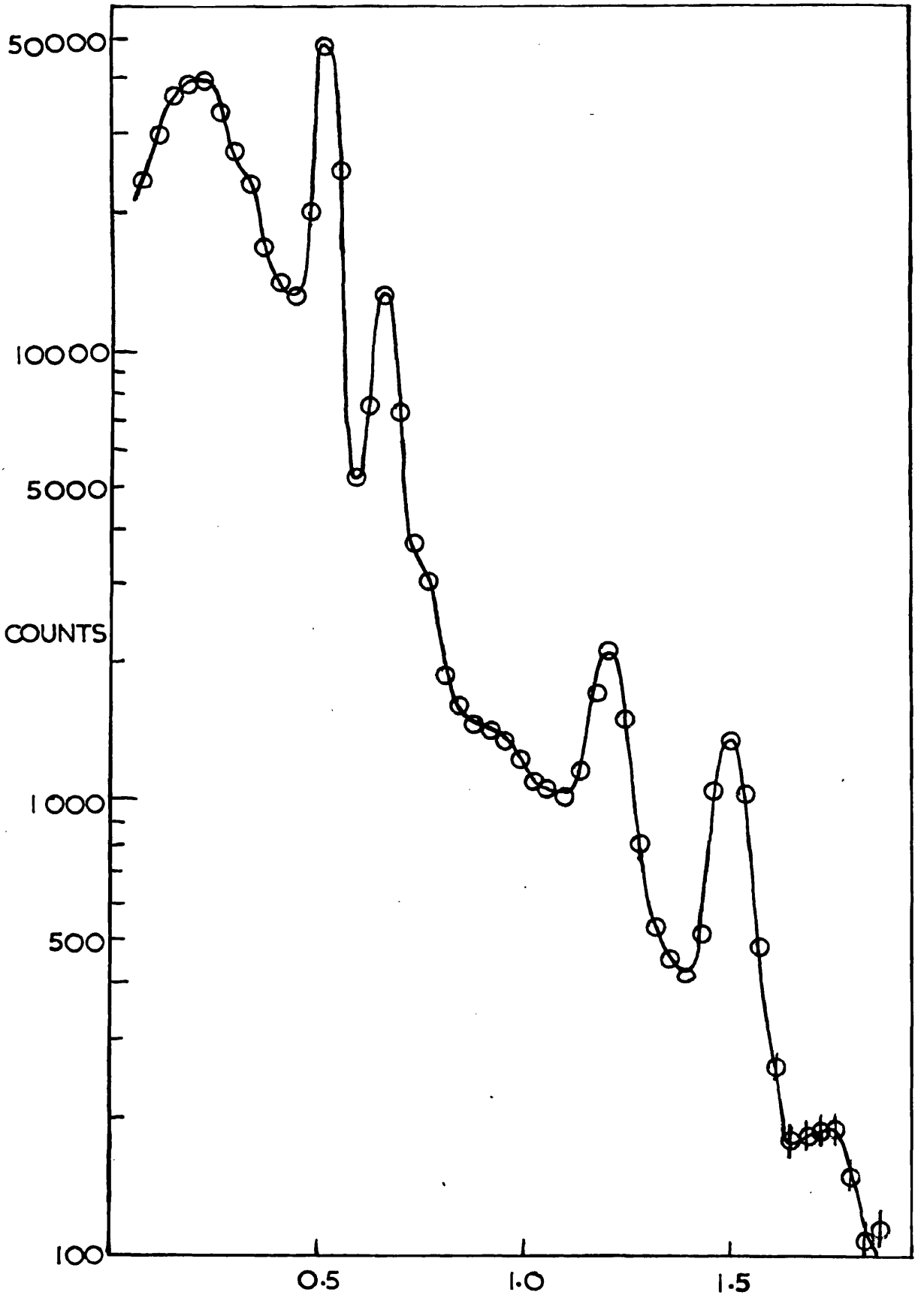

Fig. 4.1

Semi-logarithmic plot of the γ-ray spectrum of Mo^{91*}

and 2-in. thick NaI scintillators were used in conjunction with DuMont 6292 photomultipliers, conventional circuits, and a 100-channel pulse-height analyser.

In the γ-γ and γ-β^+ coincidence work, there was, in addition to the above apparatus, a 2-in. thick NaI crystal spectrometer used with a single-channel pulse-height analyser. The output from this analyser could operate a gate in the input of the 100-channel pulse-height analyser. By using this equipment, the β- and γ-spectra in coincidence with pulses from the total energy peak ("photopeak") from a particular γ-ray could be determined. Corrections were made, if necessary, for the fact that Compton recoils due to higher energy γ-rays could operate the gate as well as total absorption pulses from the desired γ-ray. In addition, corrections were made for the effects of longer lived activities induced in the other molybdenum isotopes.

A typical γ-ray spectrum of Mo^{91} and Mo^{91*} obtained in this work is shown in fig. 4.1. The spectrum shows the presence of lines at 0.51, 0.65 $\pm$ 0.02, 1.20 $\pm$ 0.02, and 1.50 $\pm$ 0.02 MeV. The 0.51 MeV γ-rays were identified as positron annihilation quanta. In some of the runs weak peaks were also present at 1.7 MeV and 2.0 MeV, but these were thought to be due to the addition of 0.51 with 1.20 MeV γ-rays and 0.51 with 1.50 MeV γ-rays. This was confirmed by measurements taken with the source at varying distances from the crystal. No other evidence was found for lines

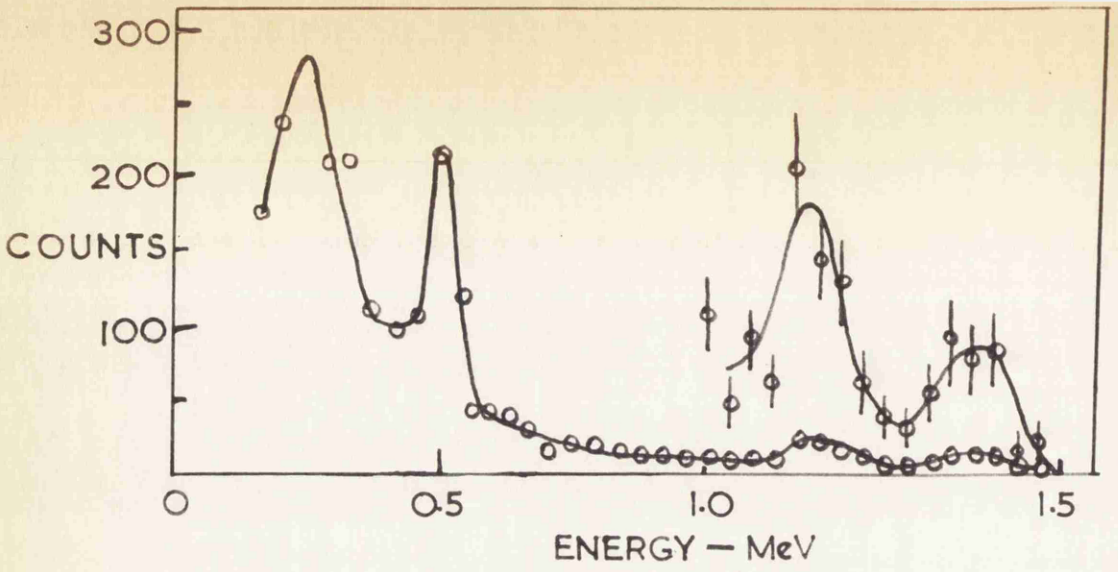

Fig. 4.2(a)

γ-ray spectrum in coincidence with 0.51 MeV γ-rays
($0.2 < E_\gamma < 1.8$ MeV)

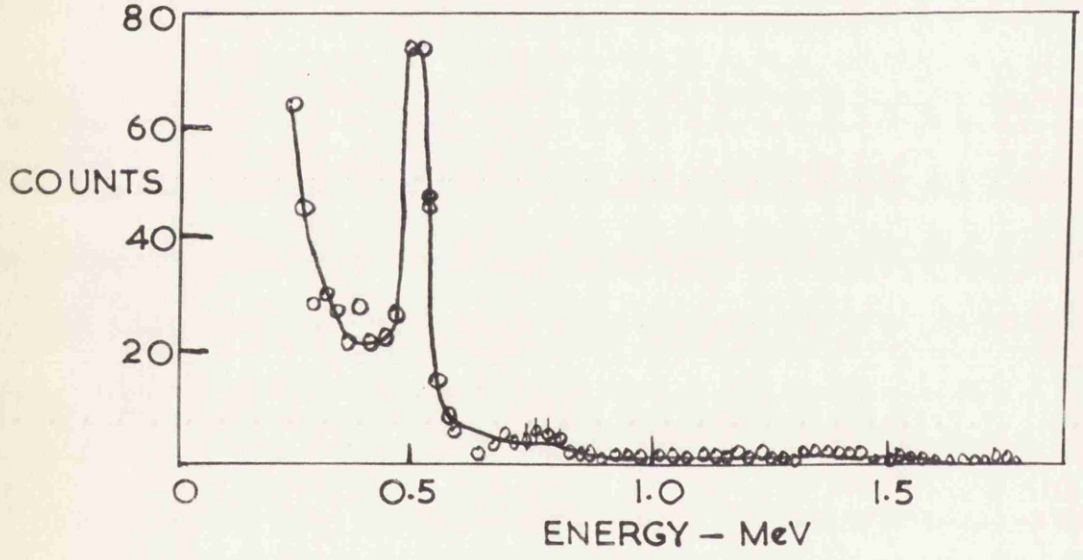

Fig. 4.2(b)

γ-ray spectrum in coincidence with 1.2 and 1.5 MeV γ-rays
($0.3 < E_\gamma < 2.0$ MeV)

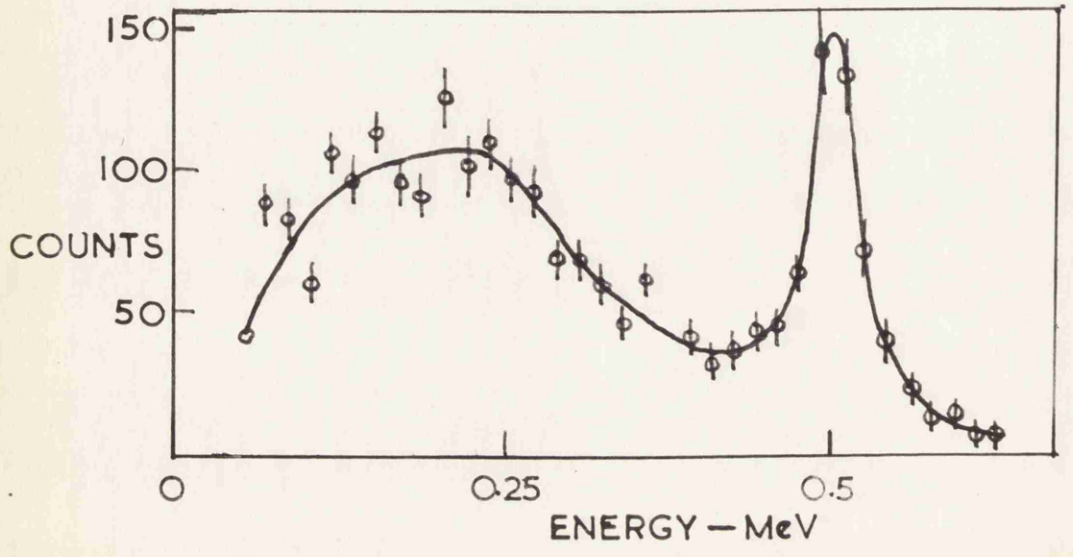

Fig. 4.2(c)

γ-ray spectrum in coincidence with 1.2 MeV γ-rays
($0.1 < E_\gamma < 0.7$ MeV)

other than the four first given above.

By using the γ-spectra obtained in a number of runs, and knowing the relative efficiency of the crystal for the different γ-ray energies, the relative strengths of the 0.65, 1.20 and 1.50 MeV lines were computed. It was found that the intensities of the rays were in the ratios

0.65 MeV:1.20 MeV:1.50 MeV = 100:39:39.

It will be seen that the two higher energy lines are of approximately equal intensity.

By using the single-channel pulse-height analyser, set to accept pulses from the photopeaks of the three lines, measurements were made of the half-lives of the three γ-rays. All three had the same half-life to within the experimental accuracy, the average value being 64 ± 1 seconds.

With the single-channel pulse-height analyser set on the photopeaks of the 0.51, 1.20 and 1.50 MeV lines, respectively, determinations were made of the spectra of γ-rays in coincidence with these three lines. These γ-γ coincidence results are presented graphically in figs. 4.2 (a), (b), (c), and are summarized below. The range of energy investigated in each case is given in parentheses.

(a) In coincidence with 0.51 MeV γ-rays ($0.2 < E < 1.8$ MeV) —0.51 MeV, 1.20 and 1.50 MeV γ-rays.

(b) With 1.20 and 1.5 MeV γ-rays ($0.3 < E < 2.0$ MeV)—0.51 MeV γ-rays.

(c) With 1.20 MeV γ-rays ($0.1 < E < 0.7$ MeV)—0.51 MeV γ-rays.

Thus while the 1.20 and 1.50 MeV lines are associated with a positron decay of the isomeric state, the 0.65 MeV line is not. Moreover, the 1.2 MeV and 1.5 MeV γ-rays are not in coincidence, even though this is suggested by their having equal intensities. A special search was made for a 0.3 MeV γ-ray which might be expected to be in coincidence with the 1.20 MeV line (1.5 MeV minus 1.2 MeV) but no such line was found (fig. 4.2(c)). The large number of counts between 0.1 and 0.3 MeV is due to scattering of the 0.5 MeV annihilation quanta, and is relatively high because of the thickness of the source being used. This explanation was confirmed by using a thick Cu^{62} positron source for comparison.

A 0.01-inch-thick molybdenum sheet was irradiated in the X-ray beam for 30 minutes, and then placed before a 1-inch-thick plastic scintillator, the spectrum from which was displayed on a 100-channel pulse-height analyser. After allowing time for the isomeric-state activity to die away, the positron spectrum of the 15-minute activity was determined. The average of several runs gave an end-point energy of 3.3 ± 0.2 MeV, in agreement with previous measurements of this energy by Katz (1953).

The observed coincidences between 0.51 MeV quanta and 1.2 and 1.5 MeV γ-rays showed that the γ-rays followed positron emission and the complex β^+-decay of the 64 second state was therefore investigated. Immediately after a 2

minute irradiation in the X-ray beam, a 0.01" thick sheet of molybdenum was placed between a plastic scintillator and a 2" thick NaI crystal. As described in a previous paragraph, the output from the plastic scintillator went to the 100-channel pulse-height analyser, while pulses from the NaI crystal spectrometer were fed to a single-channel pulse-height analyser, which in turn operated the coincidence gate of the 100-channel pulse-height analyser circuit. By a suitable setting of the single-channel analyser, the spectrum of positrons in coincidence with either 1.5 or 1.2 MeV γ-rays could thus be obtained.

The attainable counting rates were small and the results of fourteen irradiations were combined for each of the spectra. The small numbers of counts made an absolute measurement of the end points of the β^+-spectra unreliable but a comparison of the curves obtained in coincidence with the 1.20 MeV and 1.50 MeV lines, respectively, showed that the former had an end point energy 0.2 $\pm$ 0.1 MeV higher than the latter. It is therefore concluded that the β^+-decay proceeds via two excited states of Nb^{91} one of which de-excites by means of a 1.20 MeV γ-ray and the other by a 1.50 MeV γ-ray.

All sources which decay by positron emission can also decay by orbital electron capture and the two processes compete. The relative numbers of the two types of decay to each of the excited levels of Nb^{91} were calculated from the

theoretical results of Feenberg and Trigg (1950), and the values obtained are shown in the table of fig. 4.4.

The possibility of a third branch in the positron decay must be investigated for the following reasons. There is an isomeric state of Nb^{91} at an energy 0.105 MeV above the ground state and these two levels were assigned spins and parities $\frac{1}{2}-$ and $\frac{9}{2}+$ respectively (Nuclear level schemes, 1955). Either of the probable shell model assignments for the 64 second state, $p_{1/2}$ or $g_{9/2}$, would permit allowed transitions to the corresponding state of Nb^{91}: such transitions would be expected to compete with the decays to the higher excited states. The positron energy of the decay would be (3.3 + 0.65) MeV or (3.3 + 0.65 - 0.105) MeV (see fig. 4.4). The ungated β^+-spectra from thin molybdenum sheets were therefore observed, following 2 minute irradiations in the bremsstrahlung beam. The fifteen minute activity was also present; to reduce its effect the spectrum obtained between 4 and 6 minutes after the source was placed on the counter was subtracted from that obtained in the first two minutes. The results of four irradiations were added. The combined spectrum showed evidence of a high energy positron branch with end-point energy 3.9 ± 0.2 MeV energy. The large errors were due to the thickness of the source which could not be reduced because the activity attainable was extremely weak. These difficulties also prevented an accurate measurement being made of the relative

intensity of the high energy branch. It was estimated to be less than 15% of the total positron decay of the 64 second level.

An alternative method for finding the strength of this transition is to measure the intensity of the 0.51 MeV radiation associated with the 64 second decay relative to the 1.2 and 1.5 MeV γ-rays. Each positron decay gives two 0.51 MeV quanta so one half of the number measured is equal to the total number of positrons, that is $\beta_1 + \beta_2 + \beta_3$. (The β^+ branches are numbered in order of increasing energy, see fig. 4.4). The 1.5 and 1.2 MeV γ-rays follow either a positron decay or an electron capture event and thus $\gamma_1 + \gamma_2 = \beta_1 + \epsilon_1 + \beta_2 + \epsilon_2$. The geometrical effects on the counting rates were the same for the γ-rays and the annihilation radiation because with the thick sources used in this part of the experiment virtually all the positrons stopped in the source or in the aluminium absorber between it and the scintillator.

Measurement of the ratio of the intensity of the 0.51 MeV line associated with the 64 second activity to the intensity $\gamma_1 + \gamma_2$ was complicated by the necessity of subtracting the contribution of the 15 minute annihilation radiation from the observed spectrum. The longer lived activity arises both from direct production during the irradiation and from the γ-decays of the 64 second state. Axel et al. (1955) estimated from their own preliminary experiments and from a re-analysis, using the correct decay

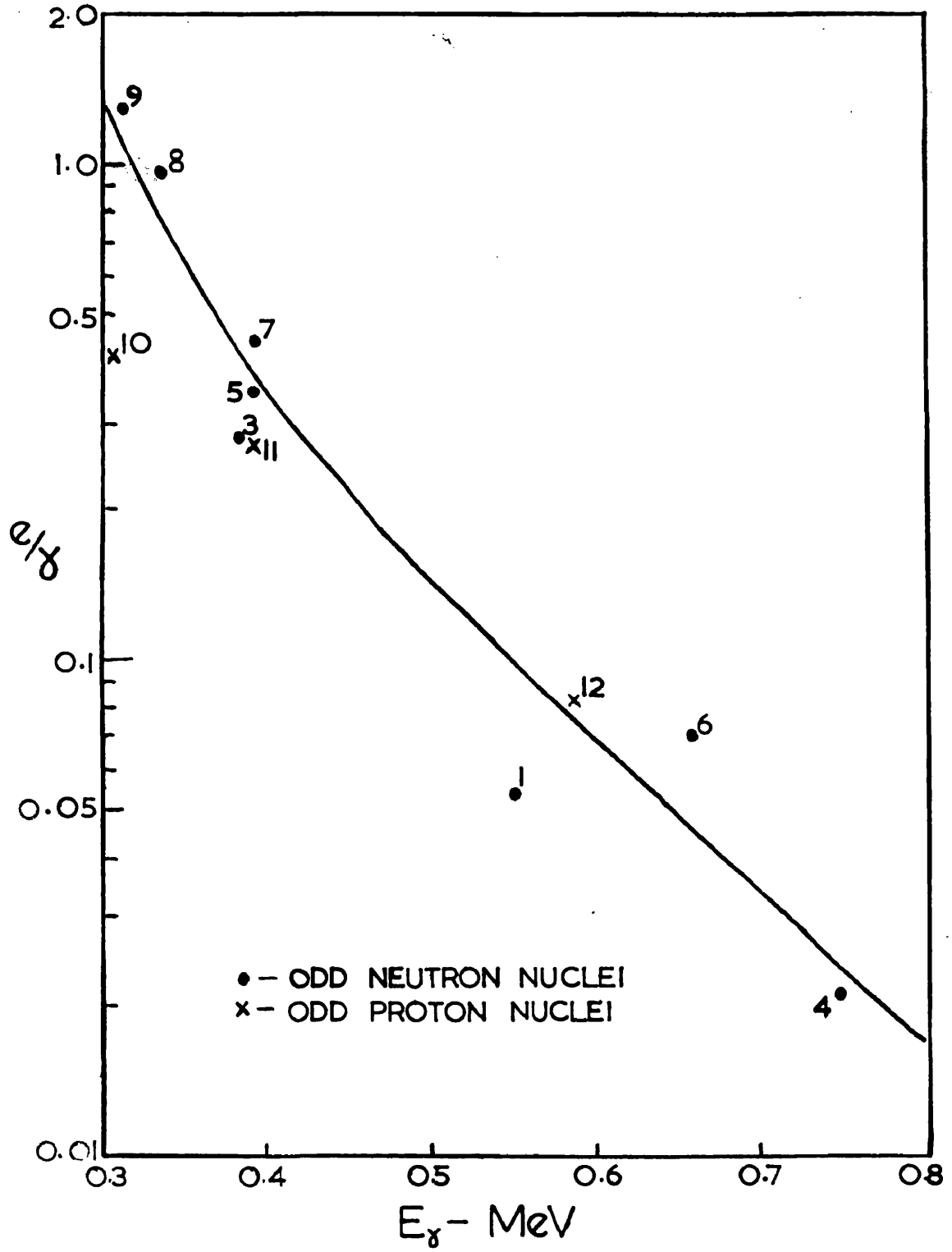

Fig. 4.3

Logarithmic plot of the total internal conversion coefficient, e/γ, against the energy of the transition, E_γ, for M4 transitions in the $g_{9/2}$ shell.

Legend

Point	1	2	3	4	5	6	7	8	9	10	11	12
Isotope	Y^{91}	Y^{89}	V^{87}	Nb^{97}	Tc^{93}	In^{109}	In^{113}	In^{115}	In^{117}	Kr^{85}	Sr^{87}	Zr^{89}

scheme, of the measurements of Katz et al. (1953) that for bremsstrahlung energies well above threshold approximately one half of the 15 minute activity resulted from the decay of the isomeric state and half was produced directly. Using this ratio and assuming a small value for β_3, the relative contributions of short and long lived decays to the 0.51 MeV peak were calculated. The ratio of β^+ emission from the 64 second state to the combined intensity $\gamma_1 + \gamma_2$ was found to be 1.0. The transition β_3 is therefore equal in intensity to the sum of the electron capture transitions to the higher excited states, i.e. $\beta_3 \simeq 6\%$, which justifies the assumption made above.

Finally, the 64 second state can also decay to the Mo^{91} ground state by the emission of conversion electrons. Taking account of the contributions from both the K and L shells the ratio of conversion electrons to γ-rays was estimated from the tabulated theoretical values given in Siegbahn (1955). The value thus obtained was $e/\gamma = 0.036$. It is of interest to see how this value compares with experimental results for other M4 transitions between $\frac{1}{2}-$ and $\frac{9}{2}+$ states in the same region of the periodic table. Values of e/γ for nine odd-neutron and three odd-proton M4 isomeric transitions, obtained from Strominger (1958) are plotted against the energy of the transition, $E\gamma$, in fig. 4.3. The values of e/γ are plotted on a logarithmic scale just to facilitate interpolation. The points lie close to a curve which gives

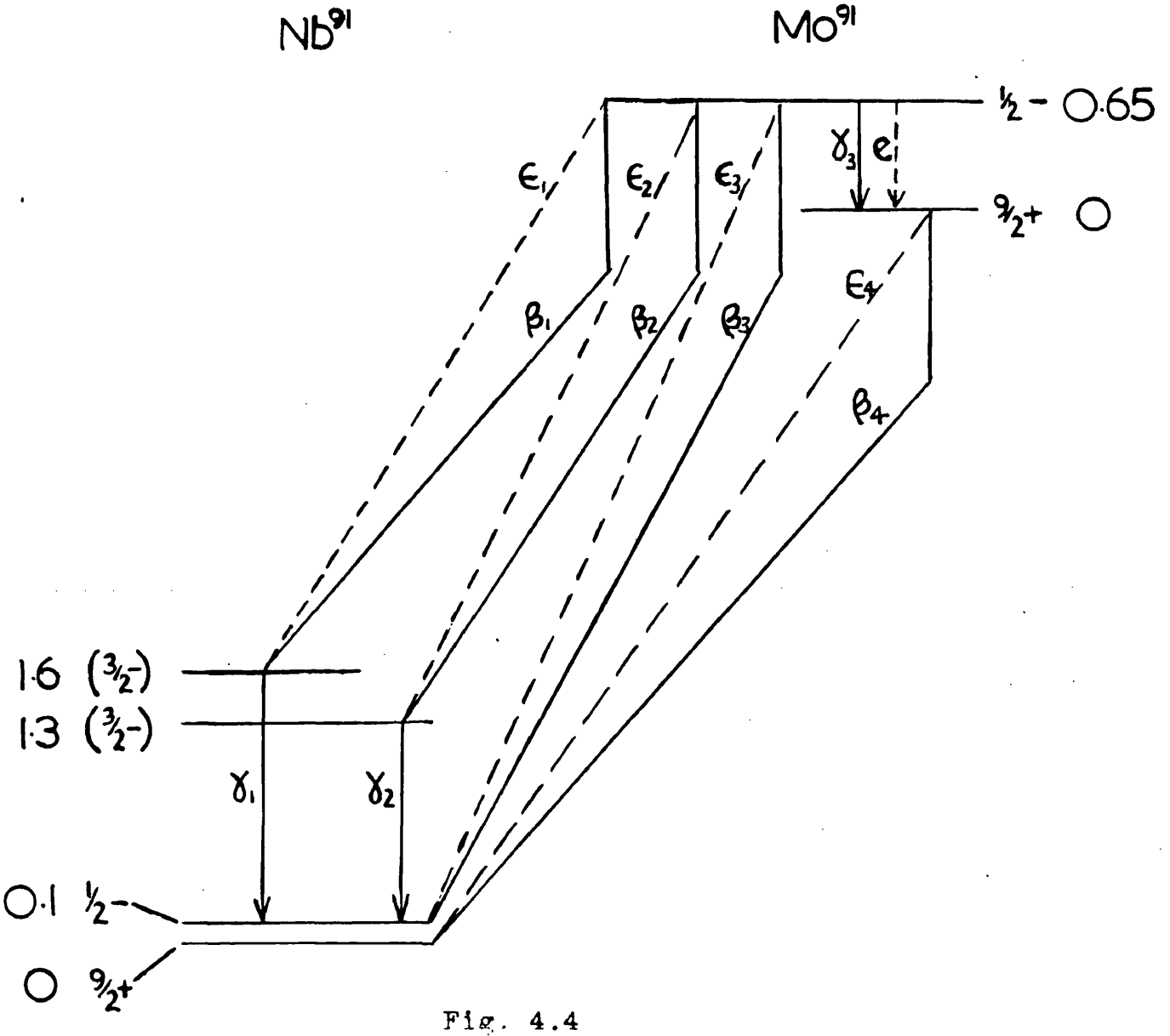

Fig. 4.4

The radioactive decay scheme of Mo^{91} and Mo^{91*}

Table

The relative intensities of the radiations from Mo^{91*}

Radiation	β_1	ϵ_1	β_2	ϵ_2	β_3	ϵ_3	γ_3	e
Percentage of total decays	16.8	3.3	17.7	2.3	5.5	0.3	52.0	2.1

e/γ = 0.05 for $E\gamma$ = 0.65 MeV. There is thus close agreement between the value predicted theoretically and that obtained by comparison with experimental values for other similar transitions. The best estimate will lie between the two given above and e/γ = 0.04 has been used in the decay scheme.

The relative intensities of all the radiations from the 64 second state of Mo^{91} are shown in fig. 4.4.

Section 4.3 Discussion of the Decay Scheme

The radioactive decay scheme shown in fig. 4.4 has been drawn up on the basis of the experimental results described above together with certain information from previous experiments by other authors.

The assignment of the 0.65 MeV γ-ray to a transition between two states of Mo^{91}, suggested on the basis of intensity measurements (Axel, 1955) is conclusively established by the present experiment which shows that it is not in coincidence with positrons or with other γ-rays. The 64 second activity must then characterize the decay of the excited state and the 15 minute half-life be associated with the ground state of Mo^{91}. The arguments of Axel et al. concerning the spins of the states are thus strengthened and the assignments of $p_{1/2}$ and $g_{9/2}$ to the upper and lower states, respectively, are confirmed. Reasons for accepting a similar order for the levels of Nb^{91} are given in Nuclear level schemes (1955).

The relative energies of all the states can now be established. The measured end point of β_4 (fig. 4.4) locates the Mo^{91} ground state relative to the Nb^{91} ground state and the energy of the isomeric transition gives the position of the metastable state of Mo^{91} as 0.65 MeV above the ground state. The transitions β_1 and β_2 have allowed ft values and therefore involve a spin change of 1 or 0 and the succeeding γ-rays most probably go to the low spin member of the Nb^{91} isomeric pair. The energies of the second and third excited states of Nb^{91} are then fixed at 0.1 + 1.2 MeV and 0.1 + 1.5 MeV. The possibility of the two γ-rays starting from the same level and de-exciting to two lower levels is excluded by the absence of 0.3 MeV γ-rays and by the measured difference in energy of the positrons in coincidence with them. Knowledge of the positions of these levels permits the calculation of the end point energies of β_1, β_2 and β_3 as 2.35 MeV, 2.65 MeV and 3.85 MeV, respectively. The first two of these values are consistent with the coincidence positron spectra obtained and the energy difference of 0.3 MeV between β_1 and β_2 is in agreement with the measured value of 0.2 ± 0.1 MeV.

The percentages shown express the relative strengths of the possible decay channels of Mo^{91*} and from these, the partial half-lives of all the branches are calculable.

The transition probability for the 0.65 MeV γ-ray is of particular interest for the reasons discussed in section

1.4(ii), dealing with isomeric states. The partial half-life of the 0.65 MeV γ-ray, obtained from the measured half-life of the state and the percentage of the transitions proceeding by this branch is 123 ± 6 seconds, equivalent to a mean life of 178 ± 9 seconds. Weisskopf's formula, with the statistical weight factor included predicts a mean life of 125 seconds. As the formula makes the very simplest assumption about the nuclear wave function this is good agreement. The observed value being slightly greater than the theoretical estimate is in fact a common feature of M4 transitions.

The reasons for assigning the spins and parities shown in fig. 4.4 to the levels of Mo^{91} and to the two lowest energy states of Nb^{91} have already been given. The values shown in brackets beside the third and fourth states are tentatively suggested by the following arguments. The positron decays to the 1.3 and 1.6 MeV states of Nb^{91} have log ft values of 4.6 and 4.3 respectively and are thus certainly allowed and the states are therefore thought to be of odd parity and spin either $\frac{1}{2}$ or $\frac{3}{2}$. The latter value can be simply explained by the shell model. If the configuration of the ground state is $(p_{1/2})^2 g_{9/2}$ then the first excited state is formed by exciting a $p_{1/2}$ proton to the $g_{9/2}$ level. This state, with configuration $(p_{1/2})^1 (g_{9/2})^2$, will have a spin of $\frac{1}{2}-$: it lies very close to the ground state because the pairing energy in the $g_{9/2}$ state is much

higher than for a pair of $p_{1/2}$ protons and the difference almost compensates for the single particle excitation. The next excited state may then be formed by raising a $p_{3/2}$ proton to the $p_{1/2}$ state. This leaves $(p_{3/2})^3(p_{1/2})^2(g_{9/2})^2$ and the three $p_{3/2}$ protons can couple in different ways to give a resultant spin $\frac{3}{2}$. If the interactions between the protons remove the degeneracy of these states then both the 1.3 and 1.6 MeV states may be assigned to the same configuration and the resultant spin and parity $\frac{3}{2}-$ would permit allowed β^+ transitions from Mo^{91*}.

The 3.85 MeV positrons, β_3, connect two states of spin and parity $\frac{1}{2}-$ and the transition is therefore an allowed one. Its log ft value of 6.3, found in this experiment, is therefore rather large. In the table of β-decays of odd A nuclei given in Siegbahn (1955) there are listed fifty-three allowed transitions of which only four have log ft values over 6.0: however, of the four, three are positron decays in the same region of the periodic table as Mo^{91}, and two of these transitions are between $p_{1/2}$ initial and final states. It therefore appears that some effect, as yet not understood, may operate in this shell to inhibit β-transitions in which a $p_{1/2}$ neutron or proton transforms into a $p_{1/2}$ proton or neutron and the measurement of the decay constants of other examples of these transitions would be of particular interest.

By establishing the details of the decay scheme the

validity of the shell model description of the nucleus in this region of the periodic table has been further confirmed. The transition probability for the M4 γ-rays from the isomeric state has been shown to be in good agreement with the experimental values for other M4 transitions and to agree with the present theory as nearly as may be expected in view of the approximations used in its derivation.

CHAPTER V THE DECAY SCHEME OF I^{128}

Section 5.1 The Nucleus I^{128} (Z = 53, N = 75)

In section 2.2(ii) the method of detecting photoneutrons by the activity which they induced in a NaI(Tl) crystal was described. The neutrons captured in the I^{127} nucleus produced radioactive I^{128}. At the time of these experiments the decay scheme of I^{128} had not been clearly defined. A more complete knowledge, it was seen, might yield information about the I^{128} ground state and the low lying excited states of the neighbouring stable isobars Te^{128} and Xe^{128}. The spins and parities of odd nuclei can throw light on the mode of coupling of several particles outside closed shells. The known first and second excited states of medium weight even nuclei showed some remarkably regular features (Scharff-Goldhaber, 1955) which could be interpreted in terms of collective oscillations of the nuclear core. Further experimental evidence to confirm or refute the empirical trends could contribute to the strength of the theoretical conclusions.

The shell model assignments for the odd proton and odd neutron of $_{53}I^{128}$ are subject to some doubt. The three protons outside the closed shell at Z = 50 might be expected to occupy the $g_{7/2}$ level (see fig. 1.1) but I^{127} has a ground state spin of $\frac{5}{2}$ (Mack, 1950) suggesting that the proton $2d_{5/2}$ state lies just below the $1g_{7/2}$ level. With 75

neutrons the $1h_{11/2}$ sub-shell, which closes at N = 82, must be partially full. The large pairing energy in the $h_{11/2}$ state prevents the occurrence of any $\frac{11}{2}-$ ground states for odd neutron nuclei in this region. Considering the pairing energy and fig. 1.1 one might predict the configuration $(3s_{1/2})^1(1h_{11/2})^6$ and a ground state spin and parity of $\frac{1}{2}+$ like Xe^{129}, one of the adjacent isotones of I^{128}, but Te^{127} which is the other neighbouring isotone of I^{128} was assigned a $\frac{3}{2}+$ ground state because of its allowed β-decay to I^{127} (Day, 1955). Thus the probable states are either $2d_{3/2}$ or $3s_{1/2}$ for the odd neutron and $2d_{5/2}$ or possibly $1g_{7/2}$ for the odd proton. The $d_{3/2}$ and $d_{5/2}$ combination gives, according to Nordheim's strong rule, the definite assignment of 1+ to the I^{128} ground state but the other possibilities yield many possible values for the resultant spin.

The β-decay of I^{128}, of half-life 24.99 minutes (Hull, 1941) was shown to be complex (Siegbahn, 1946) and to have a maximum energy of 2.02 MeV. Siegbahn also found a γ-ray of 0.429 MeV but more recent work (Wapstra, 1953a) amended its energy to 0.455 ± 0.005 MeV and reported a second γ-ray at 0.98 MeV. The fraction of the I^{128} decay proceeding to Te^{128} by orbital electron capture and β^+-decay was measured relative to the β^--decay by means of a mass spectrometric analysis of the decay products (Reynolds, 1950). Scintillation counter studies showed that $\frac{\beta^+}{\beta^-} < \frac{1}{1000}$, so that the decay to Te^{128} must be electron capture, which was confirmed

by measurements of the accompanying Te X-rays (Mims, 1951). The same authors showed that K-capture accounted for 6.3 ± 0.7% of the decays. Another γ-ray measurement (Germagnoli, 1953) gave an energy of 0.439 MeV. Thus the γ-ray spectrum and the decay scheme required further clarification.

[Note: The experiments described below were begun during July, 1955, and studies of the γ-ray spectrum, β-γ and γ-γ coincidences had determined the decay scheme prior to receipt of two publications on the same subject (Benczer, 1955 and 1956, and Gupta, 1956). The experiments to show that the 0.75 MeV γ-ray was in coincidence with the electron capture branch were completed after this date. However, the possibility of an unreported γ-ray in that branch and the confirmation of the previous results by a different experimental technique was deemed adequate justification for continuation of the work in progress.]

Section 5.2 Experimental

The investigation of the decay scheme was carried out in four parts: (i) measurements of the energies and relative intensities of the γ-rays, (ii) γ-γ coincidence experiments, (iii) measurements of the maximum energies of the β^--components in coincidence with three of the γ-rays and (iv) a coincidence experiment to show that one of the γ-rays was in the electron capture branch.

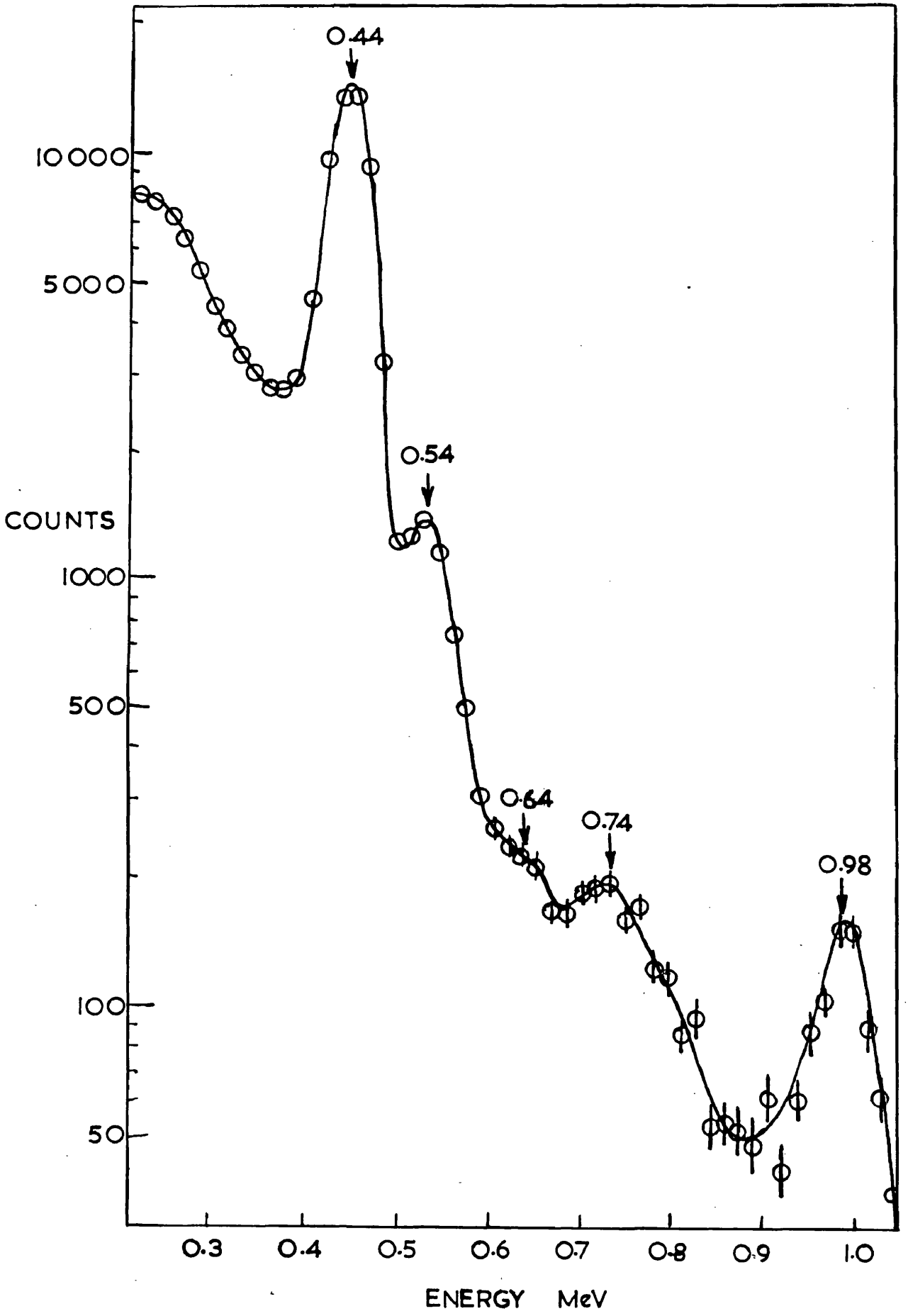

Fig. 5.1

Semi-logarithmic plot of the ɣ-ray spectrum of I^{128}

(i) The γ-ray spectrum

I^{128} was produced by exposing iodine to neutrons from a set of antimony-beryllium sources. The five sources were situated near the centre of a tank of water for shielding purposes and the iodine samples were placed near their geometric centroid. The sources had a combined antimony activity of 2 curies. The water also served as a moderator and increased the number of neutrons with energies in the range from 2 to 600 eV in which the strong neutron capture resonances of iodine occur.

The γ-rays were detected in a 2" long by $1\frac{3}{4}$" diameter NaI(Tl) crystal mounted on a DuMont 6292 photomultiplier and after amplification the resultant pulse-height spectrum was recorded on a 100-channel pulse-height analyser. An aluminium absorber was placed between the crystal and the source to prevent the β^--particles from entering the scintillator. A semi-log plot of a typical spectrum is shown in fig. 5.1. The energy scale was calibrated using Hg^{203}, Cs^{137}, Na^{22} and Zn^{65} sources which give γ-rays of energy 0.279, 0.662, 0.51 and 1.276, and 1.114 MeV respectively. The spectrum was analysed using experimental spectra for single γ-rays to determine the contribution of the compton distribution of each peak to the lower part of the energy spectrum.

Having thus found the total number of counts from each of the γ-rays it was possible to correct theoretically for the total absorption efficiency of the crystal at each

energy and determine the relative intensities of the γ-rays. The measured energies and relative intensities of the γ-rays are given in table V.1.

Table V.1

Transition	Energy (keV)	Intensity
γ_1	440 ± 8	100
γ_2	540 ± 8	12.2
γ_3	745 ± 9	2.65
γ_4	980 ± 10	5.0

The analysis of the spectrum showed that there was a larger number of counts in the region of 640 keV than could be explained by the compton distributions of the other γ-rays but several attempts failed to resolve a peak in this region. This evidence, however, suggested that a search for a γ-ray of 640 keV should be made using coincidence techniques.

(ii) γ-γ coincidences

In these experiments a source prepared as described above was placed between two NaI(Tl) scintillation spectrometers of the type described above. The output of one was amplified and fed to a single-channel pulse-height analyser with an acceptance channel which could be varied in width and energy. Its output was used to gate the 100-channel pulse-height analyser to which was fed the spectrum of pulses from the second spectrometer.

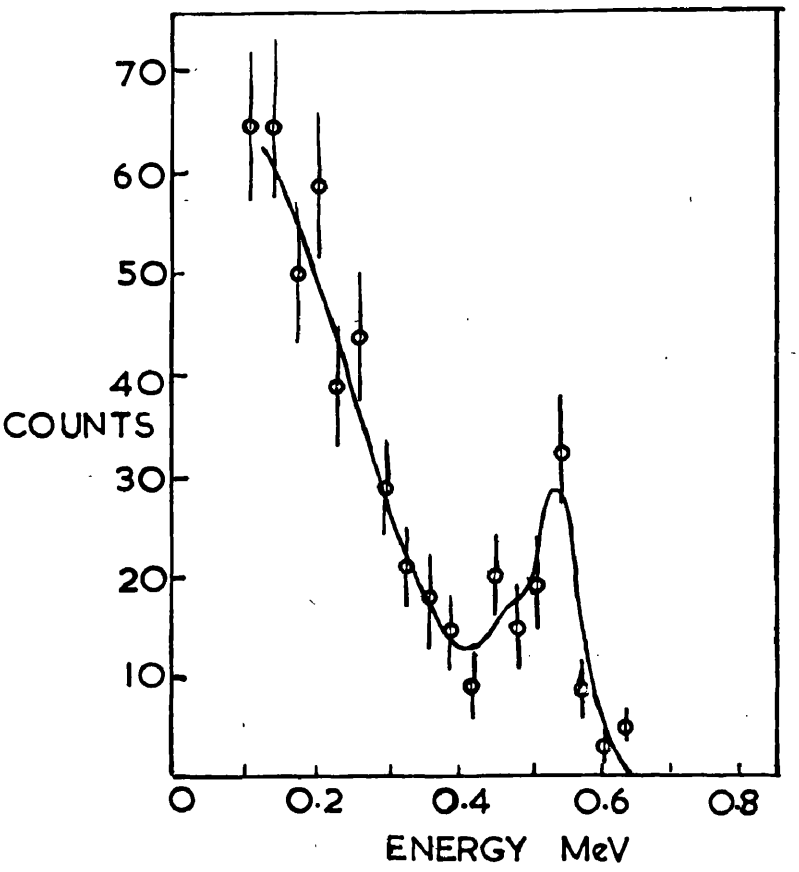

Fig. 5.2

The γ-ray spectrum in coincidence with 0.44 MeV γ-rays

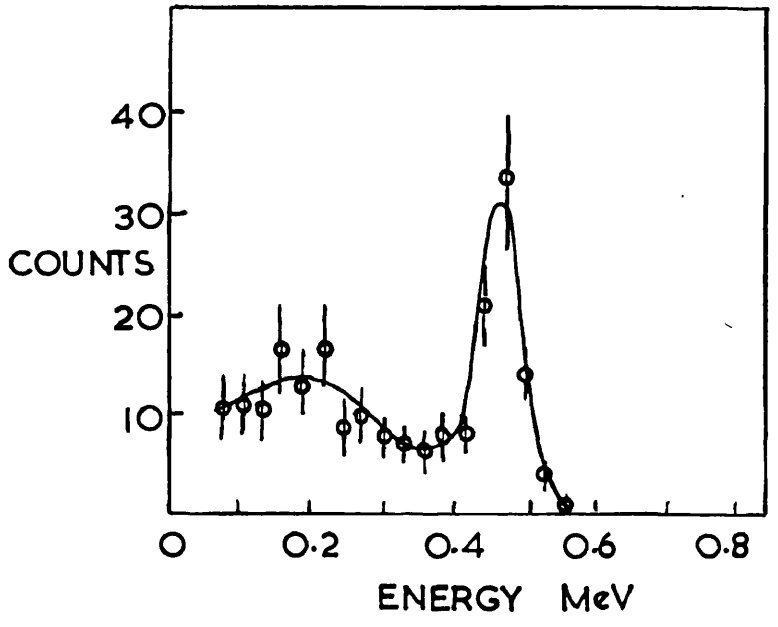

Fig. 5.3

The γ-ray spectrum in coincidence with 0.54 MeV γ-rays

Spectra were taken with the single channel set to accept pulses from each of the photopeaks in turn. Those obtained with the gate set on the 0.44 MeV peak and the 0.54 MeV peak are shown in figs. 5.2 and 5.3. In the former some low energy pulses from the 0.54 MeV peak operate the gate and the coincident 0.44 MeV γ-rays have almost prevented the resolution of the 0.54 MeV line. The latter, however, clearly shows that the 0.54 MeV pulses are in coincidence with 0.44 MeV pulses. No γ-rays were found in coincidence with 0.98 MeV γ-rays. The strongest I^{128} sources which could be obtained were not sufficiently intense to deny emphatically the possibility of γ-rays in coincidence with the 0.75 MeV line. An upper limit of $\sim$ 50% of the intensity of the 0.75 MeV line could be placed on such coincidences if they existed.

(iii) β-γ coincidences

The technique of producing I^{128} in a NaI(Tl) crystal was employed to provide "zero thickness" sources for a study of the low energy branches of the β^--decay. Crystals were packed in aluminium cans with aluminium oxide as diffuse reflector and thin glass windows, 0.035" thick. The neutron irradiation produced no confusing activities in the aluminium and those from such thin glass were of negligible intensity. Crystals were irradiated in the same position as the iodine sources. It was found, however, that a strong phosphorescence was produced in the crystal which decayed at first exponentially

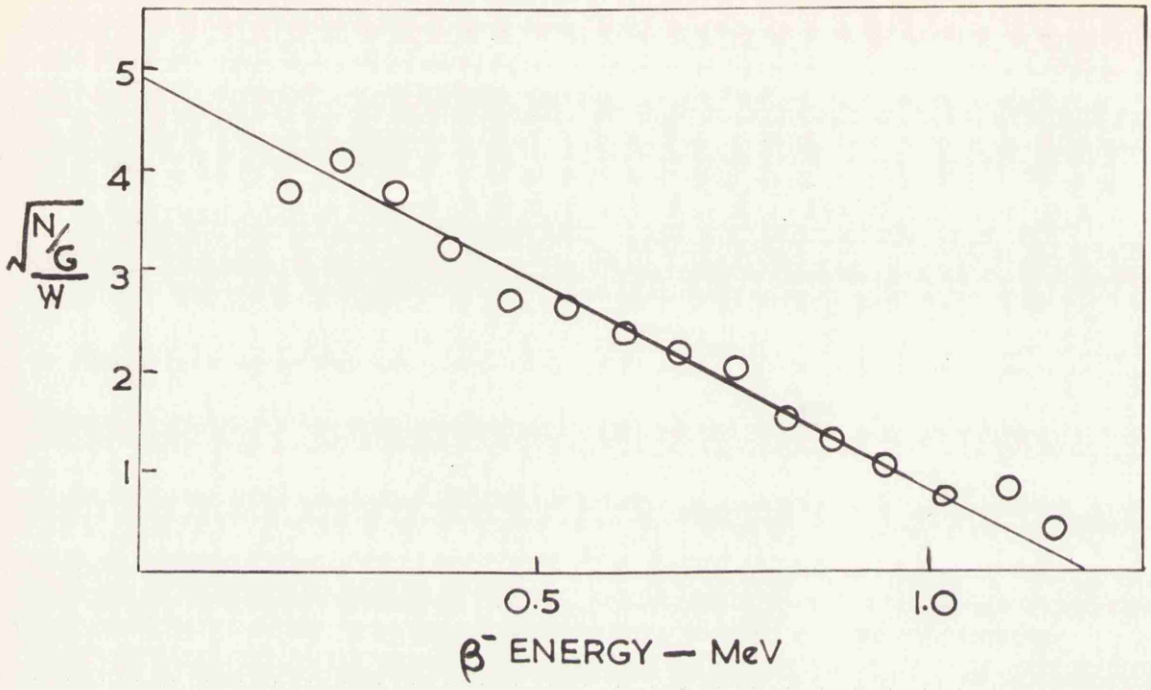

Fig. 5.4(a)

The β-spectrum in coincidence with 0.98 MeV γ-rays.

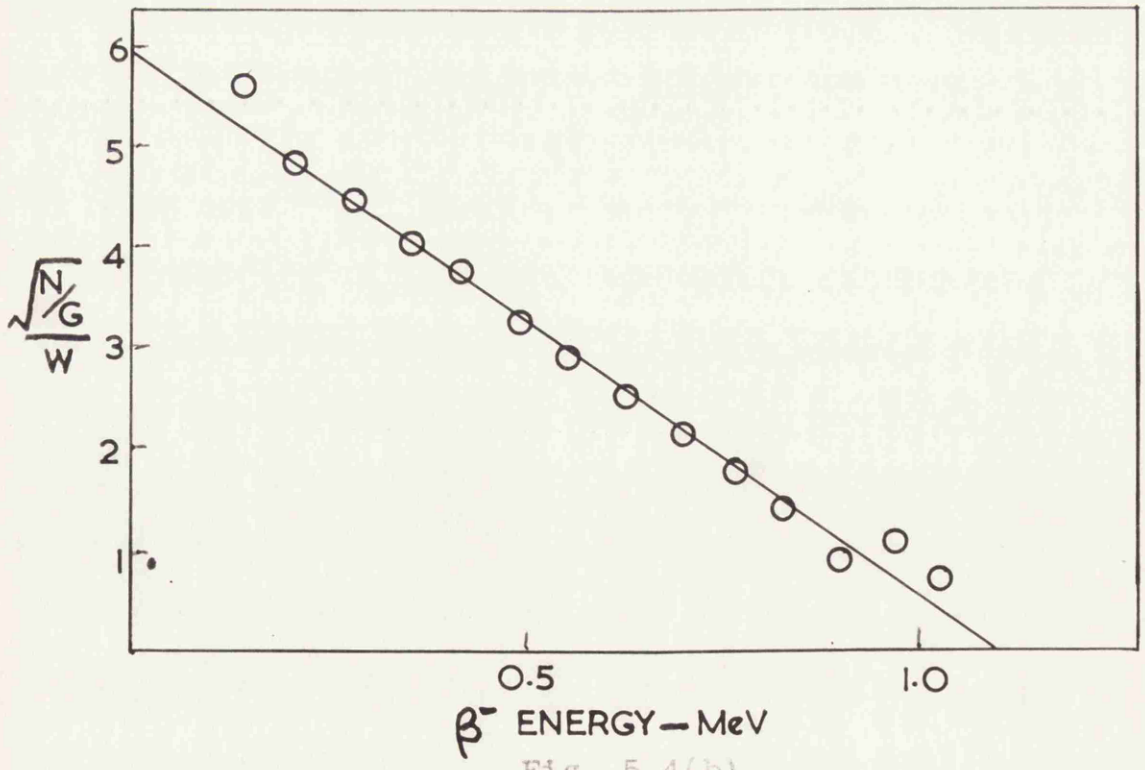

Fig. 5.4(b)

The β-spectrum in coincidence with 0.54 MeV γ-rays.

N = number of β-particles per channel
G = modified Fermi functions (Siegbahn, 1956)
W = total energy (including rest energy) of β-particle, in units of the rest energy of the electron

with a 6 minute half-life but contained a long lived non-exponential decay which reached half its original intensity in about 65 minutes. These effects were thought to be caused by the strong flux of γ-rays from the source and not by the neutrons. They were satisfactorily reduced by surrounding the crystal by a 1" thickness of lead.

The irradiated crystal was mounted on a DuMont 6292 photomultiplier and the spectrum from it fed to the 100-channel analyser. γ-rays leaving the radioactive crystal were detected in the scintillation spectrometer described above, the pulses from which, after selection by the single-channel analyser, were again used to gate the 100-channel analyser. The resultant spectrum thus contained pulses from β-particles in coincidence with γ-rays.

The spectra shown in figs. 5.4a and 5.4b were obtained with the window set on the 0.98 MeV and 0.54 MeV photopeaks respectively. The graphs shown are Kurie plots of the spectra after a correction had been applied for the small amount of Na^{24} formed in the crystal during the neutron irradiation. As its decay contained γ-rays some coincidence counts resulted from it. But the half-life of Na^{24}, 15 hours, is long compared to that of I^{128}, so its coincidence spectrum was measured after the I^{128} had decayed away, and was subsequently subtracted from the observed spectrum.

The measured end point energies are 1.13 $\pm$ 0.03 MeV for the β^- in coincidence with the 0.54 MeV γ-rays and

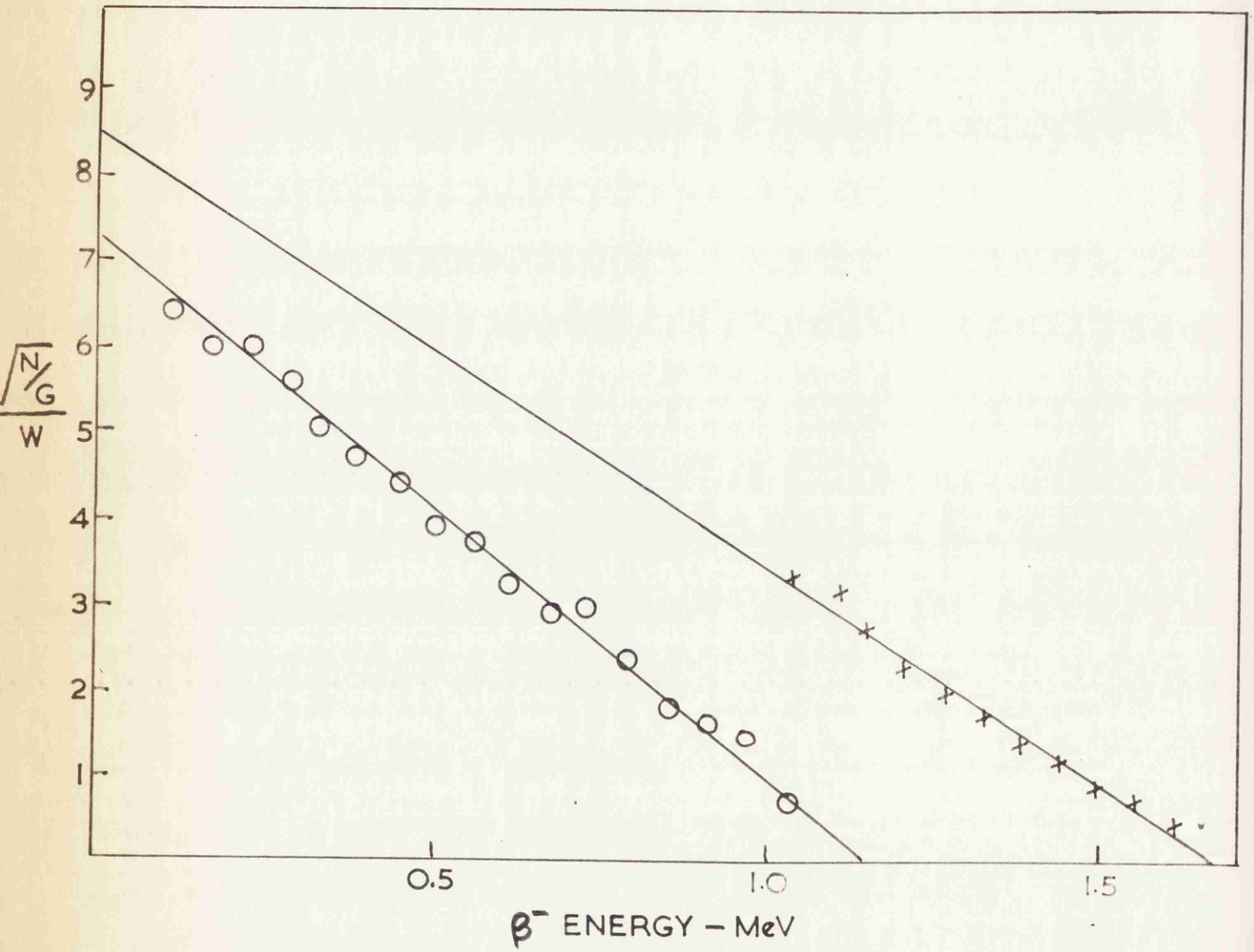

Fig. 5.5

The β-spectrum in coincidence with 0.54 and 0.45 MeV γ-rays

1.20 ± 0.05 MeV for the β^- in coincidence with the 0.98 MeV γ-rays. The estimated error for the latter value is larger because of the lower counting rate available owing to the low intensity of the 0.98 MeV γ-ray.

The spectrum in coincidence with the 0.44 and 0.54 MeV photopeaks together was found to be complex. The higher energy component has an end point energy of 1.67 ± 0.03. It was assumed to have a linear Kurie plot and its contribution below 1 MeV was estimated from the extrapolated straight line. The remaining counts, after subtraction give a straight line Kurie plot with an end point energy of 1.15 ± 0.03 MeV.* All these results are consistent with the decay scheme shown in fig. 5.7 which shows that the 0.98, 0.54 and 0.44 MeV γ-rays all follow β^--emmision.

The place of the weak 0.75 MeV γ-ray in the decay scheme was still undetermined. Owing to its low intensity and the confusion caused by low energy pulses from the 0.98 MeV γ-rays, the method described above for studying the spectra of β^--particles in coincidence with the other γ-rays was impracticable. An attempt was therefore made to find out whether the 0.75 MeV γ-rays followed β^--decay or electron capture.

The spectrum of γ-rays from the irradiated crystal was observed by feeding the output of the scintillation spectrometer to the 100-channel analyser and was compared to the same spectrum gated in coincidence with any pulse above

* See Fig. 5.5.

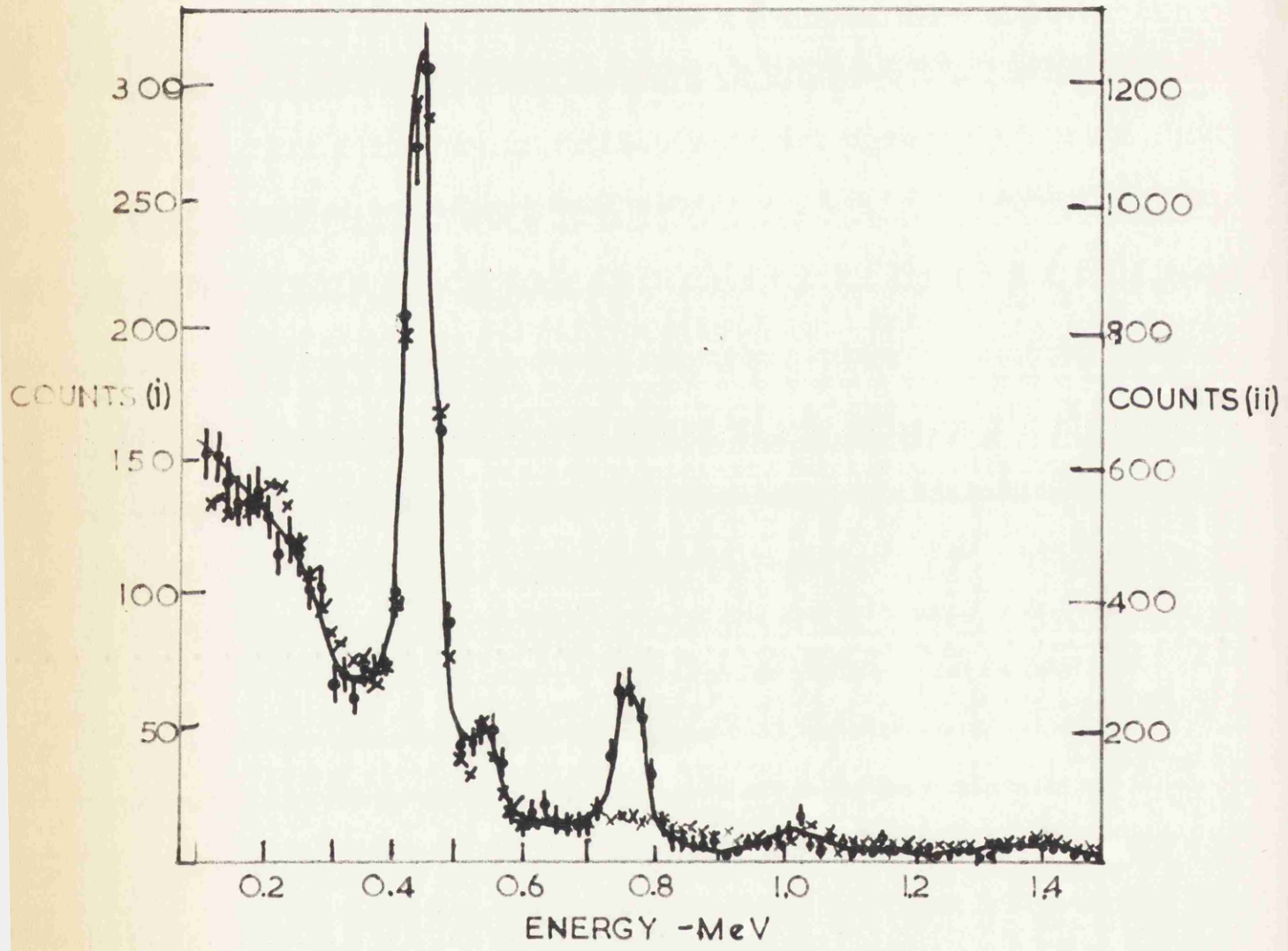

Fig. 5.6

The spectrum of γ-rays from a neutron irradiated NaI crystal (i) gated in coincidence with pulses in the crystal between 20 and 34 keV (circles) and (ii) ungated (crosses).

0.1 MeV in the radioactive crystal. The 0.98, 0.54 and 0.44 MeV γ-rays appeared in the gated spectrum. However, the 0.75 MeV γ-ray appeared in the ungated spectrum but not in the coincidence spectrum. This suggested that the 0.75 MeV γ-ray was not in the β^- branch, but as the peak was scarcely resolved the evidence was inconclusive. Further experiments were therefore undertaken, to see if the 0.75 MeV γ-ray was in coincidence with Te X-rays and therefore in the electron capture branch.

(iv) X-ray - γ-ray coincidences

In these experiments a NaI(Tl) crystal was irradiated and the pulses from the I^{128} decay in it were fed to the single-channel analyser set to accept 20 to 34 keV pulses. The spectrum of γ-rays emitted by the radioactive crystal was detected by a 2" NaI scintillation spectrometer and displayed on the 100-channel analyser. The spectrum was gated by the output of the single-channel analyser.

The pulses accepted by the single-channel analyser were those due to (i) low energy β^--particles, (ii) Te X-rays of 27 keV following electron capture in I^{128}. Thus the coincidence spectrum will contain γ-rays in coincidence with β-particles and X-rays but the ratio of the latter to the former should be enhanced relative to the ungated spectrum as only a small fraction of the β^- pulses are accepted by the single-channel analyser.

Fig. 5.6 shows the ungated spectrum and a coincidence

spectrum with roughly equal numbers of counts in their 0.44 MeV peaks. It is seen that the 0.75 MeV peak appears in the coincidence spectrum and not in the ungated one. Thus the 0.75 MeV line is shown to be in coincidence with X-rays of about 27 keV energy. The 47 keV γ-ray from RaD was used to calibrate the gain of the single-channel analyser, before irradiation of the crystal.

Many similar runs were carried out to try to decide whether there was also a very weak γ-ray at 0.63 MeV. In most of them there is slight evidence for a peak at that energy but it is inconclusive. As the gain of the 100-channel analyser varied by 2 or 3% from day to day it was impossible to add all these runs directly and thus obtain good statistics in that region.

If the transition exists and is in the electron capture branch then it is a Te^{128} γ-ray. Sb^{128} is thought to decay to Te^{128} and if such a γ-ray were found in its decay the energy of the state in Te^{128} might be determined. An attempt was therefore made to study the decay of Sb^{128}.

The isotope can be made by $Te^{128}(n,p)Sb^{128}$. Irradiation of natural tellurium with 14 MeV neutrons produced predominantly the radioactive tellurium isotopes by (n,2n) reactions. It was therefore necessary to separate the Sb from the Te after irradiation.

A chemical procedure was evolved by which the Sb could be extracted from 20 grams of sodium tellurate in about 10

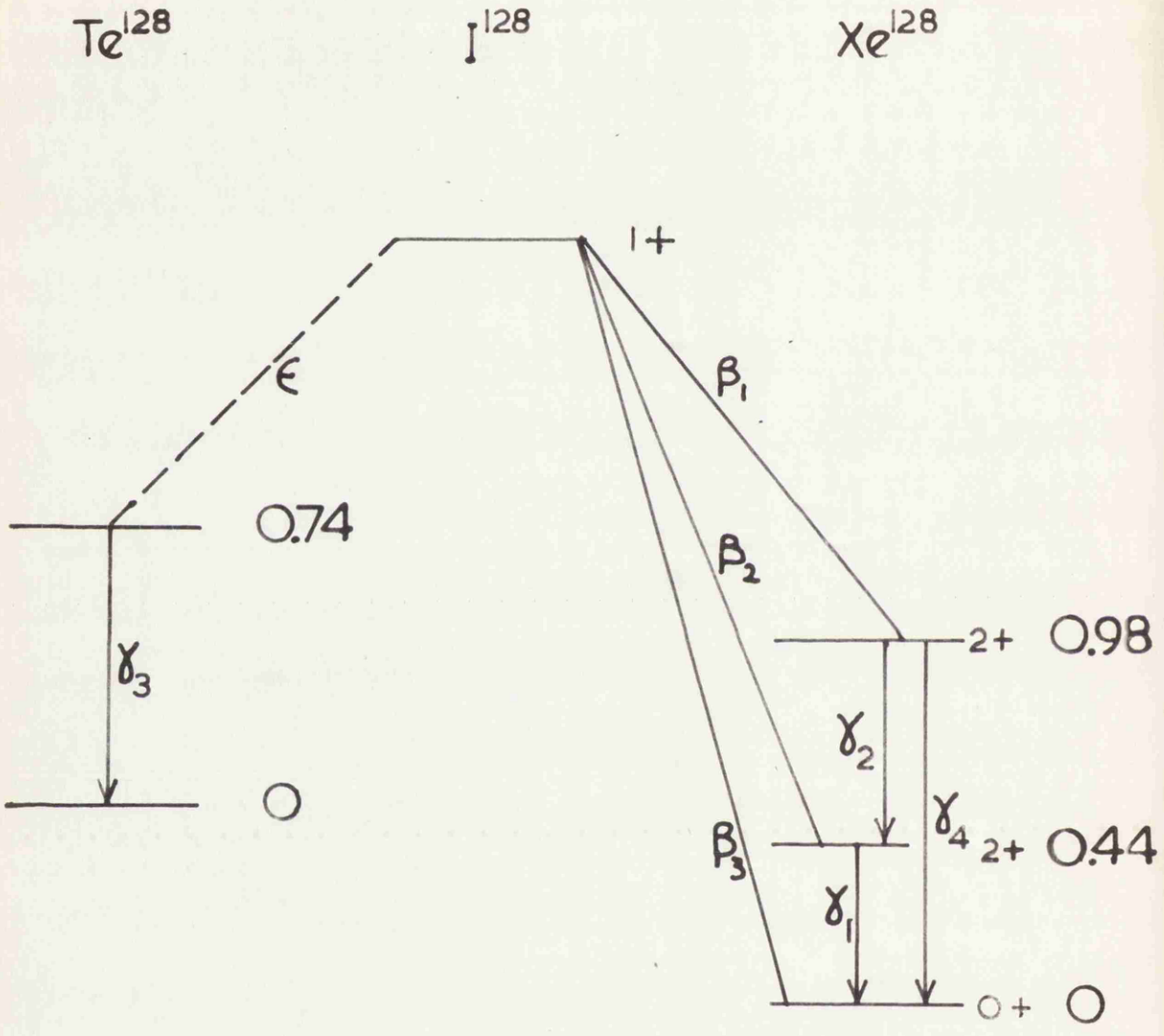

Fig. 5.7

The radioactive decay scheme of I^{128}.

minutes. Samples of sodium tellurate were irradiated with the maximum flux of 14 MeV neutrons available and then the Sb was separated as quickly as possible. Y-ray spectra showed prominent lines at 0.32, 0.42, 0.50, 0.70 and 0.77 MeV associated with decays having half-lives from about 10 to 20 minutes. Attempts were made to find coincidences between the various transitions but with the neutron flux available ($\sim 10^9$ neutrons/second) it was impossible to make sufficiently strong sources to distinguish the several decays. At least five half-lives between 7 and 40 minutes have been variously assigned to Sb isotopes between A = 126 and A = 130. With considerably stronger sources the application of coincidence techniques and the knowledge, from other experiments, of the energy levels of the corresponding Te isobars might permit a more definite assignment of these decay schemes. However, no evidence was found for a γ-ray of 0.63 MeV.

On the basis of the experimental results a decay scheme can be drawn for I^{128} and is shown in fig. 5.7. Supplemental notes on this decay scheme follow:

(i) The fact that γ_2-γ_1 coincidences were found shows that they are in cascade.

(ii) The presence of negatrons of the same energies in coincidence with both γ_2 and γ_4 shows that the latter is the crossover transition from the second excited state to the ground state.

(iii) The 1.67 MeV negatrons feed the first excited state and thus explain the greater intensity of γ_1 than γ_2.

(iv) The 0.75 MeV γ-ray is assigned to the electron capture branch because of its coincidence with K X-rays.

(v) The energy of the ground state transition, β_3, was estimated from the energy of β_2 + the energy of γ_1. An ungated spectrum of the pulses in an irradiated crystal confirmed this value.

The ratio of the ungated counting rate in the irradiated crystal to the counting rate in coincidence with 0.54 and 0.45 γ-rays, together with the calculated efficiency for detection of the γ-rays gave an estimate of the intensity of the ground state transition relative to the other two β^- branches of

$$\frac{\beta_3}{\beta_2 + \beta_1} \simeq 4$$

Section 5.3 Discussion of the Decay Scheme

From the experimental results and knowledge of some of the common properties of nuclei, it is possible to deduce many features of the energy level schemes of the isotopes involved in this radioactive decay.

All known ground states of even nuclei have spin 0 and even parity and all the measured first excited states in the medium weight region, N = 22 to N = 88, have spin and parity 2+. The second excited states with a few exceptions have

0+, 2+ or 4+ (Way, 1956). For the second excited state of Xe^{128} the first of these values is ruled out by the existence of a 0.98 MeV γ-ray which cannot connect two 0+ states. Neither is an assignment of 4+ probable because the predicted intensity (single particle approximation) of an E4, 0.98 MeV γ-ray is only 0.25×10^{-8} of the intensity of the 0.54 MeV, E2 transition to the first excited state.

The sequence of spins and parities 0+, 2+, 2+ for the first three states of Xe^{128} is consistent with the observed properties of medium weight nuclei which were summarized by Way et al. (1956). The observed ratio of excitation energies $\frac{E2}{E1} = \frac{0.98 \text{ MeV}}{0.44 \text{ MeV}} = 2.2$ and the product of first excited state energy times mass number, E1A = 56 MeV, support the view that Xe^{128} is a typical member of this medium weight group. Since neither N nor Z for this nucleus is near a magic number these excited states may be interpreted as vibrational levels with some interaction between the collective and independent particle motions which perturbs the energies away from the simple ratio of 2:1. Furthermore the γ-ray intensities support this interpretation; the conflict between the single particle prediction for the intensity ratio, $\gamma_4/\gamma_2 \simeq 20$, and the observed value $\gamma_4/\gamma_2 = 0.4$, is resolved if the crossover transition is thought to be inhibited by its 2 phonon nature and γ_2 enhanced, over its single particle value, by the collective motion of the nucleons.

The β-decay results substantiate the 0+, 2+, 2+ sequence for Xe^{128}. The log ft values although somewhat high are more consistent with allowed transitions than first forbidden ones: the 1+ assignment for the ground state of I^{128} which was shown in section 5.1 to be the most probable would give allowed β-decay to the three states of Xe^{128}. These values for the spins and parities of the ground state of I^{128} and the first three states of Xe^{128} are thus shown to be consistent with current understanding of the nucleus and most probable in the light of the experimental results. There is some evidence of vibrational excitations in Xe^{128} and the empirical trends noted by Way et al. (1956) are further substantiated.

CONCLUSIONS

The experiments described in this thesis, like most contemporary experiments in nuclear physics, do not suggest a new nuclear model or even provide an unique critical test of a current theory. The results obtained do, however, contribute to the body of knowledge of nuclear properties which is the basis of all the successful models of the nucleus. Each of the experiments contributes confirmation or criticism of a part of the accepted theory and some of them point the way to further investigations which might extend our understanding of the nucleus.

The work described in Chapter II on the relative yields of the ground and isomeric states of Pb^{207} produced by a photoneutron reaction, extended a type of investigation, initiated by others, to a heavy element in which the spin difference between the isomeric and ground states was much larger than in those previously studied. The discussion in section 2.4 showed that the large spin change involved in the production of the isomeric state leads to the interesting conclusion that the results could be much more easily understood in terms of Wilkinson's theory of photonuclear reactions than in terms of statistical emission of a neutron from a compound nucleus. A study of the yields of ground and isomeric states of In^{117} following the photoproton reaction in Sn^{118} might yield even more conclusive results as in this case the statistical emission of protons would be very

strongly inhibited by the coulomb barrier. With a very high intensity bremsstrahlung beam the experiment might be possible with about 1 gm of separated Sn^{118}; such a quantity is currently available from A.E.R.E., Harwell.

The negative result obtained in the search for an isomeric state of Mn^{54} strongly suggests that the reported radioactivity was due to some other isotope. This conclusion removes the difficulty of understanding the decay of the isomer in the light of the available information about Mn^{54} and its neighbouring isobars and the difficulty of explaining why such an isomeric state should be easily produced by (n,p) and (d,2p) reactions but not by a photoneutron reaction.

The clarification of the decay scheme of Mo^{91} added further confirmation of the similarity of the nuclear matrix elements for all the known M4 isomeric transitions. It also demonstrated again the reliability of shell model predictions for nuclei near closed shells. Finally it revealed a third example of an allowed β-transition between two states of spin and parity $\frac{1}{2}-$, which has a rather large log ft value. A similar transition has been found in the decay of Nb^{89*} (Diamond, 1954) but its energy has not been sufficiently well measured to allow calculation of its log ft value. Such a measurement would be of considerable interest to confirm or deny this apparently common feature of these particular transitions.

The study of the I^{128} decay scheme yielded information

about two excited states of Xe^{128} which suggested that they could be better described in terms of collective nuclear vibrations than single particle motions. The similarity of the properties of this nucleus to other even nuclei in the same general region of the periodic table is confirmation of the importance of collective motions.

Each of the experiments then made some contribution to the extension of our understanding of the atomic nucleus.

REFERENCES

Axel, P., Fox, J. D., and Parker, R. H., 1955, Phys. Rev. 97, 975.

Benczer, N., Farrelly, B., Koerts, L., and Wu, C. S., 1955, Phys. Rev. 100, 955A.

Benczer, N., Farrelly, B., Koerts, L., and Wu, C. S., 1956, Phys. Rev. 101, 1027.

Bendel, W. L., Toms, M. E., and Tobin, R. A., 1955, Phys. Rev. 99, 672A.

Bohr, A., and Mottelson, B. R., 1953, Dan. Mat. Fys. Medd. 27, no. 16.

Caldwell, D. O. and Stoddart, H. F., 1951, Phys. Rev. 81, 660A.

Caldwell, D. O., 1955, private communication.

Campbell, E. C. and Goodrich, M., 1950, Phys. Rev. 78, 640.

Cohen, B. L., Charpie, R. A., Handley, T. H., and Olson, E. L., 1954, Phys. Rev. 94, 953.

Courant, E. D., 1951, Phys. Rev. 82, 703.

Danos, M., 1952, Annalen der Physik 10, 265.

Day, M. C., Jr., Eakins, G. W., and Voigt, A. F., 1955, Phys. Rev. 100, 796.

de Shalit, A., 1953, Phys. Rev. 91, 1479.

Diamond, R. M., 1954, Phys. Rev. 95, 410.

Duffield, R. B. and Knight, J. D., 1949, Phys. Rev. 76, 573.

Feather, N. and Bretscher, E., 1938, Proc. Roy. Soc. A 165, 530.

Feenberg, E. and Trigg, G., 1950, Rev. Mod. Phys. 22, 399.

Feld, B. T., Feshbach, H., Goldberger, M. L., Goldstein, M., and Weisskopf, V. F., 1951, Final Report of the First Neutron Data Project AEC-NYO-636, page 115.

Flowers, B. H., 1952, Phys. Rev. 86, 254.

Germagnoli, E., Malvicini, A., and Zappa, L., 1953, Nuovo Cimento 10, 1388.

Goldemberg, J. and Katz, L., 1953, Phys. Rev. 90, 308.

Goldhaber, M. and Teller, E., 1948, Phys. Rev. 74, 1046.

Goldhaber, M. and Sunyar, A. W., 1951, Phys. Rev. 83, 906.

Goldhaber, M. and Hill, R., 1952, Rev. Mod. Phys. 24, 179.

Grace, M. A. and Prescott, J. R., 1951, Phys. Rev. 84, 1059.

Gupta, R. K. and Jha, S., 1956, Nuclear Physics 1, 2.

Harvey, J. R., 1953, Can. J. Phys. 31, 278.

Haxel, O., Jensen, J.H.D., and Suess, H. E., 1949, Phys. Rev. 75, 1766.

Hirzel, O. and Waffler, H., 1947, Helv. Phys. Acta 20, 373.

Hull, D. E. and Seelig, H., 1941, Phys. Rev. 60, 553.

Jensen, J.H.D., 1955, "Beta- and Gamma-ray Spectroscopy", Chapter XV, page 421. Edited by K. Siegbahn, North-Holland Publishing Co.

Katz, L. and Cameron, A.G.W., 1951, Can. J. Phys. 29, 518.

Katz, L., Pease, L., and Moody, H., 1952, Can. J. Phys. 30, 476.

Katz, L., Baker, R. G., and Montalbetti, R., 1953, Can. J. Phys. 31, 250.

Kurath, D., 1953, Phys. Rev. 91, 1430.

Lazar, N. H. and Klema, E. D., 1955, Phys. Rev. 98, 710.

Levinger, J. S. and Bethe, H. A., 1950, Phys. Rev. 78, 115.

Litherland, A. E., Paul, E. B., Bartholomew, G. A., and Gove, H. E., 1956, Phys. Rev. 102, 208.

Mack, J. E., 1952, Rev. Mod. Phys. 24, 179.

Mann, A. K. and Halpern, J., 1951, Phys. Rev. 83, 370.

Mayer, M. G., 1949, Phys. Rev. 75, 1969 and 1950, Phys. Rev. 78, 16 and 22.

McNeill, K. G., 1955, Phil. Mag. 46, 321.

McNeill, K. G., Prentice, J. D., Katz, L., and Link, W., 1957, Can. J. Phys. 35, 753.

Mims, W. B. and Halban, H., 1951, Proc. Phys. Soc. A 64, 753.

Montalbetti, R., Katz, L., and Goldemberg, J., 1953, Phys. Rev. 91, 659.

Neumann, H. M. and Perlman, I., 1951, Phys. Rev. 81, 958.

Nordheim, L. W., 1950, Phys. Rev. 78, 294.

"Nuclear Level Schemes A 40 - A 92", 1955, AEC-TID 5300, by K. Way, R. W. King, C. L. McGinnis and R. van Lieshout.

Perlman, M. L. and Friedlander, G., 1948, Phys. Rev. 74, 442.

Prescott, J.R.P., 1954, Proc. Phys. Soc. A 67, 540.

Pryce, M.H.L., 1952, Proc. Phys. Soc. A 65, 773.

Reid, J. M. and McNeill, K. G., 1953, Proc. Phys. Soc. A 66, 1179.

Reid, J. M. and McNeill, K. G., 1954a, Phil. Mag. 45, 957.

Reid, J. M. and Telfer, J.C.W., 1954b, Rev. Sci. Inst. 25, 300.

Reynolds, J. H., 1950, Phys. Rev. 79, 789.

Rose, M. E., Goertzel, G. H., Spinrad, B. I., Harr, J., and Strang, P., 1951, Phys. Rev. 83, 79.

Sagane, R., Kojima, S., Miyamoto, G., and Ikawa, M., 1940, Phys. Rev. 57, 1179.

Schardt, A. W. and Dropesky, B. J., 1956, Bull. Am. Phys. Soc. 1, no. 4, 162.

Scharff-Goldhaber, G. and Weneser, J., 1955, Phys. Rev. 98, 212.

Schwartz, C. and de Shalit, A., 1954, Phys. Rev. 94, 1257.

Siegbahn, K. and Hole, N., 1946, Phys. Rev. 70, 133.

Siegbahn, K., 1955, "Beta- and Gamma-ray Spectroscopy" North-Holland Publishing Co.

Soddy, F., 1916, Ann. Rep. Chem. Soc. 13, 247 and 272.

Strominger, D., Hollander, J. M., and Seaborg, G. T., 1958, Rev. Mod. Phys. 30, 585.

Vendryes, G., 1952, Annales de Physique 7, 655.

Wapstra, A. H., 1953, Thesis, University of Amsterdam (unpublished).

Wapstra, A. H., Verster, N. F., and Boelhouwer, 1953a, Physica 19, 138.

Way, K., Kundu, D. N., McGinnis, C. L., and van Lieshout, R., 1956, Annual Review of Nuclear Science 6, 129.

Weisskopf, V. F. and Blatt, J. M., 1952, "Theoretical Nuclear Physics", John Wiley and Sons.

Weisskopf, V. F., Gomes, L. C., and Walecka, J. D., 1958, Annals of Physics 3, 241.

Wilets, L. and Jean, M., 1956, Phys. Rev. 102, 788.

Wilkinson, D. H., 1954, Proceedings of the 1954 Glasgow Conference, p. 161, Pergamon Press.

Wilkinson, D. H., 1956a, Physica 22, 1039.

Wilkinson, D. H., 1956b, Phil. Mag. 1, 127.